The pathophysiological significance of Factor Seven (FVII) activating protease (FSAP) in Ischemic stroke

Inaugural Dissertation
submitted to the

Faculty of Medicine
in partial fulfillment of the requirements
for the PhD-Degree

of the Faculties of Veterinary Medicine and Medicine
of the Justus Liebig University Giessen

By
Amit Umesh Joshi

From
Pune, INDIA

Giessen 2014

Om Namah Shivaya

Om Sai Ram

Jai Shree Ram

The pathophysiological significance of Factor Seven (FVII) activating protease (FSAP) in Ischemic stroke

Inaugural Dissertation
submitted to the

Faculty of Medicine
in partial fulfillment of the requirements
for the PhD-Degree

of the Faculties of Veterinary Medicine and Medicine
of the Justus Liebig University Giessen

By
Amit Umesh Joshi

From
Pune, INDIA

Giessen 2014

From the Institute of Biochemistry
Director / Chairman: Prof. Dr. Lienhard Schmitz
of the Faculty of Medicine of the Justus Liebig University Giessen

First Supervisor and Committee Member: Prof. Dr. Sandip M Kanse
Second Supervisor and Committee Member: Prof. Dr. Katja Becker
Committee Member:
Committee Member

Date of Doctoral Defense:

नमस्ते सदा वत्सले मातृभूमे त्वया हिन्दुभूमे सुखं वर्धितोहम् ।
महामङ्गले पुण्यभूमे त्वदर्थे पतत्वेष कायो नमस्ते नमस्ते ।।

Forever I bow to thee, O Loving Motherland!
O Motherland of us Hindus, Thou hast brought me up in happiness.
May my life, O great and blessed Holy Land, be laid down in Thy Cause.
I bow to Thee again and again.

Shri. Narhari Narayan Bhide

I. Table of contents

II. List of figures

1. Introduction

1.1 Scientific Relevance

Stroke, by definition, is a sudden loss of neurologic function resulting from focal disturbance of cerebral blood flow due to ischemia or hemorrhage. Depending on the duration of the cerebrovascular disturbance, stroke can cause permanent neurologic damage, disability, or death (Shichita et al., 2012). A transient ischemic attack (TIA; stroke symptoms lasting < 1 hr) may not cause neurologic damage but is strongly associated with a risk for subsequent stroke within the next 90 days. Stroke by itself is the second single most common cause of death in Europe: accounting for almost 1.1 million deaths in Europe each year. This is 10% of all deaths in men and 15% of all deaths in women.

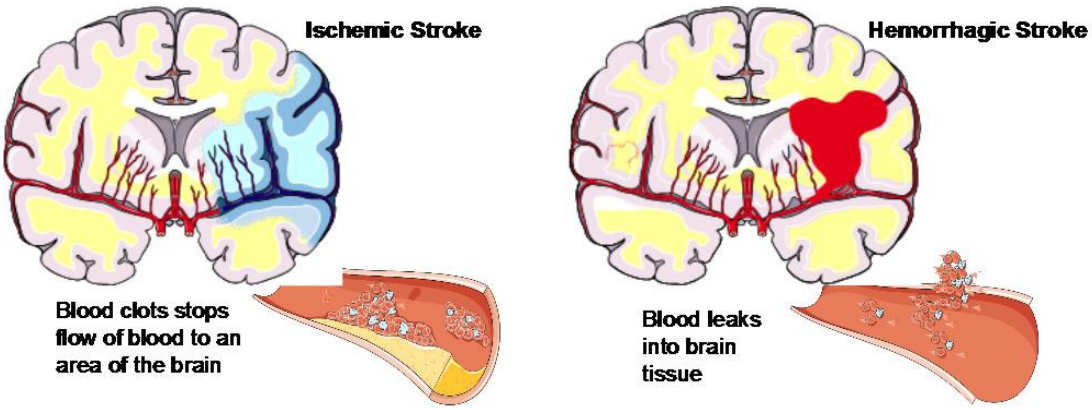

Figure 1.1: ***Classifications of Stroke.***
Ischemic stroke accounts for 80% and Hemorrhagic Stroke accounts for 20% of all stroke incidences Source: (http://www.ehnheart.org/cvd-statistics.html).

Ischemic stroke accounts for 85% of all strokes. There are two forms of ischemic stroke: focal and global ischemia. Focal ischemia is the result of lack of blood flow to an area of the brain due to a blood clot, known also as embolism *(Figure 1.1)*. Strokes may occur anywhere in the brain, including the cerebrum, brainstem, and the cerebellum. The most common area of infarct is blockage of the middle cerebral artery, which affects blood supply mainly to the striatum and forebrain. Global ischemia is the disruption of blood flow to the entire brain. Global ischemia can be the result of a heart attack, drowning, suffocation, or any sort of blockage that results in lack of blood flow to the head.

An ischemic stroke can be permanent or temporary, in which case the blood clot is eventually broken down, and reperfusion takes place. Neurons need a constant supply of oxygen and glucose, which is carried by blood. Without oxygen and glucose, neurons cannot produce energy and die. Cell death after ischemic stroke is thought to be both due to both apoptotic and necrotic pathways within the cells (Unal-Cevik et al., 2004). The occlusion of the brain blood vessel during stroke initiates the ischemic cascade, causing the activation of many signaling pathways that compromise cell survival and function, such as glutamate mediated excitotoxicity, Ca^{2+} overload, oxidative stress and blood brain barrier (BBB) dysfunction, inflammation and cell death (Mehta et al., 2007) .

The only FDA-approved treatment for ischemic stroke is tissue plasminogen activator (tPA), which has a narrow time window of only approximately 4.5 hours after the onset of stroke symptoms. tPA acts as a thrombolytic agent through the activation of plasminogen to plasmin which degrades the fibrin clot . Approximately only 3-5% of all patients that suffer a stroke benefit from tPA, mainly due to the narrow therapeutic window (Hacke et al., 2008; Martin-Schild, 2012). The lack of available therapies and the devastating effects of these diseases compel researchers and clinicians to find more effective treatments (Moskowitz et al., 2010).

1.2. Blood Brain Barrier (BBB) and Stroke

The BBB is localized at the interface between the blood and the cerebral tissue. The selective nature of this barrier is vital to protect the CNS and maintain its vital functions. The BBB is comprised of endothelial cells, which prevent the movement of molecules into the brain. The BBB consists of not only endothelial cells but also astrocytic end-feet and tight junctions, which support the selective permeability of this barrier *(Figure 1.2)*. Molecules larger than 400 daltons are unable to cross the BBB. Brain endothelial cells differ significantly from non-brain ECs by (i) the absence of fenestration correlating with the presence of intercellular tight junctions (TJs), (ii) the low level of non specific transcytosis (pinocytosis) and paracellular diffusion of hydrophilic compounds, (iii) a increased mitochondria, associated with a strong metabolic activity and (iv) the polarized expression of membrane receptors and transporters which are responsible for the active transport of blood-borne nutrients to the brain or the efflux of potentially toxic compounds from the cerebral to the vascular compartment.

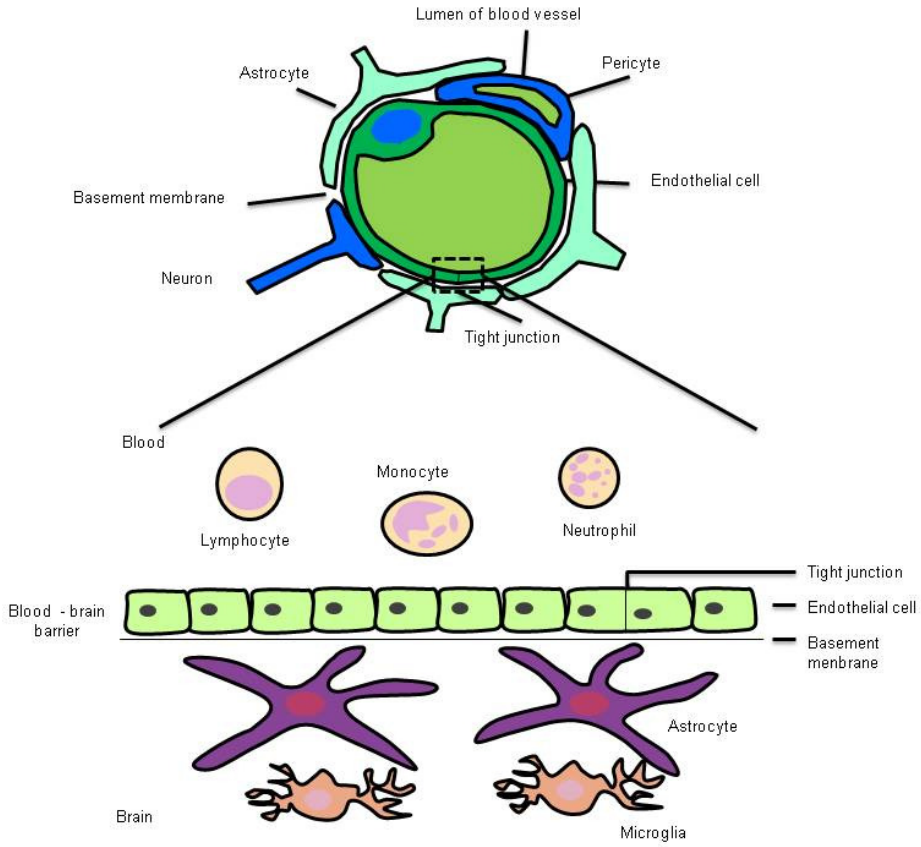

Figure 1.2: ***Structure of the Blood brain barrier***
Morphology of the brain microvascular capillary endothelium and the surrounding region. Modified from Expert **reviews** in molecular medicine ©2003 Cambridge University Press (http://journals.cambridge.org/fulltext_content/ERM/ERM5_15/S1462399403006252sup001.pdf)

Acute obstruction of cerebral blood vessel by clot formation triggers a complex series of cellular and molecular events in the brain parenchyma (membrane depolarization of neurons and astrocytes, release of excitatory amino acids and K+ ions in interstitial fluids, increase of intracellular Ca^{2+} levels), ultimately leading to dramatic cell damage within hours. Up-regulation of the matrix metalloproteinases (MMP)-2 and -9, as well as of the vascular endothelial growth factor (VEGF) are closely associated with BBB disruption (Yang et al., 2007; Bauer et al., 2010). Release of oxidants, proteolytic enzymes and inflammatory cytokines were shown to alter the BBB permeability properties, leading to brain edema formation (Dirnagl et al., 1999).

BBB dysfunction under ischemic conditions results in an increased paracellular permeability, which contributes to cerebral edema, hemorrhagic transformation, and increased mortality. Various mechanisms which occur is multiple phases, contribute to the ischemic damage of the BBB. Initially, the dissolution of the endothelial basal lamina takes place and this is rapidly followed by an increase in BBB permeability. After reperfusion, a biphasic increase of BBB permeability may occur. The multi-phasic phenomenon of this permeability change is determined by various factors, including the duration of ischemia and degree of reperfusion.

The increase of paracellular permeability is generally associated with the alteration of tight-junction protein expression and/or the redistribution of tight-junction protein along the cellular membrane. It has been shown that a reduction in Trans-Endothelial Electrical Resistance (TEER) is accompanied by a decreased claudin-5 expression under the hypoxic conditions, whereas hypoxia induced increase of paracellular permeability has been observed along with the disruption of occludin, ZO-1, and ZO-2 membrane localization (Mark and Davis, 2002; Koto et al., 2007).

In response to brain ischemia, accumulated bradykinin, VEGF, and thrombin initiate the increase of intracellular calcium concentration, whose primary effect in the endothelial cells is the activation of calcium/calmodulin-dependent myosin light chain kinase (MLCK) (Goeckeler and Wysolmerski, 1995), inducing actin reorganization, changes of cell morphology, and increased BBB paracellular permeability. Oxidative stress is also an early stimulus for BBB disruption and triggers the cellular release of MMP-9 from neurons, astrocytes, pericytes, and endothelial cells, resulting in digestion of the endothelial basal lamina. In the later phase, severe BBB damage resulting from more complicated mechanisms appears, such as induction of pro-inflammatory cytokines, followed by chemokines and adhesion molecules expression on the activated endothelium.

The expression of cytokines and adhesion molecules precedes the infiltration of leukocytes, which, together with activated microglia, further enhances the inflammatory responses and the production of toxic free radicals (Huang et al., 2006). The damaged BBB allows leakage of blood constituents into the brain parenchyma (Lo et al., 2003). Extravasation of high molecular weight components, which is followed by water due to osmosis, leads to vasogenic edema and intracranial hypertension. In particular, the extravasation of red blood cells may lead to hemorrhagic transformation in the brain.

1.3 Astrocytes in Ischemic Brain

Astrocytes are the most abundant glial cells within the central nervous system (CNS) and comprise of approximately 50% of the total number of cells in the cerebral cortex. These cells can be identified by staining for glial fibrillary acidic protein (GFAP), revealing star shaped morphologies. Astrocytes are classically divided into three major types according to their morphology and spatial organization, protoplasmic astrocytes in grey matter, fibrous astrocytes in white matter and radial astrocytes surrounding ventricles (Ransom and Ransom, 2012).

In response to different types of stimulation, astrocytes are known to release various factors including brain-derived neurotrophic factor (BDNF), nerve growth factor (NGF), glial-cell-line-derived neurotrophic factor (GDNF), transforming growth factor- β1 (TGF-β1), neurotrophin (NT), nitric oxide (NO), reactive oxygen species (ROS), interleukins (ILs) and tumor necrosis factor-α (TNF-α). Astrocytes express chemokines and cytokines in response to inflammatory stimulators. Other hand, they prevent excessive inflammatory responses of microglia thus contributing to inflammation positively or negatively (Lin et al., 2006). The primary response of the astrocytes following cerebral ischemia is likely to be important for neuronal protection. Astrocyte activation process is commonly known as reactive gliosis. The reactive astrocyte morphology is altered accompanied by differential expression of hundreds of genes compared to the non-reactive astrocyte (Eddleston and Mucke, 1993). Astrocyte reactivity is generally associated with microglial reactivity and, in some cases, leukocyte recruitment.

Activated astrocytes migrate to the injured area and contribute to glial scar formation. Glial scars may act as a barrier by sealing off the injured tissue from the healthy tissue. Axons cannot regenerate beyond glial scars, which may inhibit neuronal recovery processes after damage as shown by Silver *et. al.* (Silver and Miller, 2004). Astrocytes have been suggested to play a detrimental role following ischemia as the gap junctions may remain open (Martinez and Saez, 2000), allowing substances such as pro-apoptotic factors to spread through the syncytium thereby expanding the size of the infarct (Lin et al., 1998).

In-vitro studies have provided substantial insight into the mechanisms governing the survival of astrocytes following simulated ischemia. It has been shown that astrocytes are generally more resistant than neurons to oxygen-glucose deprivation (OGD) (Sochocka et al., 1994). Most neurons in a cortical astrocytic-

neuronal co-culture show signs of cell death after 60-70 min of OGD while astrocyte cultures require several hours to develop such extensive damage (Almeida et al., 2002). However, it appears that not all groups of astrocytes are similarly resistant to ischemic insults. The *in-vitro* studies have also provided a better understanding of what mechanisms influence astrocytic cell death. For example, a combination of hypoxia and acidosis has been found to be very effective in killing astrocytes (Giffard et al., 1990; Swanson et al., 1997; Bondarenko and Chesler, 2001).

1.4. Ischemia Reperfusion Injury in Stroke

During ischemia, cell death/ necrosis occurs due to energy depletion and loss of O_2 supply. The recovery of energy metabolism during the initial 20 minutes of reperfusion is accompanied by a restoration of the distribution of ions to near their pre-ischemic state. During reperfusion after ischemia, while restoration of oxygen and glucose supply reinstates the oxidative phosphorylation that helps to normalize energy demanding physiologic processes (Aronowski et al., 1997), a parallel cascade of deleterious biochemical processes can be triggered that may paradoxically antagonize the beneficial effect of reperfusion and have been summarized in *Figure 1.3*. Thus, reperfusion injury is the tissue damage caused when blood supply returns to the tissue after a period of ischemia or lack of oxygen (Sari et al., 2013). This phenomenon was observed in the middle cerebral artery occlusion model (MCAO, a model mimicking clinical stroke). In this study, they observed that rats with permanent occlusion resulted in smaller infarct volume than rats with 2 h occlusion followed by 24 h reperfusion. Multiple studies and reviews have described the mechanisms by which leads to injury. In brief, during reperfusion, activated leukocytes interact with endothelial cells and plug capillaries. This is followed by disruption of BBB through the release of neutrophil-derived oxidants, proteolytic enzymes, which extravasate from capillaries and infiltrate brain tissue releasing cytokines which then mediate inflammation (Pan et al., 2007). Also the plugging of capillaries results in secondary cerebral ischemia.

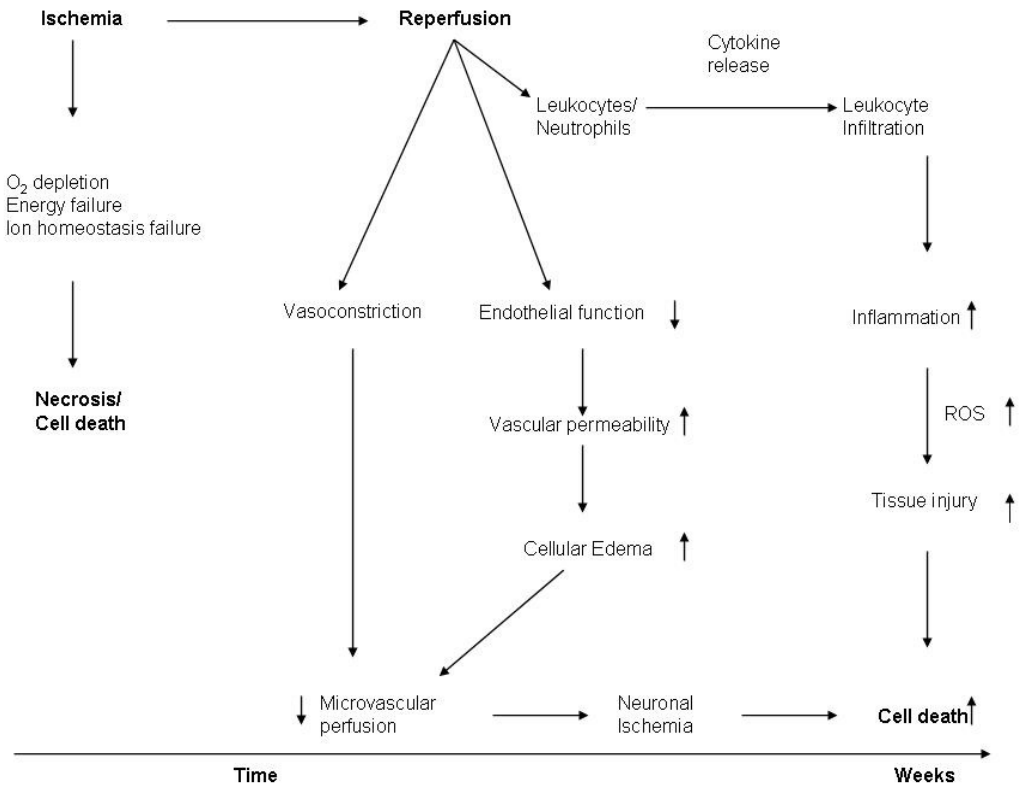

Figure 1.3: ***Scheme of events following ischemia reperfusion injury.***
Ischemia reperfusion affects endothelial function, leads to vasoconstriction and infiltration of leukocytes and neutrophils which further enhances inflammation and cell death, Modified from (Pan et al., 2007)

Once the leukocytes infiltrate the parenchyma, they release various chemical mediators like leukotrienes, and prostaglandins, reactive oxygen species (ROS), resulting in increased microvascular permeability, edema, thrombosis and parenchymal cell death (Pan et al., 2007). Platelets are known to play a synergistic role with leukocytes in reperfusion injury. Multiple mouse and clinical studies suggest that platelets are activated after cerebral ischemia and reperfusion. Activated platelets also release a variety of biochemical mediators which result in further tissue damage (del Zoppo, 1998). Complement activation has also been described to be an important component of reperfusion injury (Arumugam et al., 2009). Complement activation results in the formation of several inflammatory mediators which enhance the reperfusion injury. Studies have also shown that hyperperfusion may contribute to the development of reperfusion injury by causing brain edema or hemorrhage (Arumugam et al., 2009). Thus, breakdown of the BBB during cerebral reperfusion

may lead to the development of vasogenic edema, hemorrhagic transformation and infarction.

1.5. Inflammation in ischemic stroke

Inflammation is a defense reaction against diverse insults that serves to remove noxious agents and to limit their detrimental effects. Ischemia initiates a complex process in which inflammation contributes to stroke-related brain injury (Huang et al., 2006). Ischemia leads to the activation of microglia and astrocytes with subsequent production of inflammatory mediators. Cytokines stimulate the expression of adhesion molecules which mediate the adherence and extravasation of neutrophils and monocytes into the ischemic tissue (Wang et al., 2007). The pattern of cytokine inflammation response differs depending on stroke type and localization. IL-1β is an endogenous pyrogen which centrally contributes to an exacerbation of neuronal loss (Rothwell and Luheshi, 2000). IL-1β also contributes to the activation and proliferation of microglia and astrocytes. It has been shown that IL-1β induces edema formation and primes the endothelium for leukocyte adherence (Rothwell, 2003; del Zoppo, 2009). TNF-α like IL-1 β shows a biphasic release pattern with a first peak 1-3 hours and a second peak 24-36 hours after an ischemic insult (Hosomi et al., 2005; Nilupul Perera et al., 2006; Pan and Kastin, 2007). Activated microglia and macrophages are major producers of soluble TNF-α within the first 6 hours after cerebral ischemia (Clausen et al., 2008). Yang *et al* showed that inhibition of TNF-α attenuates infarct volume and ICAM‐1 expression in ischemic mouse brain (Yang et al., 1998). TNF-α stimulates apoptosis of endothelial cells contributing to vasogenic edema and, concomitant BBB breakdown, infiltration of circulatory inflammatory cells are stimulated (Christov et al., 2004). IL-6 is detected 4 hours after stroke onset, with peak concentrations after a day. Activated microglia, followed by astrocytes, neurons and invading cells of the immune system, comprise the main source for IL-6 (Amantea et al., 2009). Recently however, Gertz et al showed that IL-6 produced locally by resident brain cells promotes post-stroke angiogenesis and thereby affords long-term histological and functional protection (Gertz et al., 2012).

IL-10 is constitutively expressed anti-inflammatory cytokine with peak levels 3 days after stroke onset. It is primarily produced by activated microglia and astrocytes (Wang et al., 2007; Ceulemans et al., 2010). IL-10 reduces pro-

inflammatory responses after ischemic stroke primarily by acting on glia and endothelium (Ceulemans et al., 2010; Sharma et al., 2011). Sharma *et al* reported that IL-10 directly protects cortical neurons by activating PI-3 kinase and STAT-3 pathways (Sharma et al., 2011). After stroke, intracellular adhesion molecule (ICAM) -1 and -2, vascular adhesion molecule (VCAM)-1 and platelet endothelial cell adhesion molecule (PECAM)-1 contribute to the inflammatory responses by attaching neutrophils and monocytes more tightly to the endothelial wall for facilitating and even stimulating diapedesis through the vessel wall to the site of injury (Ceulemans et al., 2010). It has been previously reported that the increases in ICAM-1 and VCAM-1 after stroke are influenced by IL-1β and TNF-α (Frijns and Kappelle, 2002). VCAM-1 is known to mediate the adhesion of lymphocytes, monocytes, eosinophils, and basophils to vascular endothelium as well as function in leukocyte-endothelial cell signal transduction (Supanc et al., 2011).

1.6. Glutamate excitotoxicity in Stroke

Glutamate released at the synapses can induce astrocytic exocytosis of glutamate, modulating the activity and strength of the synapse (Bezzi et al., 2004; Liu and Neufeld, 2004). A large proportion of the glutamate taken up by the astrocytes is converted to glutamine by an enzyme, glutamine synthethase (GS), exclusively localized in astrocytes which is up-taken by neurons thus maintaining neurotransmitter pool (Martinez-Hernandez et al., 1977).

Excitotoxicity is the pathological process by which neurons are damaged and killed by the overreactions of receptors for the excitatory neurotransmitter glutamate, such as the N-Methyl-D-aspartate (NMDA) receptor and α-amino-3-hydroxy-5-methyl-4-isoxazolepropionic acid receptor (AMPA) receptor (White et al., 2000) *(Figure 1.4)*. In stroke, excitotoxicity is a determining factor in the extent of the resulting lesion. Following a stroke, there is a disruption of ionic gradients across membranes (Nakka et al., 2008). This disruption causes an increase in extracellular K^+ and an influx of Na^+, Cl^- and Ca^{2+} in the cell. The extracellular K^+ triggers depolarization and reversal of the amino acid transporters which results in a massive release of glutamate.

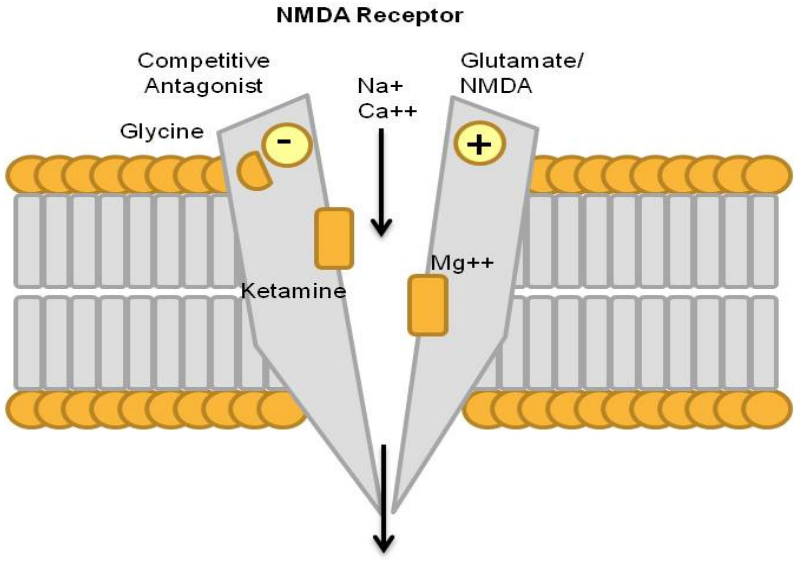

Figure 1.4: ***Example of an NMDA receptor.***
When glutamate/ NMDA binds to this receptor, it promotes the excessive influx of Ca^{2+} and Na^{+} into the cell which eventually leads to excitotoxic injury. Adapted from http://www.medical-horizons.net

The binding of glutamate to NMDA promotes excessive Ca^{2+} influx which triggers a range of downstream phospholipases and proteases that degrade membranes and proteins which in turn compromises cellular integrity (Mehta et al., 2007). The excitatory amino acid glutamate is released in large quantities during ischemia, and the removal of this neurotransmitter, predominantly accomplished by astrocytes, is important for neuronal survival in the post-ischemic tissue (Romera et al., 2004).

1.7. Apoptosis after ischemic stroke

Caspase-3 has been widely studied as a key mediator of apoptosis in animal models of ischemic stroke. It was shown that there is up-regulation of caspase-3 mRNA, caspase-3 and its cleavage products in rat brain immediately after the onset of focal ischemia (Namura et al., 1998; Asahi et al., 1999). Both genetic disruption and pharmacological inhibition of caspases have been found to have a strong neuroprotective effect in experimental stroke (Fink et al., 1999; Harukuni and Bhardwaj, 2006). It has been shown that oxygen glucose deprivation injury caused apoptotic cell death, induced cytochrome C release from mitochondria and caspase-3 activation, decreased mitochondrial membrane potential, and increased levels of pro-apoptotic Bax translocated to the mitochondrial membrane in PC12 neural cells, all of

which were reversed by overexpression of Bcl-2 (Koubi et al., 2005). Zhao *et. al.* demonstrated that Bcl-2 overexpression protects against neuron loss within the ischemic margin following experimental murine stroke and inhibits cytochrome c translocation and caspase-3 activity (Zhao et al., 2003). Thus, various studies have demonstrated the vital role of Bcl-2 in providing neuroprotection against ischemic event (Soane and Fiskum, 2005).

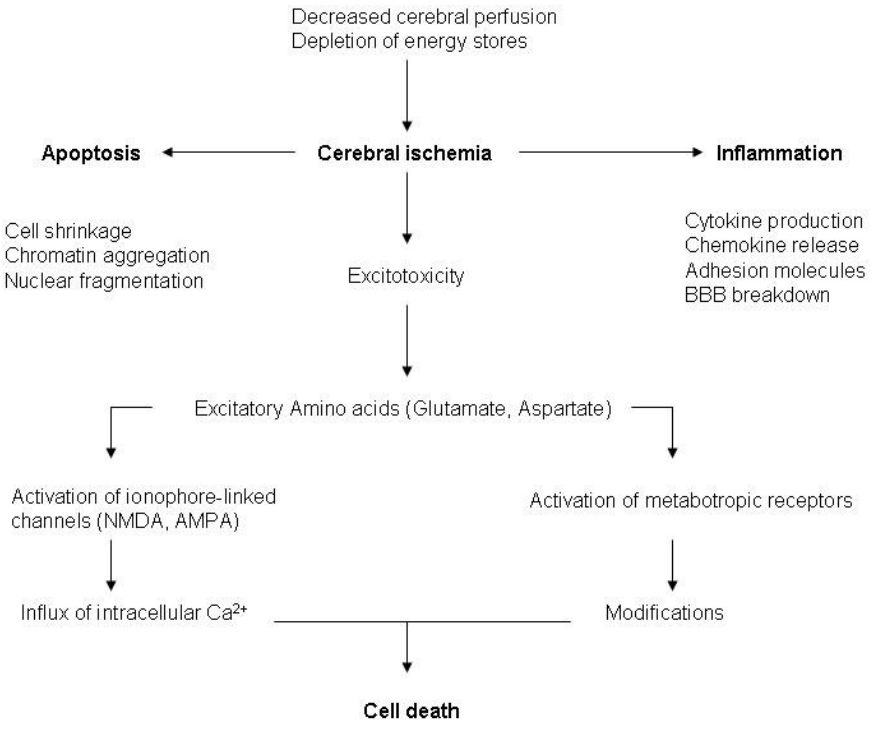

Figure 1.5: ***An overview of pathophysiology of ischemic stroke.***
Ischemia in the brain leads to a cascade of changes through apoptosis, inflammation and excitotoxicity which culminate into cell death and morbidity. Modified from (Harukuni and Bhardwaj, 2006)

1.8. Role of Akt survival signaling pathway in Stroke

Akt was originally identified as a cellular counterpart of the oncogene derived from murine AKT8 retrovirus. The same gene product was independently isolated as a protein kinase related to protein kinase A and C and was therefore named as protein kinase B (PKB) or RAC (related to protein kinase A and C) (Neary et al., 2005) (Hu et al., 2005; Zhao et al., 2006). The phosphoinositide-3-kinase/Akt cell survival

signaling pathway has been increasingly researched in the field of stroke (Zhao et al., 2006; Arai and Lo, 2010). Akt activity has been suggested to be upregulated by phosphorylation through the activation of receptor tyrosine kinases by growth factors. Although the upstream signaling components phosphoinositide-dependent protein kinase (PDK)1 and integrin linked kinase enhance the activity of Akt, phsophatase and tensin homolog deleted on chromosome 10 (PTEN) decreases it. Upon activation, Akt phosphorylates a wide array of molecules, including glycogen synthase kinase3β (GSK3β), forkhead homolog in rhabdomyosarcoma (FKHR), and Bcl-2-associated death protein, thereby blocking mitochondrial cytochrome c release and caspase activity (Zhao et al., 2005; Endo et al., 2006). Generally, the level of Akt phosphorylation at site Ser 473 (p-Akt) transiently increases after focal ischemia. Numerous compounds have been demonstrated to reduce ischemic damage, possibly by up regulating p-Akt (Zhao et al., 2006; Li et al., 2008; Lan et al., 2013). It has been reported that effective recruitment of Akt by appropriate survival signals may lead to activation of Mdm2, inactivation of p53, and eventually inhibition of p53-dependent apoptosis (Gottlieb et al., 2002; Ogawara et al., 2002; Liu, G. P. et al., 2012). Taken together, attenuation of the Akt pathway dysfunction could contribute to neuronal and astrocytic survival after ischemic stroke.

The p53 tumor suppressor gene encodes a nuclear phosphoprotein that functions as a key regulator of cell cycle progression and apoptosis. In murine brains, it was reported that p53 deficiency played a central role in driving gliomagenesis (Wang et al., 2009). Neuronal injury, especially damage mediated by excitotoxicity, is associated with increased production of reactive oxygen species and accumulation of single-strand DNA breaks. Cell culture studies have established strong correlations between p53 expression and excitotoxic neuronal death induced by glutamate and NMDA (Culmsee and Mattson, 2005). The absence of p53 has been shown to protect neurons *in-vivo* from a wide variety of toxic insults including focal ischemia (Crumrine et al., 1994). The signaling pathways activated by Akt phosphorylation have been summarized in *Figure 1.6.*

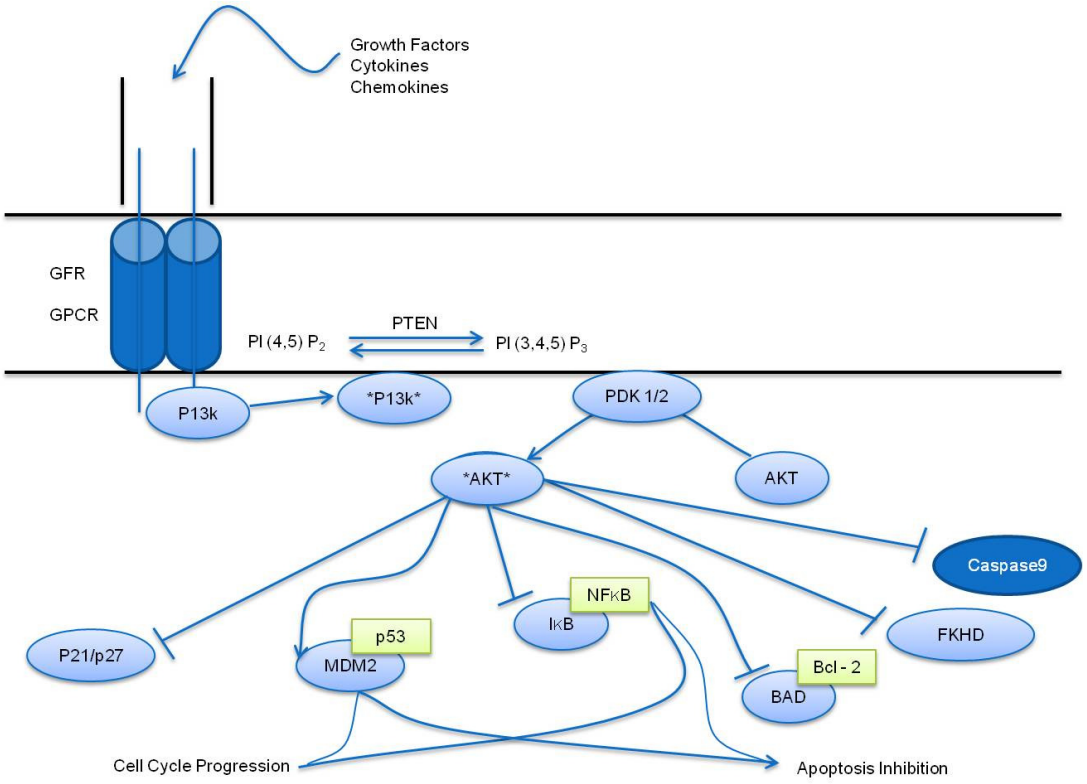

Figure 1.6: ***Akt – Master regulator for cell fate.***
Once activated Akt pathway is involved in mediating various biological responses which promote cell survival after injury. (Adapted from Cell Signaling Technology, Inc., http://www.cellsignal.com).

1.9. Role of FSAP in vasculature

FSAP is predominantly produced as an inactivate zymogen molecule of 78 kDa that can be converted in its active two-chain form consisting of a 50 kDa heavy and a 28 kDa light chain connected by a disulfide bond in the liver. FSAP consists of 560 amino acids including a 23 amino acid pro-peptide at the amino terminal part of the molecule. FSAP consists of three epidermal growth factor (EGF) domains, a kringle domain, a serine protease domain at its C terminus *(Figure 1.7)* (Choi-Miura et al., 1996). The circulating plasma concentration of FSAP is 12 µg/ml (180nM) and it can be activated by factors released from apoptotic or dead cells, e.g. histones and nucleosomes (Kanse et al., 2008). Once activated, FSAP is capable of activating other FSAP molecules in an autocatalytic fashion. Single-chain FSAP (scFSAP) in purified systems has been reported to be susceptible to auto-proteolysis. FSAP can also be auto-activated upon binding to negatively charged polyanions, such as hyaluronic acid, heparin, and nucleic acids. Apart from FVII, several other substrates for FSAP

have been identified including fibrinogen, fibronectin, high molecular weight kininogen (HMWK), single-chain urokinase -type plasminogen activator (scu-PA), FV, FVIII, and more recently the tissue factor pathway inhibitor (TFPI) (Muhl et al., 2009; Kanse et al., 2012). After *in-vivo* activation complex formation of FSAP has been observed especially with α2-plasmin inhibitor and C1 inhibitor (Stephan et al., 2011) . In *in-vitro* experiments, FSAP has been shown to promote fibrinolysis through activation of sc u-PA, and sc u-PA, in turn, can activate FSAP at a high enzyme to substrate ratio. FSAP is also a potent inhibitor of platelet-derived growth factor-BB (PDGF-BB), which has an important role in vascular smooth muscle cell proliferation and migration (Muhl et al., 2007).

1.10. FSAP Single Nucleotide Polymorphisms (SNPs) and Stroke

FSAP is encoded by the hyaluronic acid binding protein 2 *(HABP2)* gene. There are two prominent single nucleotide polymorphisms (SNP) which exist in the FSAP encoding gene, G534E (Marburg I, MI) and E393Q (Marburg II, MII), that each result in an exchange of a single amino acid in the protease domain which leads to loss of enzymatic activity *(Figure 1.7)* (Kannemeier et al., 2001; Romisch et al., 2001). About 6–9% of the Caucasian population is heterozygous carrier of each SNP (Romisch et al., 2001). Two other SNPs also lead to an exchange of a single amino-acid, but these SNPs are located in the heavy chain, in the EGF domains. These exchanges are S56T and I90V, respectively, their location in the heavy chain suggests no consequences for proteolytic activity.

In the analysis of the Bruneck Study the homozygous allele of the MI-polymorphism was shown to be strongly linked to late complications of carotid stenosis (Willeit et al., 2003). In another clinical trial, the FSAP-MI-SNP was also determined as a risk factor for cardiovascular disease in general. In one study, it was shown that FSAP-MI was associated with venous thromboembolism while others indicated no correlation (Kanse et al., 2008). In the PROSPER study, the Marburg I polymorphism was associated with an increased risk of clinical stroke (HR: 1.60, 95% CI: 1.13–2.28) and all-cause mortality (HR: 1.33, 95% CI: 1.04–1.71) (Trompet et al., 2011).

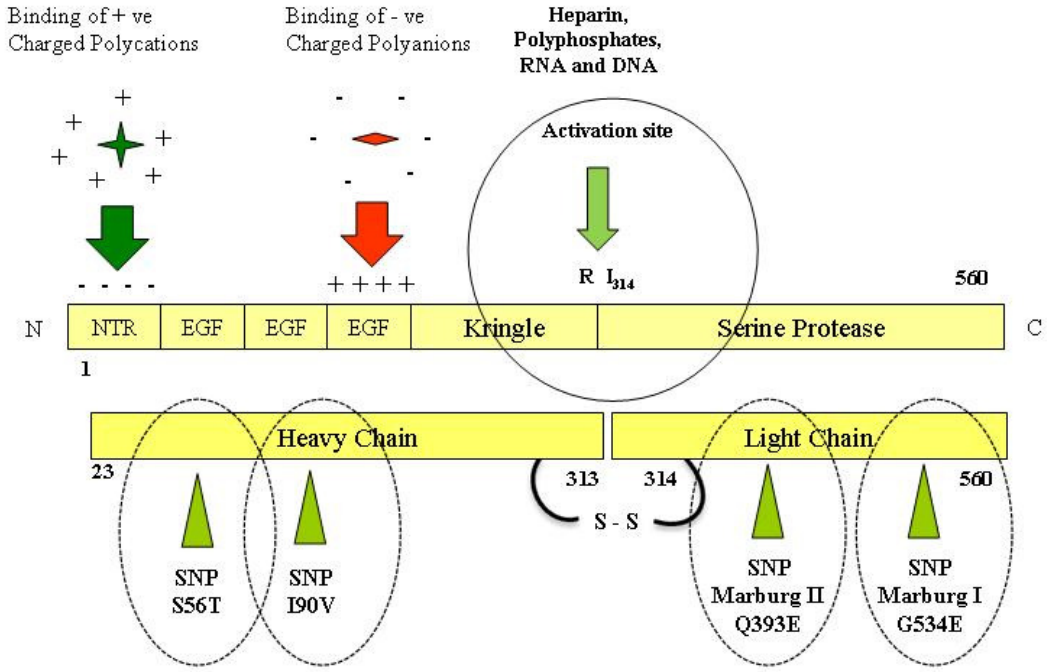

Figure 1.7: ***Structure of FSAP.***
Inactive single-chain conformation (top) and active two chain conformation (bottom) of FSAP with EGF kringle and serine protease domains indicated. The cleavage site is highlighted by the blue arrow, cleavage occurs at R▼I314. The arrows highlight locations of SNP, in either heavy-chain or light-chain Adapted from (Kanse et al., 2008).

We recently investigated whether FSAP antigen and activity levels are associated with ischemic stroke and/or etiologic subtypes of ischemic stroke (Hanson et al., 2012). To assess the potential association between FSAP and ischemic stroke, plasma FSAP antigen and activity were measured in 600 consecutive IS patients and 600 population-based controls from the case-control study the Sahlgrenska Academy Study on Ischemic Stroke (SAHLSIS). Both the FSAP antigen and activity levels were significantly increased in patients with IS, both in the acute phase and at the 3-month follow-up, as compared to controls (Hanson et al., 2012). In patients, FSAP activity was significantly higher in the acute phase compared with the follow-up measurement (mean 1274 mU/mL compared to 1214 mU/mL, $P<0.001$). It is possible that the increased acute phase FSAP activity is, to some extent, a result of tissue injury after stroke which leads to the release of apoptotic or dead cells. By contrast, there was no difference between the acute phase and follow-up FSAP antigen levels. Both FSAP antigen and activity were significantly lower in carriers of the A allele

(n=43) of the MI-SNP, compared to homozygotes for the wild-type G allele (n=546), (geometric mean 10.3 vs. 12.3 µg/mL, and mean activity 668 vs.1141 mU/mL, respectively, P<0.001 for both) (Hanson et al., 2012). However, the mechanisms by which FSAP might influence the pathophysiology of stroke remain elusive.

It is possible that FSAP through prothrombotic mechanisms (by inhibition of TFPI) might contribute to ischemic stroke (Kanse et al., 2012). However, there is no direct evidence linking TFPI levels and ischemic stroke occurrence. Recently we demonstrated a protective role for FSAP in liver fibrosis. In this study, bile duct ligation was used as a method for inducing liver fibrosis in mice (Borkham-Kamphorst et al., 2013). It is known that bile duct ligation induces hypoxia (Rosmorduc et al., 1999) and inflammation (Iredale, 2007). This role of FSAP in dampening of inflammation might also influence stroke outcome. Many studies have indicated that FSAP is also likely to have effects outside the hemostasis system analogous to plasminogen with which it shares high homology. It was shown that FSAP could influence endothelial permeability via Protease-activated receptor-1 (Mambetsariev et al., 2010). Activated protein C (APC) is similar to FSAP in that it also activates PAR-1 and recent studies have shown that APC exerts direct anti-apoptotic effects in neurons (Guo et al., 2004; Mosnier et al., 2007; Griffin et al., 2012). Protease-activated receptors (PARs) (PAR1-4) a family of G protein-coupled receptors (GPCRs), are widely expressed in the central nervous system (CNS), including neurons, microglial cells, astrocytes, and oligodendrocytes. Increasing evidence over the recent years has demonstrated that PAR-1, the main subtype of PARs, plays an important role in brain (Rohatgi et al., 2004). It was also reported that PAR-1 activation by thrombin treatment remarkably increases levels of glutathione peroxidase in human astrocytes, which protects neurons from the toxicity of thrombin at high concentration (Ishida et al., 2006). Thus, interactions of FSAP with PAR-1 receptor on astrocytes and neurons could be a possible mechanism by which FSAP may influence stroke pathophysiology.

2. Specific Aims

FSAP encoding gene has been associated with increased stroke mortality and morbidity in human genetic studies. However, to date no information is available as to what the function of FSAP may be in the context of stroke. Normally, poor outcome in stroke is associated with blood brain barrier dysfunction and secondary microinfarctions or the absence of a neuroprotective agent which finally culminates into edema formation and mortality. We have analyzed the pathophysiological role of FSAP in stroke using in-vitro cell culture based models and in-vivo using FSAP $^{-/-}$ mice. Thus, the specific aims of this thesis were:

1. *Determine if FSAP can cross through the blood brain barrier by in-vitro model and if it influences permeability under conditions mimicking stroke; identification of this will be helpful to understand if FSAP can reach the neurons and astrocytes and if it regulates BBB permeability;*
2. *To investigate the effect of FSAP on cell death/ apoptosis of primary cortical astrocytes under hypoxia reperfusion injury conditions;*
3. *Elucidate the effect of FSAP on cell death/ apoptosis of primary cortical neurons under excitotoxicity and ischemia reperfusion injury;*
4. *Examine the role of FSAP in-vivo using murine thromboembolic stroke model using FSAP $^{-/-}$ mice.*

.

3. Materials & Methods

3.1. Human plasma FSAP.

The preparation of FSAP and Phe-Pro-Argchloromethylketone (PPACK)-inactivated FSAP from human plasma has been described before (Roedel et al., 2013).

3.2. Primary Cell culture

3.2.1 Neurons

Cortical neurons were prepared from fetal mice (E15-E16). Dissociated cortical cells were resuspended in Dulbecco's modified Eagle's medium (DMEM) supplemented with 5% (vol/vol) fetal bovine serum, 5% (vol/vol) horse serum, and 1 mM glutamine, and plated in 24-well dishes previously coated with poly-D-lysine and laminin. After 3 days, the cells were exposed to 10 uM Ara-C to inhibit glial proliferation. Cultures were used after 14 DIV for excitotoxicity and hypoxia assays. Cultures from 3 different isolations were stained with neuronal nuclei antibody (Anti NeuN, MAB377, Millipore, MA, USA) and 95% of the cells were identifiable as neurons.

3.2.2 Astrocytes

Primary astrocytes were prepared as described elsewhere (Gorina et al., 2009). Following isolation of cortices and removal of the meninges, dissociated cells were suspended in Dulbecco's Modified Eagle's Media (DMEM) F12 containing 20% fetal bovine serum (FBS) and 0.25% gentamycin, and plated on 10 mm dish pre-coated with 0.1 mg/ml poly-L-lysine. Cultures were maintained for 14 days to generate a confluent glial culture. Prior to trypsinization, contaminating microglial cells were separated by mechanical agitation and removed by subsequent washing in Hank's Balanced Salt Solution (HBSS). Astrocytic monolayers were then dislodged from flasks by trypsinization (0.25% trypsin in HBSS and 1 mM EDTA). Cells were seeded in either 24 well plates (1×10^5 cells/well) or 75 cm^2 flasks (5×10^5 cells/flask) and grown for 14-16 days until confluent prior to stimulation. Cultures were routinely more than 95% pure astrocytes when assessed by glial fibrillary acidic protein (GFAP) immunostaining.

3.2.3 Primary mouse brain microvascular endothelial cells (pMBMECs)

pMBMECs were isolated from 4- to 6-week old C57BL/6 mice, cultured in DMEM, 20% (vol/ vol) FCS, 1 mmol/L sodium pyruvate, 1% (vol/ vol) minimal essential medium nonessential amino acids, 50 ug/mL gentamycin, and 1 ng/mL basic fibroblast growth factor (bFGF) as exactly as described before (Gorina et al., 2013). During the first 48h, the media was supplemented with the translator inhibitor puromycin at 4μg/mL to obtain higher pMBMEC purity. Forty-eight hours after seeding, pMBCEC monolayers growing on the inserts were set in the 24-well culture plates containing the astrocytes. The medium was changed and the media used for luminal and the abluminal compartments (co-culture medium) consisted of DMEM with 10% FBS (PAA), 2X NEAA, 2X NaPyr, gentamycin (Gibco-BRL) with bFGF. Once the cells were in co-culture, the medium was renewed every two days. Under these conditions, pMBCECs migrated from digested microvessels reached confluence about 4 days after plating. Experiments were carried out 4-5 days after setting up the co-culture.

3.3. Permeability assay

Permeability assays were performed in triplicate as published previously (Coisne et al., 2005). pMBMECs were grown to confluence on matrigel coated filter inserts, washed with wash buffer (HBSS, 10% FCS, 25 mmol/L Hepes pH 7.2 to 7.5) and permeability to AlexaFluor-680-dextran (3 kDa, 10 μg/mL, LuBioScience, Luzern, Switzerland) was measured in the presence of the assay medium (DMEM, 5% FCS, 4 mmol/L -glutamine, 25 mmol/L Hepes pH 7.2 to 7.5). Endothelial permeability was specifically measured at 2 and 24 hours of reoxygenation after OGD. Diffused AlexaFluor-680-dextran was quantified using the Odyssey Infrared Imaging System (LI-COR, Bad Homburg, Germany). To measure diffusion of FSAP across the BBB, FSAP was added to the luminal side. Medium from the abluminal side of the insert was removed at the indicated times and analysed by ELISA.

3.4. FSAP ELISA

Microtiter plates were coated with a rabbit polyclonal anti-FSAP Ab (5 μg/ml) and blocked with 3% (wt/vol) BSA, 0.1% (wt/vol) Tween 20 in TBS. Cell supernatants were incubated for 1 hour at RT. After extensive washing, anti-FSAP

mAb 570 (2 ug/ml) was added and incubated (1 hour, RT). It was followed by incubation of peroxidase-coupled mouse Ab. The resolution of the ELISA was done using 3,3‘,5,5‘-Tetramethylbenzidin (TMB-Substrate-Kit, Pierce, Rockford, Il, USA) and the optical density was measured at 405 nm using microplate reader EL808 (Biotek Instruments, Winooski, OR, USA). Using a standard curve with Standard Human Plasma from Siemens Diagnostics (Marburg, Germany), the concentration of FSAP across the BBB was calculated.

3.5. NMDA mediated Excitotoxicity

Excitotoxicity was induced at 37°C by a 24 hour exposure to 12.5 uM NMDA in DMEM supplemented with glycine (10 uM). Neuronal death was quantified by measurement of lactate dehydrogenase (LDH) release by damaged cells into the bathing medium. The LDH level corresponding to complete neuronal death was determined in parallel cultures exposed to 200 uM NMDA for 24 hours in DMEM supplemented with glycine. Background LDH levels were determined in parallel cultures subjected to sham wash and subtracted from experimental values to yield the signal specific to experimentally induced injury.

3.6. Oxygen-glucose deprivation injury in neurons and astrocytes

Primary astrocytes were subjected to oxygen glucose deprivation (OGD) by adding OGD medium containing glucose- and serum-free DMEM (OGD medium-1) and placed for 6 h under 1%O_2, 5% CO_2, 37 °C in a CO2 incubator (Innova CO-48; New Brunswick 210 Scientific, USA) for 6h followed by a period of 24 h under 20% O_2, 5%, CO_2, 37 °C (reoxygenation) in fresh medium containing DMEM with glucose supplemented with 1X NEAA, 1X NaPyr and reoxygenation medium - 1.

Primary neurons were incubated in OGD medium-1 for 2 h at 1%O_2, 5% CO_2, 37 °C in a CO_2 incubator followed by 24 h (reoxygenation) under 20% O_2, 5%, CO_2, 37 °C (reoxygenation) in fresh reoxygenation medium – 1.

3.7. Oxygen-glucose deprivation injury in BBB

For the BBB experiments, co-cultures were subjected to OGD by adding a OGD medium and placed for 6 h in an anoxic atmosphere using GasPack EZ bags (Becton Dickinson, Sparks, MD, USA). The cells were washed in OGD medium-2 containing glucose and serum free DMEM, Hepes 25nM and gentamycin After the

OGD period media was changed for fresh reoxygenation medium-2 containing DMEM with glucose supplemented with 1X NEAA, 1X NaPyr, 25mM Hepes and gentamicin. For normoxic controls, cells were exposed to DMEM containing glucose with Hepes 25mM and gentamicin during the OGD period and after that, media was changed for reoxygenation medium.

3.8. Transient H_2O_2 injury

Cultured cells were incubated at 37°C with fresh serum-free culture medium in the absence or presence of H_2O_2 (250 μM) for 3 h. After the H_2O_2 treatment, medium was changed and different inhibitors were added for 24 h.

3.9. Total RNA isolation and real-time PCR

Total RNA was extracted using the Total RNA Miniprep kit (Sigma Aldrich (Taufkirchen, Germany). Reverse transcription was performed using the High Capacity cDNA reverse transcription kit (Applied Biosystems, Germany). Quantitative real-time PCR was performed using the SensiMix SYBR kit (Bioline GmbH, Luckenwalde, Germany), and fluorescence of amplified DNA was detected by the Step One Plus real-time PCR system (Applied Biosystems, Germany). The temperature program of DNA amplification was as follows: cDNA denaturation at 95 °C for 15 s, primer hybridization at 60 °C for 30 s, and elongation at 72 °C for 30 s. The amplification plot was monitored over 40 cycles, and continuous fluorescence measurement indicated mRNA expression of analyzed genes. Fluorescent threshold cycles (*Ct*) were set and normalized against *Ct* of housekeeping gene GAPDH (Δ*Ct*). Subsequently, expression of the target gene was controlled with the reference probe, and target *Ct* was calculated as $2^{-\Delta\Delta Ct}$. Data is thus expressed as fold change compared to unstimulated cells.

3.10. Caspase 3/7 activity assay

Caspase-3 is activated in the apoptotic cell both by extrinsic (death ligand) and intrinsic (mitochondrial) pathways. The caspase-3 zymogen has virtually no activity until it is cleaved by an initiator caspase after apoptotic signaling events have occurred especially after ischemic insult. Hence, Caspases-3/7 activities were measured using Caspase 3/7 homogeneous according to manufacturer's protocol (Promega, USA). In brief, at the end of treatment, neurons and astrocytes were

washed with PBS and 300 µL of caspase- 3/7 reagent was added to each well and the cells were scraped and collected in a microfuge tube in dark. The cell lysate was incubated in dark for 30 min and the resultant fluorescence was measured. The results are expressed as fold change in Caspase 3/7 activity from control.

3.11. Viability assays

Cell death was quantified by measurement of the activity of lactate dehydrogenase (LDH) released from damaged cells into the supernatant with a kit (Roche Diagnostics, Mannheim, Germany). In addition, cytotoxicity was also quantified by measurement of the reduction of 3-(4, 5-dimethylthiazol-2-yl) 2, 5-diphenyl-tetrazolium bromide (MTT) (Sigma Aldrich, Taufkirchen, Germany) to produce a dark blue formazan product. This assay assesses the integrity of mitochondrial function. MTT was added to each culture well at a final concentration of 0.5% MTT solution (wt/vol). After incubation for 4 hours at room temperature, the medium was moved, and cells were dissolved in 150 µL DMSO for 1 hour. The formation of formazan was measured by reading absorbance at a wavelength of 570 nm with a reference setting of 630 nm on a microplate reader EL808 (Biotek Instruments, Winooski, OR, USA).

3.12. DNA fragmentation by terminal deoxynucleotidyl transferase-mediated dUTP nick end labeling (TUNEL) assay

TUNEL staining was performed with the Fluorescein *In Situ* Cell Death Detection Kit (Roche, Mannheim, Germany) according to the manufacturer's instructions. Cells were fixed with 4% (vol/ vol) formaldehyde in PBS pH 7.4 for 30 minutes and permeabilized by 0.5% (wt/ vol) Triton X-100 in TBS. DNA strand breaks were labeled with digoxigenin-deoxy-UTP using terminal deoxynucleotidyl transferase (TdT, 0.18 U/µL) using manufacturer’s protocol. The incorporation of nucleotides into the 3′-OH end of damaged DNA was detected with an anti-digoxigenin-fluorescein antibody. Slides were mounted with mounting medium for fluorescence containing DAPI for DNA staining and visualized in a fluorescence microscope. Negative control slides were incubated in absence of TdT.

3.13. Preparation of Cell Extracts and Western Blotting

Cell extracts were prepared in lysis buffer containing 200 mM HEPES at pH 7.4, 100 mM NaCl, 100 mM NaF, 1 mM Na_3VO_4, 5 mM EDTA, 1% Triton-X-100 and a protease inhibitor cocktail (COMPLETE™, Roche, Basel, Switzerland). Cells were left for 20 minutes on ice in lysis buffer. Subsequently, we obtained the cell extract and we added Laemmli sample buffer. Samples were boiled for 10 min and resolved by Tris/Glycine SDS-Polyacrylamide gel electrophoresis. Proteins were transferred onto PVDF membrane (GE Healthcare, Frankfurt, Germany). The membranes were incubated overnight with primary antibodies diluted in 5% nonfat milk (wt/ vol) or 5% BSA (wt/ vol) in TBS, and then washed and incubated with a HRP-secondary antibody for 1 hr. The relative abundance of proteins was determined by scanning densitometry and expressed relative to control groups and reference proteins that were arbitrarily assigned as 1.

3.14. Immunocytochemistry

8-well chamber slides (Nunc, Wiesbaden, Germany) containing cortical astrocytes or neurons were fixed in 4% buffered PFA in phosphate-buffered saline (PBS; Sigma-Aldrich). Fixed cells were permeabilized and blocked (1% BSA and 0.1% Triton-X in PBS) at room temperature for 1 h before overnight incubation at 4°C with Glial fibrillary acidic protein (GFAP) or neuron-specific nuclear protein (NeuN/ Neuronal Nuclei) antibody. Following primary incubation, the slides were incubated in the appropriate Alexa Fluor-conjugated secondary antibodies (Invitrogen) for 1 h at room temperature. Following secondary incubation, slides were sealed with mounting solution (Sigma-Aldrich) on cover-slips.

Confluent pMBMEC grown on trans-well inserts were washed in Tris-buffered saline (TBS) and exposed to test substances as described above for permeability assays (Gorina et al., 2013). Cells were fixed with 1% (wt/vol) paraformaldehyde in phosphate-buffered saline for 10 minutes at room temperature and blocked with blocking buffer (5% skimmed milk (wt/vol), 0.3% Triton X-100 (vol/vol) and 0.04% (wt/vol) NaN_3 in TBS) for 30 min at RT. The inserts were then incubated with rabbit anti-mouse ZO-1 (617300, Invitrogen, 1:100) 1h. After washing, cells were incubated for 60 min with Alexa Fluor 488-conjugated goat anti-rabbit IgG (Molecular Probes, Eugene, OR, USA, 1:1000), and mounted with

Mowiol. Pictures were taken using a fluorescence microscope (Leica DMRB, Leica Microsystems, Wetzlar, Germany).

3.15 Animal housing conditions and ethical considerations

Male (10–14 weeks) C57/ BL6 (Janvier, France) and $FSAP^{-/-}$ mice, backcrossed atleast 10 generations, were housed in a temperature-controlled room on a 12 hour light/12-hour dark cycle with food and water ad libitum. Experiments were performed at Cyceron, Caen France, in collaboration with Prof. Denis Vivien and Dr. Cyrille Orset. Experiments were in accordance with French ethical laws (act no. 87–848; Ministe`re de l'Agriculture et de la Foreˆt) and European Communities Council Directives of November 24, 1986 (86/609/EEC) guidelines for the care and use of laboratory animals.

3.16. Induction of Ischemic stroke and Physiological Monitoring

Mice were randomized, and experiments were performed as described before (Orset et al., 2007) in a blinded fashion. Animals were deeply anesthetized with isoflurane 5% and, thereafter, maintained with 2.5% isoflurane in a 70%/30% mixture of NO_2/O_2. MCA occlusion was induced by thrombin injection, as described elsewhere. Briefly, the skin between the right eye and the right ear was incised and the temporal muscle was retracted. To expose the MCA, a small craniotomy was performed and the dura mater was excised. A micropipette was introduced into the lumen of the MCA and 2 μL (1.5 U) of purified murine alpha-thrombin (Haematologic Technologies, Vermont, USA) was injected to induce the formation of a clot. Ten minutes after injection the clot had stabilized and the micropipette was removed. After surgery the incision wound was sutured. Rectal temperature was maintained at 37 ± 0.5°C throughout the surgical procedure using a feedback-regulated heating system.

3.17. Monitoring of Cerebral Blood Velocity by Laser Doppler Flowmetry

Cerebral blood velocity was determined by laser Doppler flowmetry using a fiberoptic probe (Oxford Optronix) glued to the skull in the MCA territory. Cerebral blood velocity was measured before the injection of alpha-thrombin (100% baseline) and throughout the duration of the experiment (60 minutes).

3.18. Stroke assessment by magnetic resonance imaging

Magnetic resonance imaging (MRI) was performed 24h after stroke on a dedicated 7T MR small animal imaging system (ClinScan, Bruker, Ettlingen, Germany). The animals were anesthetized with 1.5-2% isofluran and positioned into the magnet with a laser-controlled system for the animal cradles. Respiratory frequency and body temperature were monitored throughout the experiment and the latter was maintained with a water heating pad. The image protocol comprised T2-weighted imaging and diffusion-weighted imaging (DWI). To calculate infarct volume as the percentage of hemisphere that is infarcted (% of infarcted hemisphere), we estimated the volume of the contralateral hemisphere (CH) and that of the non-lesioned ipsilateral hemisphere (NLH). The percentage of infarcted hemisphere was then calculated using the formula = (CH-NLH/CH) X 100. Volume was normalized by edema index, which is the ratio between the volume of the contralateral and ipsilateral hemisphere.

3.19. Angiography

Magnetic resonance angiographies (MRA) were performed using a 2D-TOF sequence (TE/TR 10/50 ms). Analyses of the MCA MRA were performed blinded to the experimental data using the following score: 2: normal appearance, 1: partial occlusion and 0: complete occlusion of the MCA.

3.20. Laser Speckle Flowmetry (LSF)

Laser speckle perfusion imaging of the brain was performed using moorFLPI2, Full-Field Laser Perfusion Imager (Moor Instruments, Devon, UK) according to the manufacturer's instructions and as described previously (Manwani et al., 2013). Briefly, a midline scalp incision was made, the skull was exposed and the charge coupled device camera of LSF was installed 30 cm above the skull using an articulating arm. Complete hemispheres were used to evaluate the relative cerebral perfusion. The imaging was set up at a display rate of 25 Hz, time constant of 1 second, and a camera exposure time of 4 milliseconds.

3.21. Neuroscore

Neurological evaluation was performed 24 hours after induction of ischemia and scored on a 6-point scale. 0 = no apparent deficit, 1 = contralateral forelimb

flexion; 2 = decreased grip of contralateral forelimb grip while tail pulled; 3 = spontaneous movement in all directions, contralateral circling only if pulled by tail; 4 = spontaneous contralateral circling; 5 = no movement.

3.22. Mouse Brain Extracts for SDS page

Animals were euthanized 24 hours post stroke induction and brains were directly prepared in cold PBS. Hemispheres were separately homogenised mechanically in homogenisation buffer (140 mM NaCl; 20 mM Tris-HCl pH 7,6; 5 mM EDTA; 16 complete protease inhibitors) and extracts additionally sonicated for 30 s. Resulting extracts were centrifuged (6000 rpm) for 10 min at 4^0C. Supernatants were further centrifuged (14000 rpm) for 10 min at 4^0C.

3.23. Mouse Plasma FSAP activity

Total FSAP activity was measured by an immunocapture activity test using the buffers and procedures as described, with minor modifications. Microtiter plates were coated with 10µg/ml anti-FSAP mouse polyclonal antibody *(MENEW)* in coating buffer (15 mM Na_2CO_3, 35 mM $NaHCO_3$, pH 9.6), followed by blocking with standard buffer (20 mM Na-citrate, 150 mM NaCl, 100mM Arginin, pH 6.0) containing 3% BSA (wt/vol). Plasma probes were diluted (1:100) in a standard buffer (see above) containing 0.1% Tween 80 (wt/vol), 1% BSA (wt/vol) and 100U/ml unfractionated heparin (Liquemin, Roche, Grenzach, Germany) and applied on the plate, incubated for 1 hour at room temperature (RT) and washed three times. Recombinant single-chain uPA (10µg/ml Saruplase, Grünenthal, Stolberg, Germany in TBS with 0.1% Tween 80 /wt/vol), 2 mM $CaCl_2$, pH 7.2) was added and incubated for 5 min followed by chromogenic substrate S-2444 (2 mM) (Haemochrome, Essen, Germany) and further incubated (37°C). Absorbance at 405 nm was recorded every minute with microplate reader EL808 (Biotek Instruments, Winooski, OR, USA) over 1 hour (37°C). The maximal velocity (substrate turnover with time) over 8 min was determined and this was invariably always the initial reaction velocity. For the assay, calibration curves were established through a dilution series of Standard Human Plasma (SHP, Siemens Diagnostics, Marburg, Germany). SHP served as reference for the measured FSAP activity, which was defined as 1 plasma equivalent unit (1000 mU/ml).

3.24. Statistics

Generally each *in-vitro* experiment was performed in duplicates on at least 3 different isolations of cells from independent cell culture preparations. Results are presented as means ± S.D. Between-group comparisons were performed with one-way ANOVA and Tukey post-test. One-way ANOVA and post hoc Tukey's multiple comparison test. *P<0.05 **P<0.01 and ***P< 0.001 indicate statistically significant differences. Number of animals in each experiment and the statistical significance are presented in figure legends.

4. Results

4.1. FSAP can cross the BBB and protects the endothelial barrier integrity upon oxygen glucose deprivation (OGD) and reoxygenation-injury

To determine the effect of FSAP on the BBB permeability after an ischemic insult, we used primary mouse brain microvascular endothelial cells (pMBMECs) in co-culture with primary mouse astrocytes as an *in-vitro* model of the BBB (Enzmann et al., 2013). We observed that addition of FSAP (100nM) on the luminal endothelial side decreased the OGD/reoxygenation-induced permeability of the BBB as shown by a reduction in the permeability coefficient for 3KDa labeled-dextran (Figure 4.1 A). FSAP also reduced the release of LDH after OGD followed by 24 h of reoxygenation suggesting that FSAP could protect the endothelial cells against oxidative stress-related cell death (Figure 4.1 B). FSAP was able to cross BBB under normoxic conditions and increased passage was observed after OGD/ reoxygenation (Figure 4.1 C,D). Thus, FSAP decreased the permeability of the *in-vitro* BBB under conditions that mimick stroke followed by reperfusion. Surprisingly, although FSAP decreased permeability, the passage of FSAP itself was higher under conditions of OGD/reoxygenation.

We then analyzed Zonula occludens-1 (ZO-1) expression by staining as it is a junctional protein that regulates endothelial permeability (Fischer et al., 2002; Zehendner et al., 2011). We observed that its localization in endothelial junctions was altered after OGD/reoxygenation, but in the presence of FSAP the junctional localization of ZO-1 was preserved (Figure 4.1 E). Inhibition of the FSAP proteolytic activity with the protease inhibitor Aprotinin completely blocked the protective effect of FSAP after OGD/reoxygenation (Figure 4.1). ZO-1 expression is a surrogate marker of endothelial cell permeability and its organized junctional distribution is disturbed by OGD/ reoxygenation. FSAP prevented this disruption of ZO-1 expression, suggesting a protective effect on barrier function.

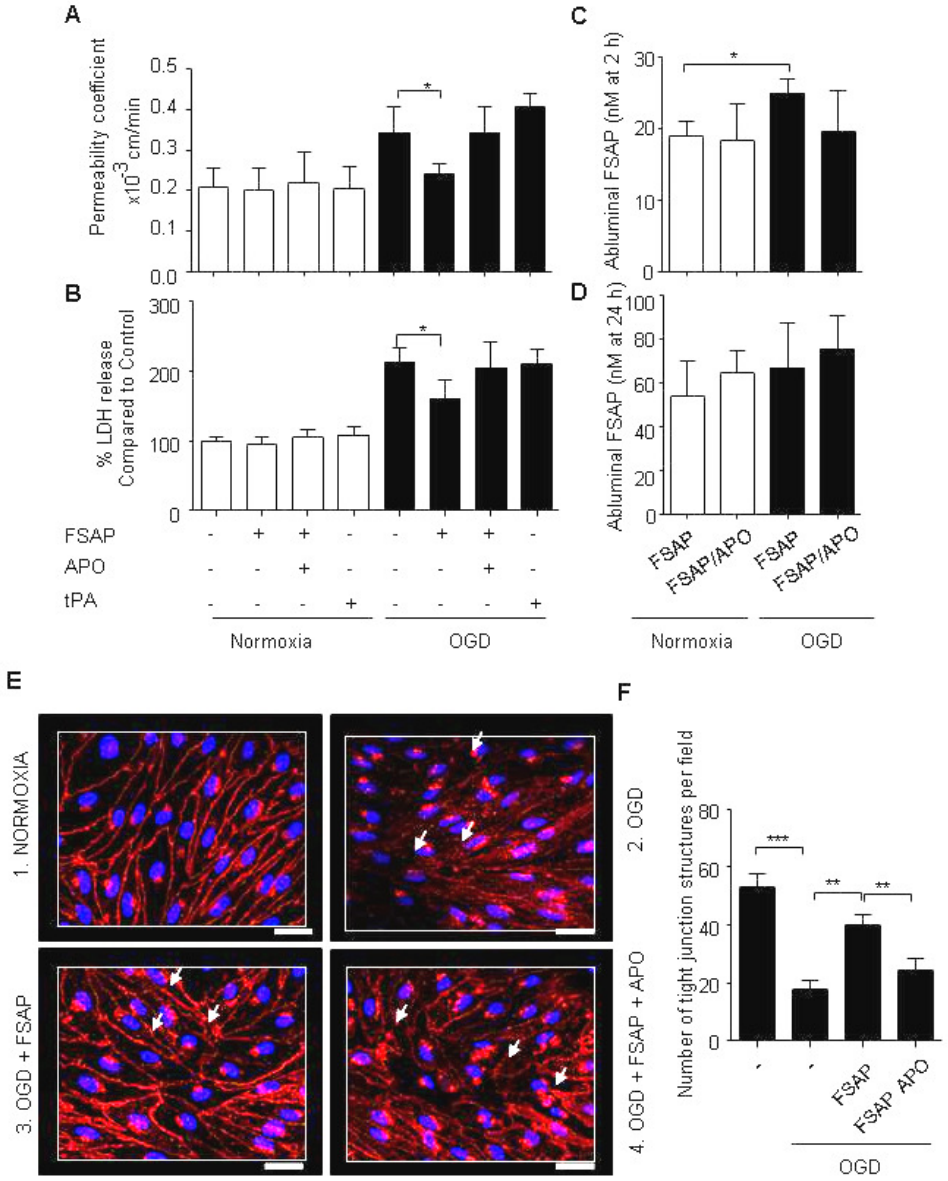

Figure 4.1: ***FSAP treatment protects the blood-brain barrier integrity during OGD/reoxygenation injury in-vitro.***

A. Effect of treatment with FSAP (100 nM) after normoxia (white bars) or OGD/reoxygenation (OGD) (black bars) on pMBMEC permeability. Aprotinin (APO) (10 µg/ml) and tPA (20 µg/ml) were used to demonstrate the specificity of the FSAP protective effect. **B**. FSAP protected pMBMEC from OGD/reoxygenation-induced cell death as quantified by LDH release. **C-D.** FSAP was added on the BBB endothelial luminal side at the beginning of the reoxygenation phase and its concentration was measured by ELISA in the abluminal side after 2 hours (C) or 24 hours of reoxygenation (D). **E**. Immunofluorescence staining for ZO-1 in pMBMECs grown in co-culture with astrocytes. ZO-1 distribution under normoxic conditions **(1)**, after OGD/reoxygenation **(2)**, in the presence of FSAP after OGD/reoxygenation **(3)** and FSAP in the presence of Aprotinin after OGD/reoxygenation **(4).** Mean ± SD, n ≥ 3 independent cultures in duplicates. One-way ANOVA and post hoc Tukey's multiple comparison test. *P<0.05 indicates statistically significant differences.

4.2. FSAP decreases cell death after OGD/reoxygenation in astrocytes

Astrocytes are known to play a critical role in the progression of ischemic stroke. After injury, astrocytes form a glial scar which helps to isolate the necrotic tissue from the rest. Multiple studies have shown the beneficial effects of astrocytic protection in improving the stroke outcome as they provide support to neurons. Hence we decided to see if FSAP could induce a protective effect on astrocytes exposed to ischemic insult. Cortical astrocytes in culture were exposed to OGD (6 hours) followed by 24 hours of reoxygenation with glucose. This has been used as a model to mimick the clinical situation wherein ischemia is followed by reperfusion that leads to cell death.

Treatment with FSAP prevented cell death in hypoxic astrocytes as measured by LDH release (Figure 4.2A) and mitochondrial-function assay (Figure 4.2B). We then evaluated the levels of apoptosis in the presence of FSAP by measuring the number of TUNEL-positive apoptotic cells and the enzymatic activity of caspase-3/7. OGD/reoxygenation induced activation of caspase-3/7 (Figure 4.2C) and the number of cells undergoing apoptosis (Figure 4.2D, 4.2E) was reduced in the presence of FSAP. Inhibition of FSAP activity by the serine protease inhibitors, PPACK and Aprotinin (Figure 4.2), inhibited the anti-apoptotic effect of FSAP. As in the case of pMBMECs, we observed that FSAP inhibited cell death and apoptosis in astrocytes. These effects also required the proteolytic activity of FSAP.

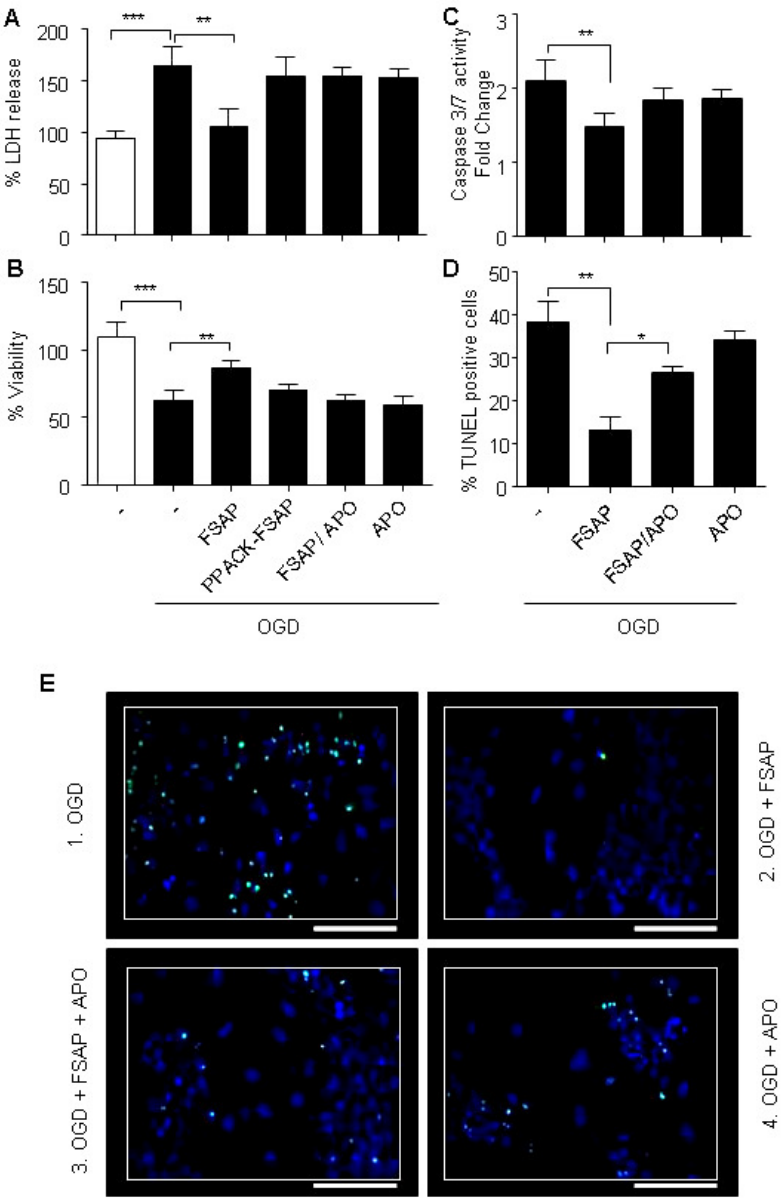

Figure 4.2: ***FSAP protects astrocytes from OGD/reoxygenation injury.***
A-B. Effect of FSAP or PPACK-FSAP (100 nM) in astrocytes after 24 h of OGD/reoxygenation (OGD) (black bars) on cell survival was quantified by LDH (A) and MTT reduction assay (B). White bars represent normoxic untreated controls. **C.** Caspase-3 activity astrocytes after 12 h of reoxygenation in the presence or absence of FSAP and/or Aprotinin (APO) (10 µg/ml) and quantified relative to untreated control. **D.** The number of apoptotic TUNEL-positive cells were quantified as described in the Methods. Fold change was calculated relative to untreated control. **E.** Representative fluorescent-TUNEL (green)/dapi (blue) staining in mouse cortical astrocytes 24 h after OGD treatment in the presence or absence of FSAP and/ or Aprotinin. Mean ± SD, $n \geq 3$ independent cultures in duplicates. One-way ANOVA and post hoc Tukey's multiple comparison test. *P<0.05 **P<0.01 and ***P< 0.001 indicate statistically significant differences.

4.3. Activation of **PI3K-Akt** *signaling pathway by FSAP protects astrocytes from OGD/reoxygenation-mediated cell death*

Cell death was prevented by FSAP as measured by LDH release (Figure 4.3.1A) and mitochondrial function test (Figure 4.3.1B) in a concentration-dependent manner (12.5 nM – 100 nM), with maximal antiapoptotic effect at 100 nM. Since the PI3K-Akt pathway has been implicated to be the most important pathway in regulating the apoptotic response to hypoxia (Li et al., 2013), we measured if FSAP was able to induce phosphorylation of Akt on Ser^{473}. We observed that FSAP was able to activate the PI3K-Akt signaling pathway in a concentration-dependent manner (Figure 4.3.1C). Inactivation of FSAP with either PPACK or Aprotinin removed the protective effects induced by FSAP mediated Akt phosphorylation (Figure 4.3.2.A,B).

To further validate our observations that FSAP induced Akt phosphorylation, LY294002 (10 μM) or Wortmannin (0.5 μM), inhibitors of PI3K-dependent Akt signaling, were added to the cultures 1 h before OGD exposure. LY294002 and Wortmannin both blocked FSAP-mediated phosphorylation of Akt as well as FSAP-mediated cell protection (Figure 4.3.1D & 4.3.1E) indicating the requirement of PI3K-dependent Akt signaling pathway. Only active FSAP was able to induce potent Akt phosphorylation at all measured time points (Figure 4.3.2.A,B). This data suggests that the activation of PI3K-Akt by only active FSAP is ultimately responsible for the antiapoptotic effect in cultured astrocytes challenged with OGD.

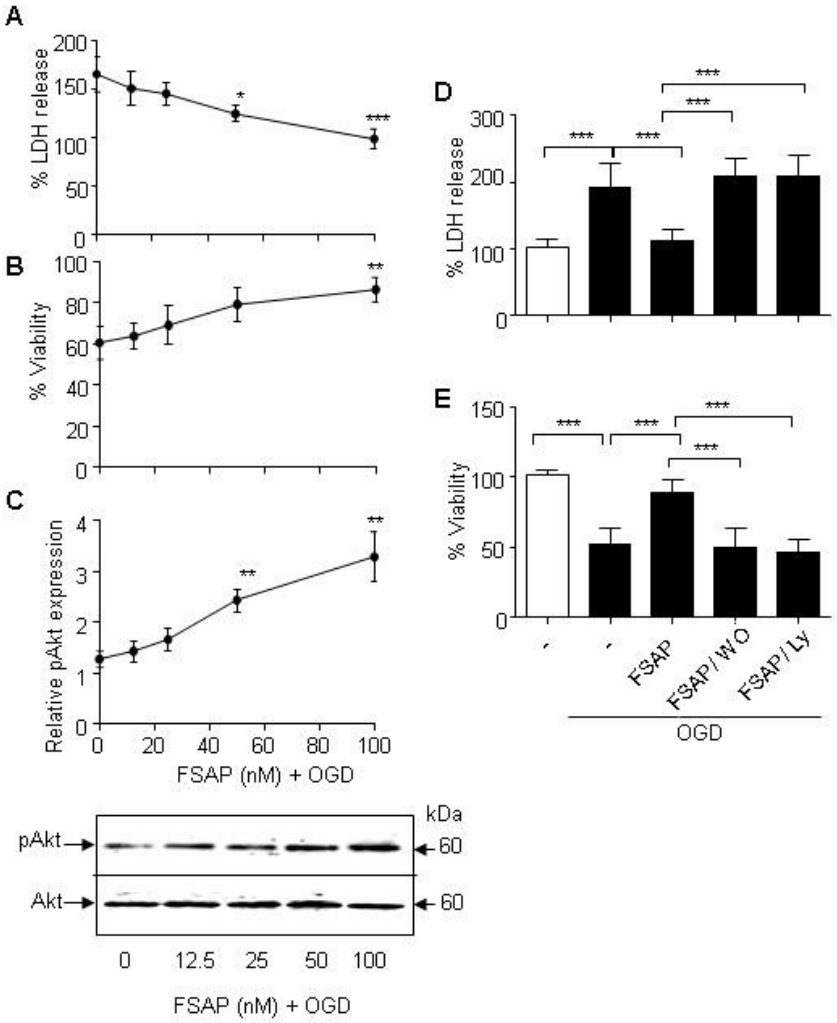

Figure 4.3.1: ***FSAP reduces cell death in OGD/reoxygenation astrocytes via the* PI3K-AKT *pathway.***

A-B. LDH release (A) and mitochondrial function (B) were quantified in astrocytes subjected to OGD and treated with FSAP (0-100 nM) during the reoxygenation phase for 24h. Values relative to normoxic cells (100%). **C.** Western blots for pAkt (Ser473) and total Akt in whole-cell extracts. Intensity of pAkt signal was measured by scanning densitometry and normalized to total Akt at 24 hours. Fold change was calculated relative to untreated control. **D-E.** Survival of mouse cortical astrocytes 24 h after OGD/reoxygenation in the presence or absence of FSAP (100 nM), LY294002 (10 μM) or Wortmannin (0.5 μM) was measured using LDH release assay (D) and MTT reduction assay (E) . LY294002 (LY) and Wortmannin (WO) were added to the culture supernatant 1 h before OGD (OGD, black bars). Mean ± SD, n ≥ 3 independent cultures in duplicates. One-way ANOVA and post hoc Tukey's multiple comparison test. *P<0.05 **P<0.01 and ***P< 0.001 indicate a statistically significant differences.

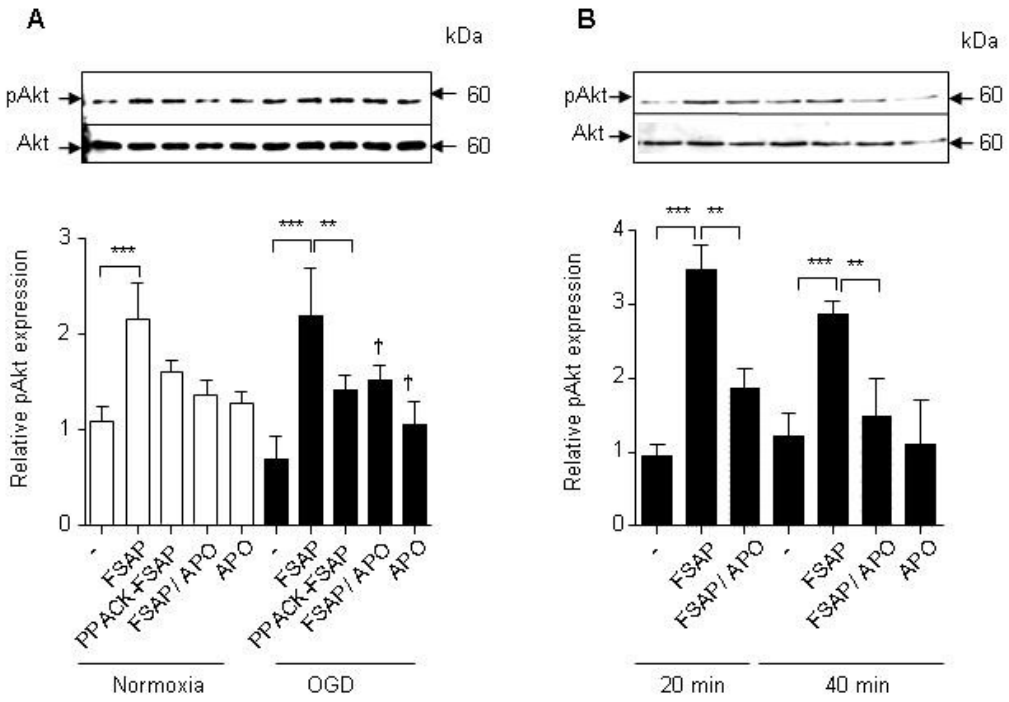

Figure 4.3.2: ***FSAP activates Akt phosphorylation in normoxic and hypoxic astrocytes.***
(A). Representative western blot of the effect of FSAP or PPACK- FSAP (100nM) in the absence or presence of Aprotinin (APO) (10 µg/ml) on Akt phosphorylation in astrocytes under normoxic and OGD/ reoxygenation for 24 h. (B) Same as (A) except that Akt phosphorylation was determined at 20 and 40 mins after reoxygenation. Intensity of pAkt signal was measured by scanning densitometry and normalized to total Akt at each of the control time points. Mean ± SD, n ≥ 3 independent cultures in duplicates. One-way ANOVA and post hoc Tukey's multiple comparison test. *P<0.05 **P<0.01 and ***P< 0.001 indicate statistically significant differences.

4.4. FSAP treatment also modulates p53 and Bcl-2 expression downstream of Akt phosphorylation

After ischemic injury, it is known that there is an increase in p53 levels which further potentiate cell death response. It has been described that there exists a cross-talk between Akt and p53 which plays a critical role in cell survival after ischemia (Li et al., 2013). Also, it has been previously reported that restoring the levels of anti-apoptotic Bcl-2 shifts the cellular response towards survival. Promoting Akt phosphorylation has been implicated to also up regulate Bcl-2 levels, further enhancing the cell survival response (Pugazhenthi et al., 2000; Bratton et al., 2010). Since we observed that FSAP treatment robustly induced Akt phosphorylation, we investigated further if FSAP treatment affected OGD/reoxygenation-mediated p53 induction. FSAP reduced p53 expression dose dependently on astrocytes exposed to

OGD/reoxygenation (Figure 4.4A). Next, we checked if FSAP induced Akt phosphorylation had any effect on Bcl-2 expression. FSAP treatment indeed increased Bcl-2 protein (Figure 4.4A) after OGD/ reoxygenation injury in astrocytes. Thus, FSAP could prevent cell death by activating the PI3K/ Akt pathway that in turn influences the activity of p53 and Bcl proteins.

4.5. The FSAP induced protective effect involves activation of protease-activated receptor-1 (PAR-1)

Activated Protein C and Thrombin mediated cleavage of PARs leads to the activation of PI3K's and promotes Akt phosphorylation in neurons, astrocytes and endothelial cells (Resendiz et al., 2007; Mosnier et al., 2012). Since it has been previously reported that FSAP can signal through PAR-1 receptor on endothelial cells (Mambetsariev et al., 2010) and PAR-1 is expressed on astrocytes, we checked if the FSAP-induced protection was mediated through the astrocytic PAR-1 receptor.

In the presence of SCH 79797, a strong, selective non-peptide PAR-1 antagonist, FSAP was unable to reduce cell death as measured by LDH release and mitochondrial function assay (Figure 4.4B & 4.4C). We also observed that FSAP induced Akt phosphorylation was blocked by treatment with SCH79797, indicating that PAR-1 is a receptor necessary for the protective effect of FSAP (Figure 4.4D).

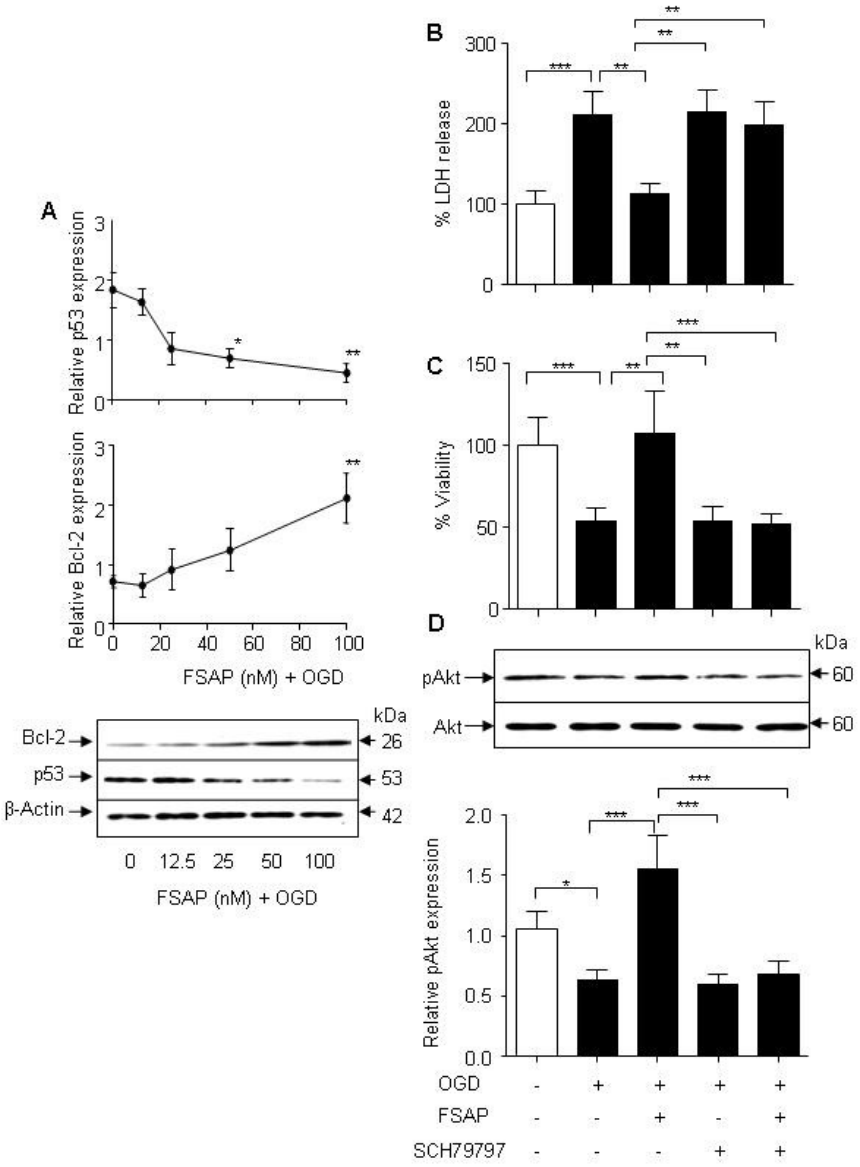

Figure 4.4: ***FSAP inhibits cell death after OGD/reoxygenation by regulating p53 and Bcl-2 expression via the PAR-1 receptor in astrocytes.***

A. Western blots for p53, Bcl-2 and β-actin in whole-cell extracts from astrocytes after 2 h of reoxygenation in the presence of FSAP (0-100 nM). Intensity of p53 and Bcl-2 signal was measured by scanning densitometry and normalized to β-actin. Relative expression in normoxic cells was set as 1. **B-C.** Survival of astrocytes 24 h after reoxygenation in the presence or absence of FSAP (100 nM) and SCH 79797 (5μM) was measured using LDH release assay (B) and MTT reduction assay (C). **D.** Representative Western blot for pAkt (Ser473) and total Akt in whole-cell extracts from the same experiment. Intensity of pAkt signal was measured by scanning densitometry and normalized to total Akt at 2 hours. SCH79797 was added to the culture 20 min before OGD exposure. Mean ± SD, $n \geq 3$ independent cultures in duplicates. One-way ANOVA and post hoc Tukey's multiple comparison test. *P<0.05 **P<0.01 and ***P< 0.001 indicate statistically significant differences.

4.6. FSAP modulates the expression of anti-inflammatory genes after OGD/reoxygenation in *astrocytes*

Since astrocytes play a critical role in regulation inflammation post ischemia in stroke, we investigated if FSAP influenced the expression of inflammatory genes. We observed the FSAP significantly increased the mRNA expression of anti-inflammatory IL-10 and IL-4 genes while down regulating the expression of pro-inflammatory COX-2 and IL-6 genes after OGD/reoxygenation injury indicating an anti-inflammatory role for FSAP (Figure 4.5). Similarly, FSAP decreased TNF-α expression after OGD/reoxygenation in astrocytes. Thus, FSAP could alter the inflammatory phenotype developed by ischemic astrocytes by promoting the expression of anti-inflammatory genes thereby reducing inflammation induced secondary cell death.

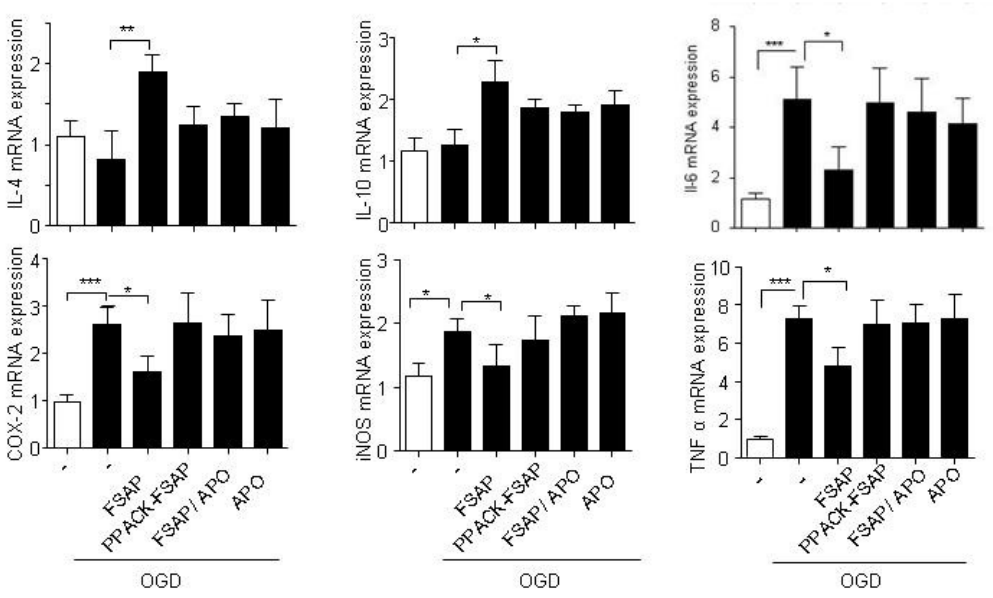

Figure 4.5: ***FSAP treatment alters the mRNA expression profile of anti-inflammatory genes in astrocytes.***
mRNA expression of different inflammatory genes was measured 24 hours after OGD/ reoxygenation in astrocytes. FSAP, PPACK-FSAP, Aprotinin were added as described in earlier sections. Mean ± SD, n ≥ 3 independent cultures in duplicates. One-way ANOVA and post hoc Tukey's multiple comparison test. *P<0.05, **P<0.01 and ***P< 0.001 indicate statistically significant differences.

4.7. FSAP protects astrocytes from hydrogen peroxide (H_2O_2) induced injury

During oxidative stress, cell apoptosis is promoted through the mitochondrial death pathway. Hence we investigated the biochemical and morphological responses of astrocytes to hydrogen peroxide-mediated cell death and define the role that FSAP might play in the apoptotic cascade. Astrocytes were exposed transiently to H_2O_2 for 3h, and cell death was measured 24 hours later. Cell death induced by H_2O_2 was reversed by FSAP treatment as measured using the LDH release (Figure 4.6A) and MTT assay (Figure 4.6B). Enzymatic activity of FSAP was required for this protective effect (Figure 4.6). As in the OGD/reoxygenation model, FSAP treatment significantly increased the Akt phosphorylation and promoted the PI3K-Akt signaling pathway activation in the presence of H_2O_2 (Figure 4.6C). Similarly, the induction of caspase activity and apoptosis by treatment with H_2O_2 (Figure 4.7A, B, C) was also reduced by FSAP. This effect was mediated via PAR-1 signaling as showed using LDH (Figure 4.7D) and MTT assay (Figure 4.7E). Thus, our results show that FSAP is able to promote cell survival in multiple form of ischemic injury in astrocytes and PAR-1 receptor mediated Akt phosphorylation by FSAP was responsible for the protective effect.

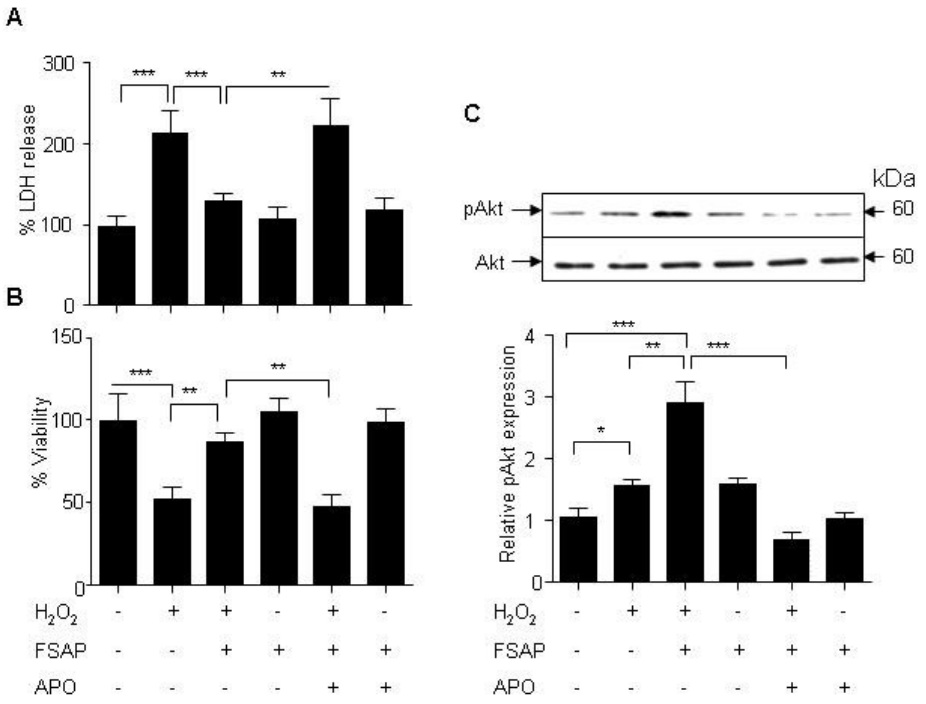

Figure 4.6: ***FSAP treatment prevents cell death and mitochondrial function via Akt phosphorylation in H_2O_2-treated astrocytes.***

Astrocytes were exposed to 250 µM H_2O_2 for 3 hours followed by 24 hours in the absence or presence of FSAP (100 nM) and APO (10 µg/ml). **A-B.** Cell viability was measured using LDH release assay (A) and MTT reduction assay (B). **C.** Representative Western blot for pAkt (Ser473) and total Akt in whole-cell extracts from the same experiment as above. Mean ± SD, n ≥ 3 independent cultures in duplicates. One-way ANOVA and post hoc Tukey's multiple comparison test. **P<0.01 and ***P< 0.001 indicate statistically significant differences.

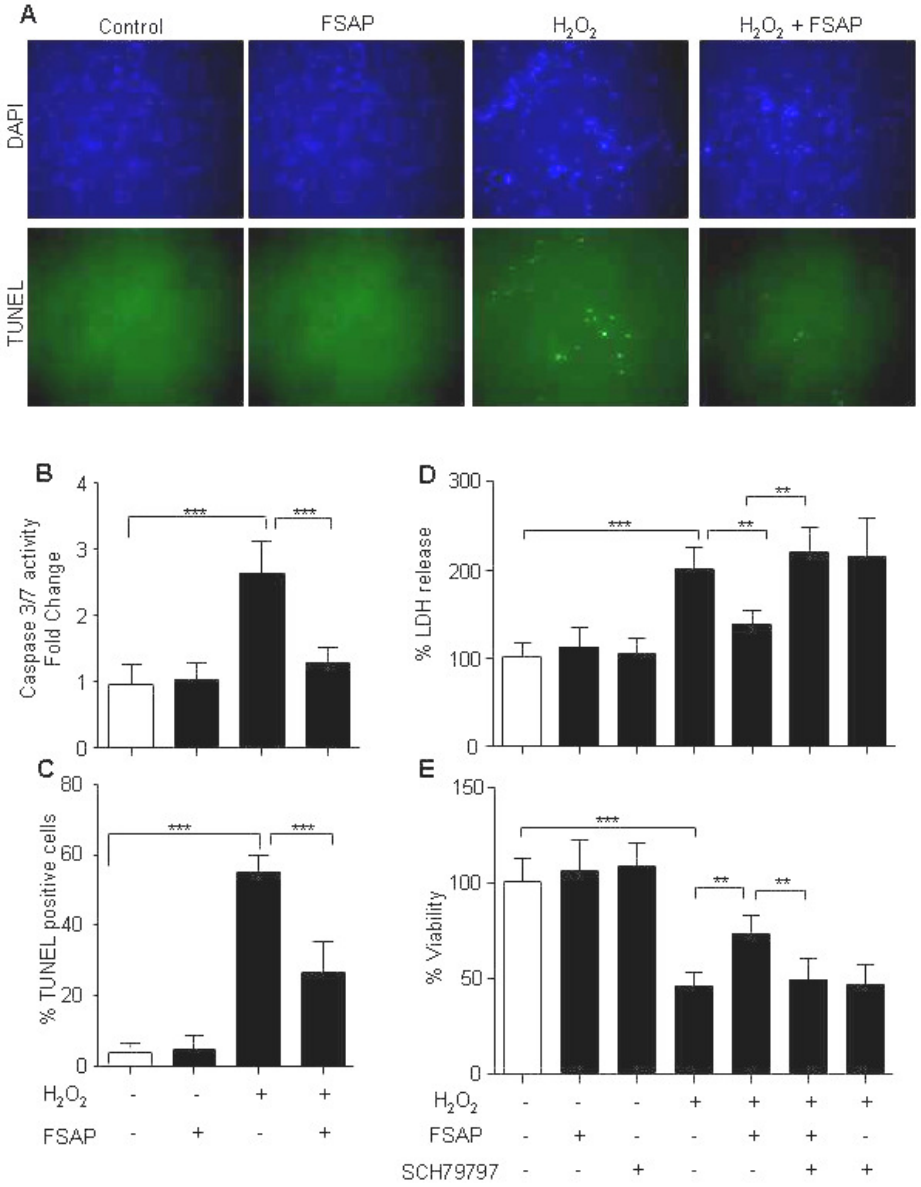

Figure 4.7: ***FSAP prevents apoptosis after oxidative stress injury in astrocytes by activating PAR-1 receptor.***

A. Representative fluorescent-TUNEL (green)/dapi (blue) staining in astrocytes 24 h in the presence or absence of FSAP (100 nM) after 3 h H_2O_2 treatment. **B.** Caspase-3 and -7 activity in astrocytes 12 h after H_2O_2 in the presence or absence of FSAP. **C.** The number of apoptotic TUNEL-positive cells quantified from the experiment in (A). **D-E.** Cell death was quantified by (D) LDH release and (E) Mitochondrial function assay in the presence or absence of FSAP and SCH79797, PAR-1 antagonist. SCH 79797 (5µM) was added to the culture 20 min before H_2O_2 treatment. Mean ± SD, n ≥ 3 independent cultures in duplicates. One-way ANOVA and post hoc Tukey's multiple comparison test. **P<0.01 and ***P< 0.001 indicate statistically significant differences.

4.8. FSAP protects mouse cortical neurons from tPA/NMDA-mediated injury

Various studies using a transient ischemia stroke models have shown direct post-ischemic neuronal toxicity of tPA. It has been also shown that tPA enhances neuronal injury in the presence of NMDA. The pathologic activation of NMDARs contributes to neuronal death after acute excitotoxic trauma such as brain ischemia. To determine whether FSAP could influence neuronal death, we used a model of excitotoxicity induced by exposure of primary cortical neuronal cultures to NMDA (12.5 uM) in the presence of tPA (20 ug/ml) as has been reported previously (Roussel et al., 2011). tPA/NMDA treatment produced acute cell swelling followed 24 hours later by neuronal degeneration, as measured by the release of LDH in supernatant. Co-application of FSAP (100 nM) prevented the pro-excitotoxic effects of tPA/NMDA-induced neuronal death (Figure 4.8.1. A, C). Neuronal viability was also assessed using the MTT reduction assay as a measure of mitochondrial dysfunction (Reddrop et al., 2005), tPA/NMDA treatment reduced mitochondrial function whereas, FSAP preserved it (Figure 4. 8.1. B, C).

We then checked if the increased survival of the cells was related to the process of apoptosis by measuring the enzymatic activity of caspase-3/7 as well as TUNEL assays. Treatment with FSAP blocked the tPA/NMDA-mediated activation of caspases (Figure 4.8.2.A). A few TUNEL-positive staining cells were noted in control cells whereas cultures treated with tPA/NMDA for 24 hours had a large numbers of cells undergoing apoptosis. However, FSAP treatment reduced the numbers of apoptotic cells (Figure 4.8.2.B, C). Inactivation of FSAP with aprotinin reversed the effect of FSAP (Figure 4.9.A, B). Thus the enzymatic activity of FSAP protected against tPA/NMDA excitotoxicity in neurons.

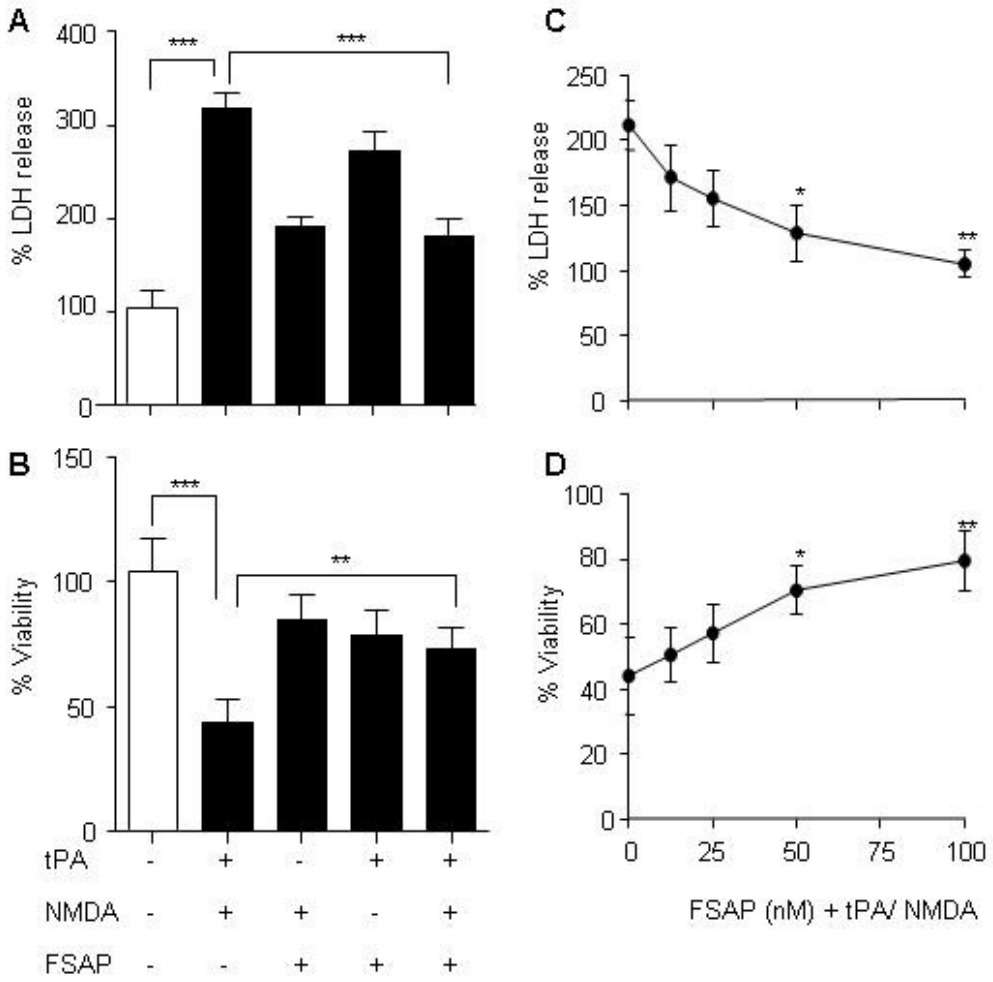

Figure 4.8.1: ***FSAP protects neurons from tPA/NMDA-mediated injury.***
Effect of FSAP (100 nM) on neuronal cultures 24 h after tPA/NMDA treatment. FSAP was used at 100 nM and was added simultaneously with tPA (20 µg/ml) and NMDA (12.5 µM). Cell survival was quantified with a LDH assay (A) & MTT reduction assay (B) relative to normoxic controls (100%). FSAP treatment promoted cell survival in dose dependent manner in neuronal cultures 24 h after tPA/NMDA treatment as quantified by LDH assay (C) and MTT reduction assay (D) and expressed relative to normoxic controls (100%). For the dose response, cells were treated with 12.5 nM, 25 nM, 50 nM & 100 nM FSAP. Mean ± SD, $n \geq 3$ independent cultures in duplicates. One-way ANOVA and post hoc Tukey's multiple comparison test. *P<0.05 **P<0.01 and ***P< 0.001 indicate statistically significant differences.

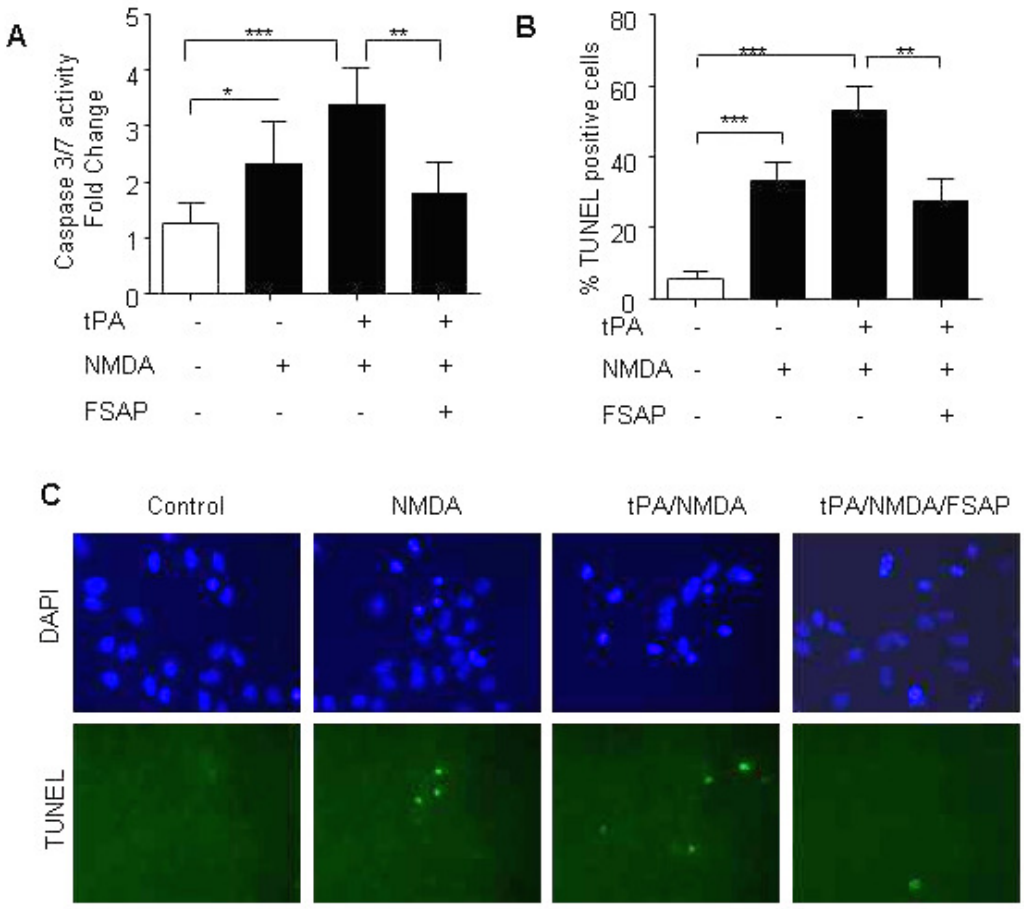

Figure 4.8.2: ***FSAP treatment reduces apoptosis in neurons after tPA/NMDA-mediated injury.***
(**A**) Caspase-3/-7 activity in neurons 12 h after tPA/NMDA in the presence or absence of FSAP. (**B**) The number of apoptotic TUNEL-positive cells quantified as described in the Methods in the presence of NMDA with and without tPA or FSAP. (**C**) Representative fluorescent-TUNEL (green)/dapi (blue) staining in neurons 24 h after tPA/NMDA treatment in the presence or absence of FSAP. Mean ± SD, n ≥ 3 independent cultures in duplicates. One-way ANOVA and post hoc Tukey's multiple comparison test. *P<0.05 **P<0.01 and ***P< 0.001 indicate statistically significant differences.

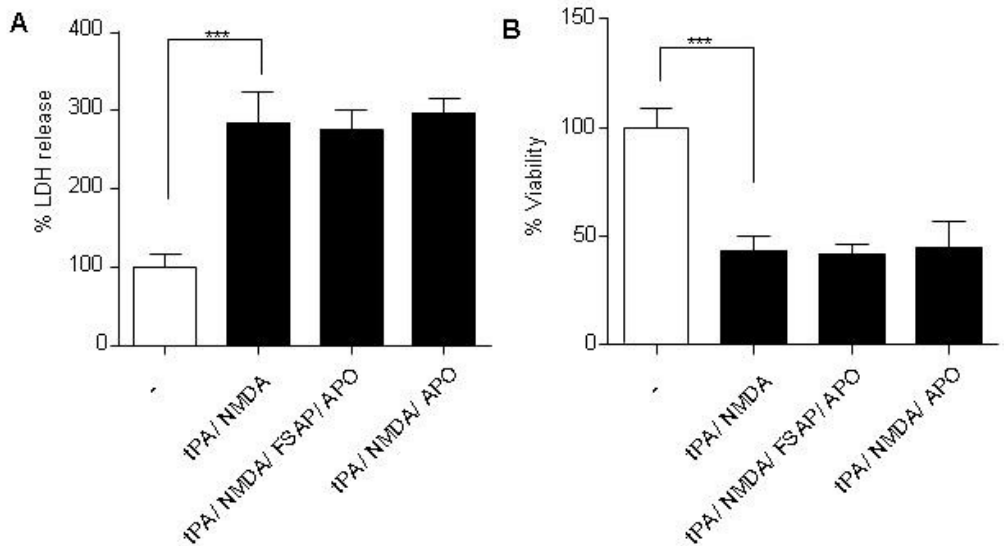

Figure 4.9: ***Inactive FSAP does not protect neurons against*** **tPA/NMDA** ***excitotoxic injury.***
Survival of neurons 24 h after tPA/NMDA exposure in the presence/ absence of FSAP (100 nM) and APO (10 µg/ml) was measured using (A) LDH release assay and (B) MTT reduction assay. In all experiments FSAP was added simultaneously with tPA (20 µg/ml) and NMDA (12.5 µM). Mean ± SD, n = 3 independent cultures in duplicates. One-way ANOVA and post hoc Tukey's multiple comparison test. ***P< 0.001 indicates statistically significant differences.

4.9. FSAP neuroprotection requires activation of Akt signaling

Various studies show that tPA/NMDA injury involves a decrease in Akt phosphorylation in neurons (Liu et al., 2004; Guo et al., 2011). We tested whether the ability of FSAP to protect neurons from tPA/NMDA-mediated injury requires PI3K-Akt activation. FSAP treatment stimulated phosphorylation of Akt on Ser473 in neurons after tPA/NMDA challenge (Figure 4.10 A, B) indicating that FSAP is able to activate the Akt signaling pathway in a sustained manner. LY294002 and Wortmannin, PI3K inhibitors, blocked FSAP-mediated phosphorylation of Akt and neuronal protection after tPA/NMDA exposure as measured by LDH release (Figure 4.11. E) and MTT reduction (Figure 4.11. F). This data suggests that FSAP's neuroprotective effects are modulated through the PI3K-Akt pathway. Since it has been previously reported that tPA/NMDA induces p53 activation (Liu et al., 2004) and FSAP treatment increased Akt, we investigated if FSAP treatment had any effect of p53 induction. FSAP treatment, indeed, reduced the tPA/NMDA induced p53 levels in excitotoxic neurons as seen in the representative western blot and its

densitometry analysis (Figure 4.10 A,C). FSAP treatment also increased Bcl-2 protein expression after tPA/NMDA injury (Figure 4.10 A, D) indicating a pro survival signaling pathway comprising of Akt/ p53/ Bcl-2. PAR-1 receptor antagonist, treatment blocked the FSAP induced neuroprotection as measured by LDH release and mitochondrial function (Figure 4.11. A, B respectively). FSAP down-regulation of caspase 3/7 activity (Figure 4.11 C), activation of Akt phosphorylation (Figure 4.11 D,E) and up-regulation of anti apoptotic Bcl-2 protein (Figure 4.11 D,F) in tPA/NMDA treated excitotoxic neurons was also inhibited by the PAR-1 antagonist.

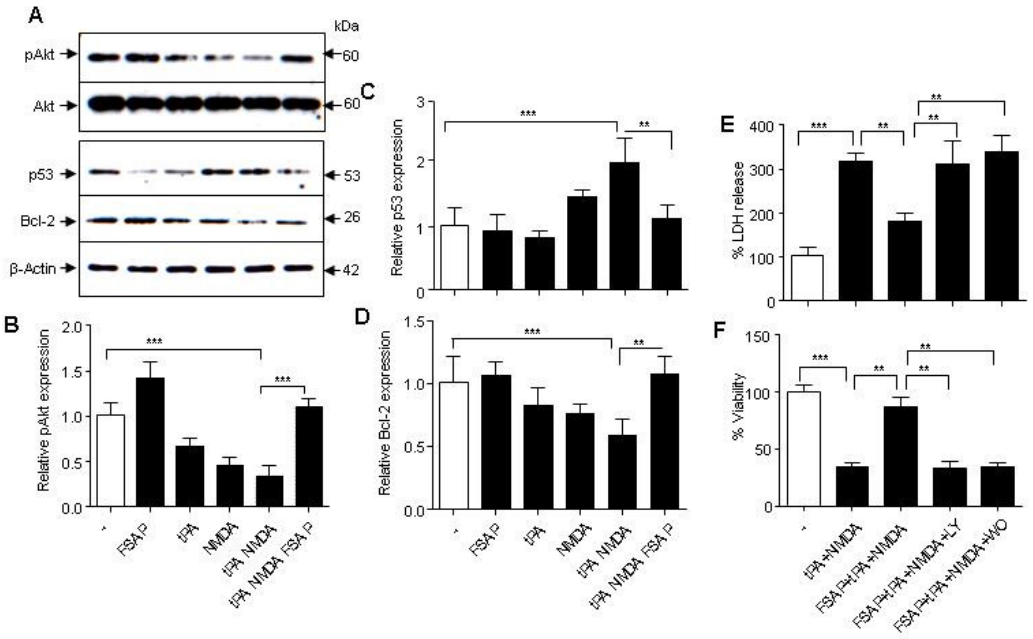

Figure 4.10: ***FSAP protects neurons from tPA/NMDA excitotoxicity via Akt survival pathway.***

Representative western blots for pAkt (Ser473), total Akt, p53, Bcl-2 and β-actin in whole-cell extracts from neurons 2 h (A) after tPA/NMDA exposure in the presence or absence of FSAP (100 nM). Intensity of pAkt signal was measured by scanning densitometry and normalized to total Akt at 2 hours. Intensity of p53 and Bcl-2 signal was measured by scanning densitometry and normalized to β-actin at 2 hours. Survival of neurons 24 h after tPA/NMDA exposure in the presence or absence of FSAP (100 nM), LY294002 (10 μM), Wortmannin (0.5 μM) was measured using (B) LDH release assay and (C) MTT reduction assay. LY294002 and Wortmannin were added to the culture 1 h before tPA/NMDA treatment. When applied alone, neither Wortmannin nor LY294002 was toxic. In all studies, FSAP was added simultaneously with tPA/NMDA. Mean ± SD, n ≥ 3 independent cultures in duplicates. One-way ANOVA and post hoc Tukey's multiple comparison test. *P<0.05 **P<0.01 and ***P< 0.001 indicate statistically significant differences.

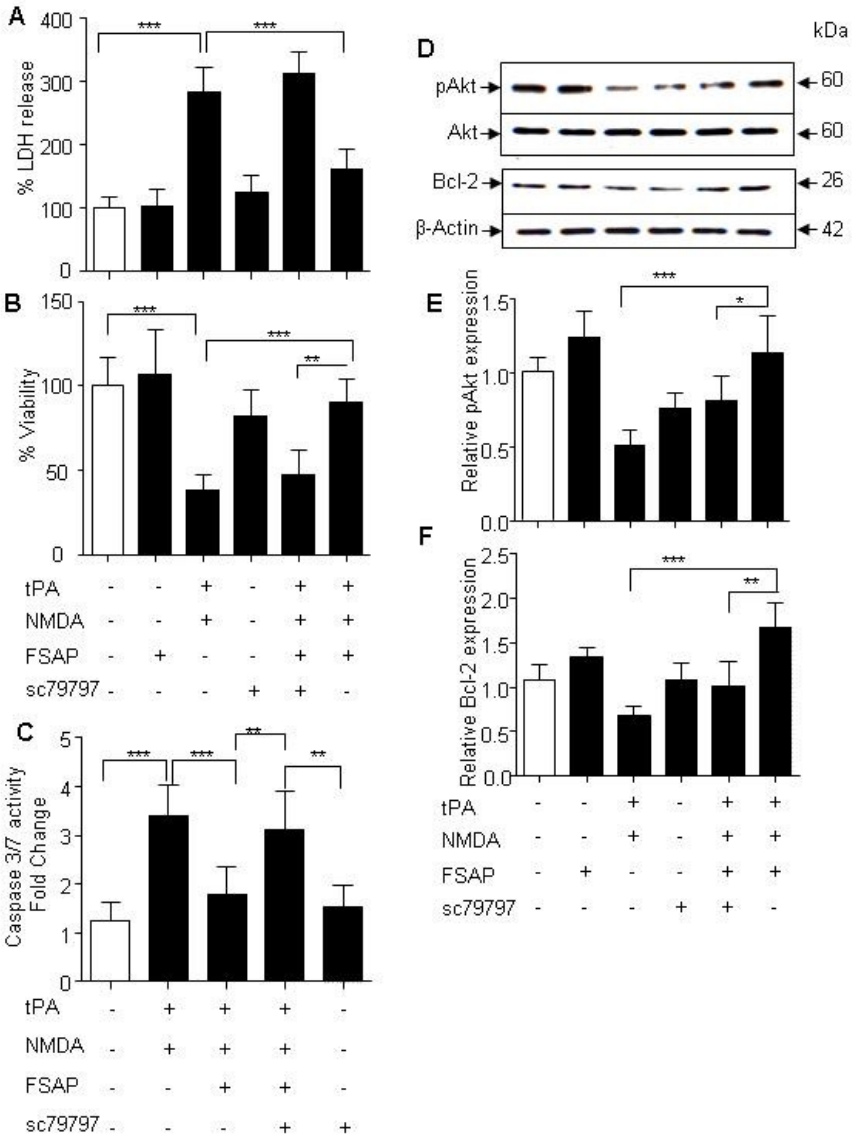

Figure 4.11: ***FSAP protects neurons from tPA/NMDA excitotoxicity via PAR-1 receptor signaling.***

Survival of neurons 24 h after tPA/NMDA exposure in the presence or absence of FSAP and SCH 79797 (5µM) was measured using (A) LDH release assay and (B) MTT reduction assay. (C) Caspase-3/-7 activity in neurons 12 h after tPA/NMDA in the presence or absence of FSAP 100 nM and SCH79797 (5µM). (D) Representative western blots for pAkt (Ser473), total Akt, Bcl-2 and β-actin in whole-cell extracts from neurons 2 h after tPA/NMDA exposure. Intensity of pAkt signal and Bcl-2 was measured by scanning densitometry and normalized to total Akt and β-actin at 2 hours respectively SCH79797 was added to the culture 20 min before tPA/NMDA treatment. Mean ± SD, n ≥ 3 independent cultures in duplicates. One-way ANOVA and post hoc Tukey's multiple comparison test. *P<0.05 **P<0.01 and ***P< 0.001 indicate statistically significant differences.

4.10. FSAP protects neurons from OGD-reperfusion damage

To further validate the neuroprotective effect of FSAP, we subjected cortical neurons in culture to oxygen glucose deprivation (OGD) (90 min) followed by 24 hours reperfusion with glucose containing medium. It is know that OGD exposure in neurons induces cell death via the apoptotic signaling which leads to activation of caspases and involves p53 accumulation. Cell death induced by OGD/reoxygenation was attenuated by FSAP treatment as measured by LDH release and MTT assay. Exactly, as with the excitototoxicity-mediated cell death, OGD induced cell death was reversed by blocking the enzymatic activity of FSAP (Figure 4.12 A, B). Also, FSAP regulated Akt phosphorylation and promoted PI3K-Akt signaling pathway (Figure 4.12 C, D). Similarly, the down-regulation of caspase -3/-7 activity (Figure 4.13 E) and apoptosis (Figure 4.12 F,G) was reduced in the presence of FSAP and this effect could also be blocked by aprotinin. The neuroprotective effect of FSAP was mediated by PAR-1 dependent signaling as indicated by the LDH release (Figure 4.13 A) and mitochondrial function (Figure 4.13 B) in inhibitor treated cells. Also, FSAP failed to activate Akt survival pathway signaling (Figure 4.13 D, E) in the presence of SCH 79797. FSAP induced reduction in p53 protein expression (Figure 4.13 D, F) was diminished with the treatment of the antagonist. FSAP failed to reduce Caspase 3 activity in hypoxic neurons with the blockage of the PAR-1 signaling pathway (Figure 4.13 C).

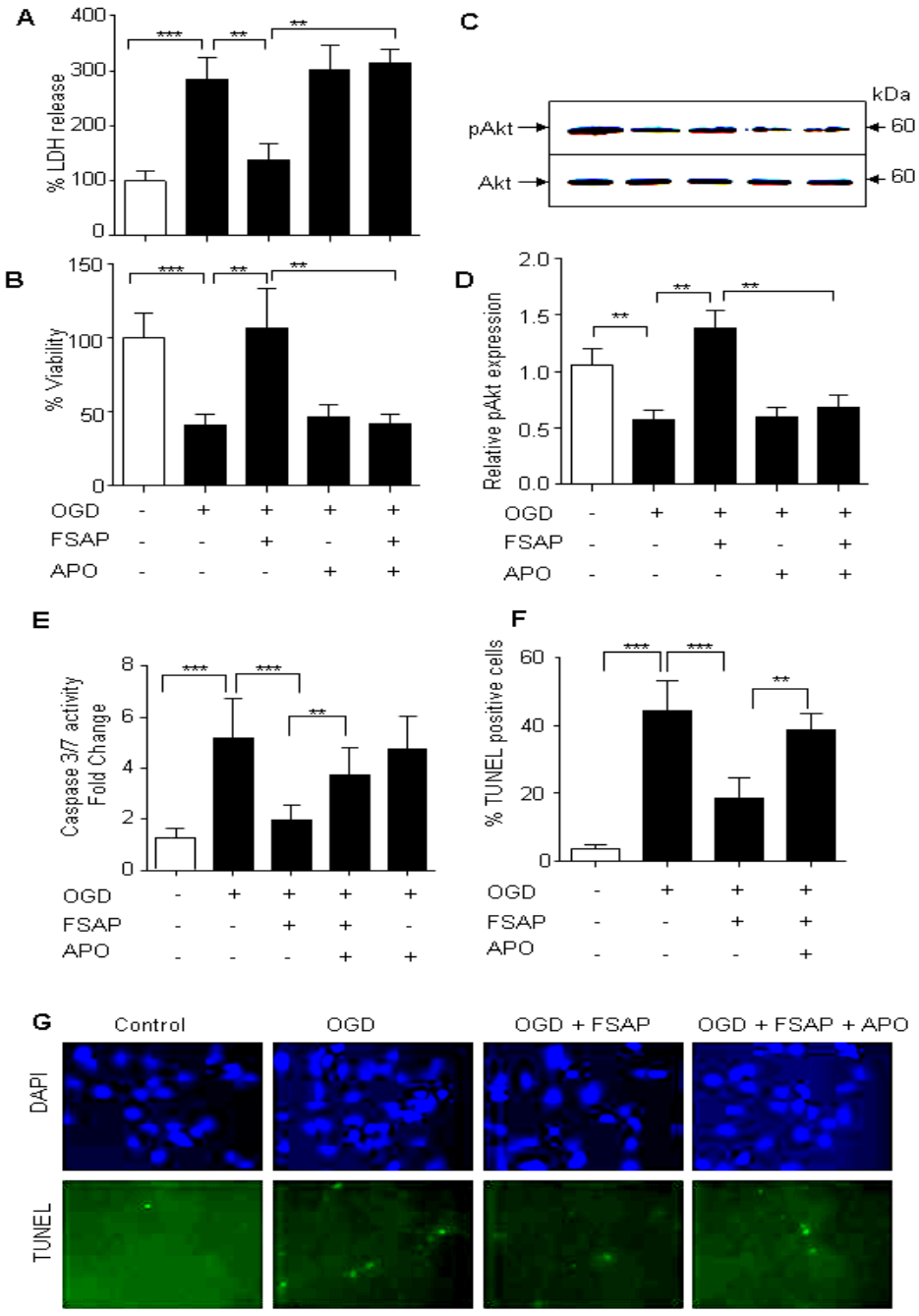

Figure 4.12: ***Inactive FSAP does not protect neurons from OGD/reoxygenation injury.***
Cell death was quantified by (A) LDH release and (B) MTT reduction assay from neurons 24 h after 90 min exposure to OGD in the presence or absence of FSAP (100 nM). (C) Representative western blots for pAkt (Ser473) and total Akt in whole-cell extracts from neurons after OGD/ reoxygenation. (D) Intensity of pAkt signal was measured by scanning densitometry and normalized to total Akt. (E) Caspase 3/7 activity in neurons 12 h after OGD/ reoxygenation was reduced with FSAP (100 nM) treatment. (F) The number of apoptotic TUNEL-positive cells was quantified as described in the methods 24 hours after OGD in the presence or absence of FSAP. (G) Representative fluorescent-TUNEL (green)/ DAPI (blue) staining in neurons after OGD/ reoxygenation.

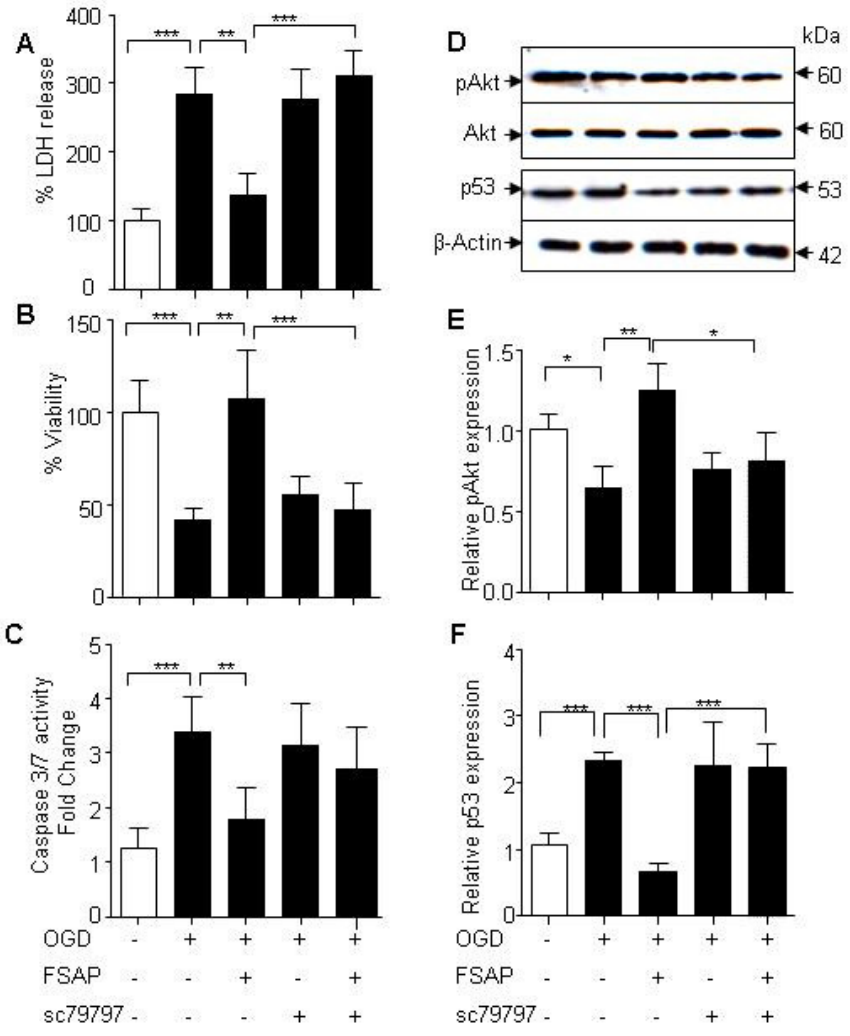

Figure 4.13: ***FSAP protects neurons from* OGD/reoxygenation *via PAR-1 receptor signaling.***

Cell viability was quantified (A) LDH release and (B) MTT reduction assay from neurons 24 h after 90 min exposure to OGD in the presence or absence of FSAP (100 nM) and SCH 79797(5µM). (C) Caspase-3/-7 activity in neurons 12 h after OGD in the presence or absence of FSAP and SCH 79797. (D) Representative western blots for pAkt (Ser473), total Akt, p53 and β-actin in whole-cell extracts from neurons 24 hours after OGD/ reoxygenation. Intensity of pAkt and p53 signal was measured by scanning densitometry and normalized to total Akt and β-actin respectively. Mean ± SD, n ≥ 3 independent cultures in duplicates. One-way ANOVA and post hoc Tukey's multiple comparison test. *P<0.05 **P<0.01 and ***P< 0.001 indicate statistically significant differences.

4.11. Endogenous FSAP influences stroke outcome in thromboembolic stroke model

After having seen the protective effects of FSAP *in-vitro* on the cells of the BBB, we sought to analyze the role of FSAP using mouse stroke model. The development of neuronal damage in $FSAP^{-/-}$ mice following cerebral ischemia was studied in a model that depends on thromboembolism in the microvasculature of the middle cerebral artery (MCA). These experiments were conducted in cooperation with Prof. Denis Vivien/ Dr. Cyrille Orset at Cyceron, University of Caen, Caen, France. The advantage of this model compared to other embolic stroke models is the high reproducibility as the clot is always located at the same place.

To initiate cerebral ischemia, murine thrombin, was directly injected into the MCA to form a stable clot in about 10 min and reduced the regional cerebral flow by >90%. Post surgery, the mice were kept under anesthesia for a further 50 min on a heated pad at 37 ^{0}C. 24 h after the surgery, animals were analyzed for infarct volumes and reperfusion using MRI. To account for differences in the brain size, we measured the infarct volumes as % of contralateral hemisphere. We observed that infarct volumes 24 h after reperfusion were significantly increased in $FSAP^{-/-}$ mice compared to WT mice. The infarcted region appears more hyperintense in the T2-weighted images (Figure 4.14 A) .The infarct size of WT mice was 12.6 ± 4.09 % *versus* 18.6 ± 5.35 % in $FSAP^{-/-}$ animals (Figure 4.14 B). All animals showed infarction that was restricted to the cortex. The lesion volume was distributed from the anterior (position + 3.2 from the bregma) to the posterior brain (- 4.8 mm from the bregma) with a distribution that was homogeneous between animals.

Next, edema formation was calculated as a ratio of Contralateral and Ispilateral hemispheres, which significantly correlates with absolute brain water content. This analysis revealed that $FSAP^{-/-}$ mice developed relatively pronounced cerebral edema as compared to WT mice (Figure 4.14 C). We then investigated whether the tissue damage in $FSAP^{-/-}$ mice was also functionally relevant. Neurological deficit was analyzed as described in the methods and we observed that $FSAP^{-/-}$ mice performed significantly worse compared to WT mice showing multiple deficits (Figure 4.14 D) correlating well with the increased infarct volumes. These results obtained from the above experiments provide further evidence of the role of

FSAP in the pathophysiology of stroke and correlate well with the human population data wherein FSAP-MI patients are at more risk of fatal stroke.

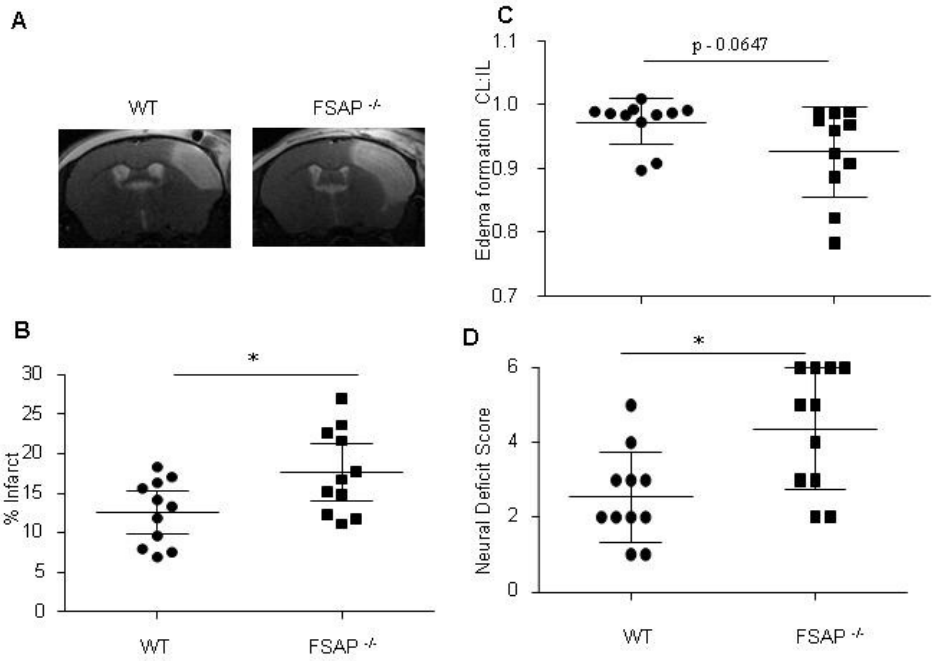

Figure 4.14: ***Loss of endogenous FSAP enhances infarct volumes and worsens stroke outcome.***
A. Longitudinal T2-weighted images for WT and FSAP$^{-/-}$ 24 hours after thromboembolic stroke indicating the infarcted area. B. Infarct volumes are represented as % of the infarcted hemisphere. C. Edema formation was calculated as described in methods. Edema formation is represented as ratio of contralateral to the infarcted hemispheres. D. FSAP $^{-/-}$ show higher neural deficit as compared to WT. Data represented as mean ± SD. n=11 in each group. **P*<0.05; Data from % Infarct (B) and edema (C) were analyzed with unpaired 2-tailed Student´s t-test; Neural deficit score (C) was evaluated with the Mann-Whitney-U test.

4.12. FSAP $^{-/-}$ mice have cerebral vasculature comparable to WT mice

Reperfusion plays a dual role after ischemia, while restoring the blood flow ensures the supply of O_2, it also leads to the influx of leukocytes, neutrophils and other cells which further worsen the outcome. Next, to check if the observed increase in infarct volumes was associated with decreased perfusion in the FSAP$^{-/-}$ mice, we evaluated the cerebral reperfusion after stroke. Using, laser doppler flowmetry, we evaluated the relative reperfusion in both hemispheres. However, there was no significant difference in the relative cerebral reperfusion 24 h after stroke onset in WT and FSAP $^{-/-}$ mice (Figure 4.15 A, B). Then using non-invasive MRI, we calculated

the mean angiography score to evaluate existing embolism in the larger arteries, which revealed no difference between the WT and FSAP$^{-/-}$ mice (Figure 4.15 C, D). The MRI angiogram also revealed no difference in the cerebral vasculature of the WT and FSAP$^{-/-}$ mice (Figure 4.15 C) indicating that FSAP deficiency lead to poor outcome independent of fibrinolytic mechanism.

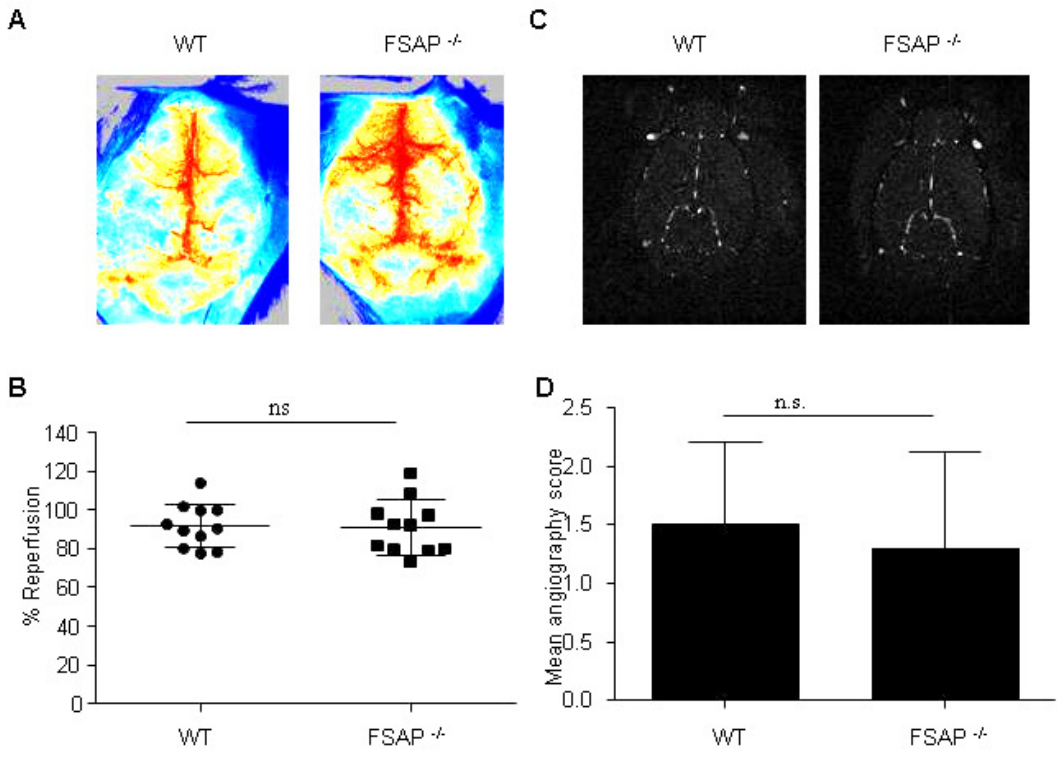

Figure 4.15: ***Endogenous FSAP shows no effect on cerebral reperfusion after embolic stroke.***
A. LSF flux images (perfusion images) showing cerebral blood flow (CBF) post reperfusion in WT and FSAP $^{-/-}$ mice. B. No difference observed in the relative reperfusion in WT and FSAP$^{-/-}$ mice after stroke. C. Represenative angiogram showing cerebral vasculature in WT and FSAP $^{-/-}$ mice. D. Mean angiography score was calculated as described in methods and indicates no difference between WT and FSAP $^{-/-}$ mice. Data represented as mean ± SD. n=11 in each group. Data from % Reperfusion (B) and Mean angiography score (D) were analyzed with unpaired 2-tailed Student´s t-test.

4.13. FSAP antigen and activity levels are elevated after stroke

Previously, we had reported that FSAP antigen and activity levels were elevated in human patients after ischemic stroke. In our model of thromboembolic stroke, we observed that the circulating levels of FSAP did increase appreciably (Figure 4.16 A, B) and the activity increased substantially (Figure 4.16 C) as compared to sham operated mice indicating a role for FSAP in recovery in the WT

mice. We could not detect any FSAP antigen or activity in the FSAP$^{-/-}$ mice confirming the associated increase in infarction was associated with the complete loss of FSAP.

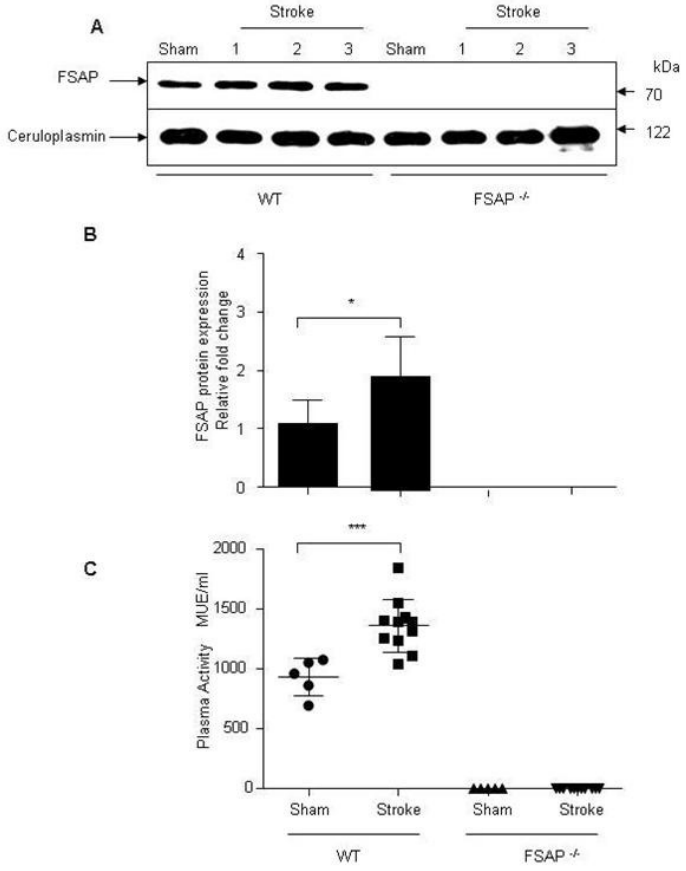

Figure 4.16: ***Endogenous FSAP levels are elevated after embolic stroke.***
A. Representative western blot for FSAP and Ceruloplasmin in mouse plasma in sham and stroke samples. B. Intensity of FSAP signal was measured by scanning densiometry and normalized to Ceruloplasmin. C. Circulating FSAP activity increased in mouse plasma in WT mice and was measured as described in methods. Data represented as mean ± SD. 5 sham mice per group and 11 stroke mice per group were used for the analysis. One way anova followed by Tukey's multiple comparison test. *P<0.05, ***<P<0.001.

4.14. Increased pro-inflammatory cytokine transcription in FSAP$^{-/-}$ mice after stroke

The inflammatory response in stroke involves not only leukocytes, endothelial and glial cells but also neurons. At the molecular level, inflammation is mediated by a complex cascade of mediators. Since in our earlier experiments with astrocytes we observed that FSAP influenced the expression of inflammatory genes, we analyzed if the increased infarct volumes were associated with the modulation of inflammation. A

strong up-regulation of TNF-α, IL-1β, IL-6 and COX-2 was observed at 24 h in the ischemic hemisphere after occlusion in WT and FSAP$^{-/-}$ mice. IL-6 is a pleiotropic cytokine that coordinates inflammatory processes between the periphery and the central nervous system, and can be released by various cell types in response to injuries. Moreover, IL-6 influences the expression and function of several other inflammatory mediators. Several studies have reported that higher levels IL-6 are associated with worse outcome after ischemic stroke (Cojocaru et al., 2009). IL-6 expression was significantly higher in FSAP$^{-/-}$ mice as compared to WT mice.

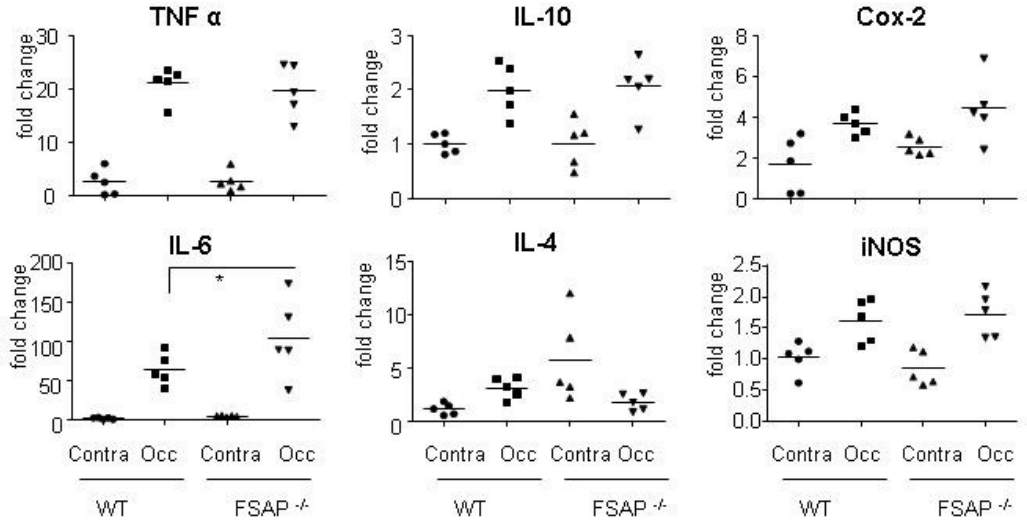

Figure 4.17: ***Expression of inflammatory genes is increased in after thromboembolic stroke***
mRNA expression of TNF-α, IL-10, COX-2, IL-6, IL-4 and iNOS were analyzed by quantitative real-time polymerase chain reaction 24 after reperfusion. Mean fold increase was calculated relative to contralateral WT hemisphere (n-5). Data represented as median. One-way ANOVA and post hoc Tukey's multiple comparison test. *P<0.05

Expression of IL-4, a potent anti-inflammatory cytokine was decreased further in FSAP$^{-/-}$, while the expression of COX-2 was increased. The expression of iNOS mRNA tended to be elevated *per se*, however it was not significantly up-regulated in the FSAP$^{-/-}$ mice. Both injurious and beneficial roles of TNF-α have been proposed for TNF-α in the pathogenesis of cerebral ischemia (Pan and Kastin, 2007). However, no difference was observed in the TNF-α expression in WT and FSAP$^{-/-}$ mice. IL-10 deficiency was shown exacerbates damage, while its over-expression reduced infarct volumes after ischemic brain injury (Planas et al., 2006). The post-ischemic IL-10

mRNA response was also not found to be significantly altered between the two groups. There was however, a tendency towards a pro-inflammatory phenotype in the $FSAP^{-/-}$ mice after embolic stroke as represented in Figure 4.17, which suggests a possible role for FSAP in modulating post-ischemic inflammation and associated increase in infarct volumes.

4.15. Endogenous FSAP modulates Akt phosphorylation in-vivo after embolic stroke

Akt activation is one of the principal factors that prevent apoptosis in many cellular systems. In our *in-vitro* analysis, we observed that exogenous FSAP was able to prevent cell death in neurons and astrocytes after ischemic insults via up-regulation of PI3K-Akt signaling pathway. To study the role of endogenous FSAP on Akt phosphorylation, we performed western blot analysis of Akt phosphorylated at serine 473 in brain extracts of WT and $FSAP^{-/-}$ 24 hours after stroke. Akt did not show a prominent modification after reperfusion. However, Akt phosphorylation was significantly down-regulated in ipsilateral hemisphere of $FSAP^{-/-}$ mice and also showed a tendency towards decrease in the contralateral hemisphere confirming the *in-vitro* findings that FSAP *appears* to be an activator of Akt survival signaling pathway (Figure 4.18).

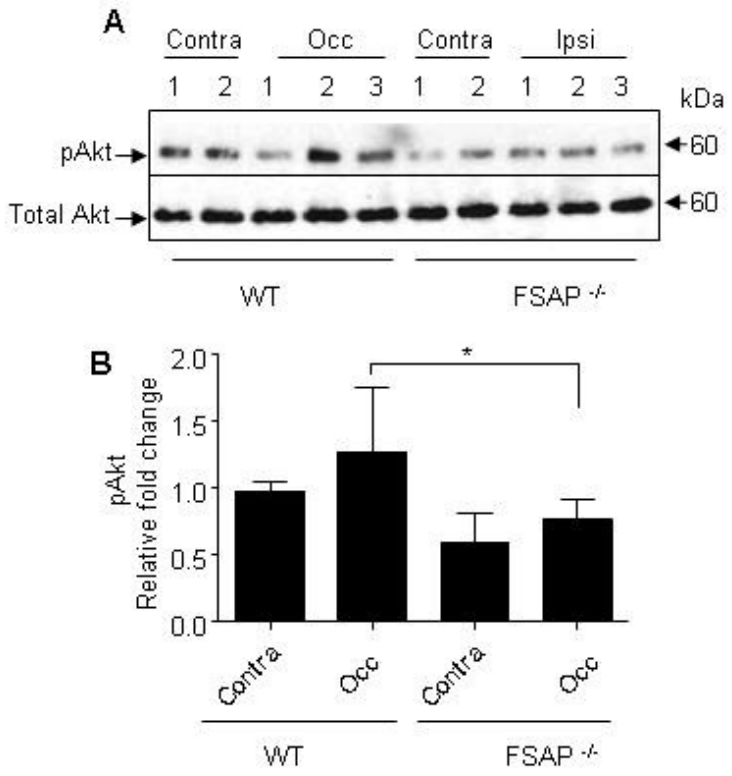

Figure 4.18: ***Western blot analysis of phospho-Akt (serine-473) and Akt from WT and FSAP $^{-/-}$ mice after embolic stroke.***
(A) Representative Western blot analysis for Akt phosphorylated at serine 473 (pAkt) and total Akt in brain extracts from WT and FSAP$^{-/-}$ mice 24 hours after stroke. (B) Mean density of the band for pAkt in wild-type and FSAP$^{-/-}$ mice 24 hours after occlusion as measured by scanning densiometry. n = 6. Data represented as Mean ± SD. One-way ANOVA and post hoc Tukey's multiple comparison test. *P<0.05

4.16. FSAP regulates p53 and Bcl-2 protein levels in mice after stroke

Pro-apoptotic p53 expression after ischemic stroke is one of the most prominent markers of the extent of cell injury (Vaseva et al., 2012). We observed that the protein levels of p53 were increased in the occluded hemispheres of WT and FSAP$^{-/-}$ mice as compared to the contralateral hemisphere. However, significant increase in the p53 levels in FSAP$^{-/-}$ mice as compared to WT indicated the severity of the ischemic injury suggesting a role for endogenous FSAP in modulating p53 levels *in-vivo* (Figure 4.19 A,B). Since p53 and anti-apoptotic Bcl-2 participate in the modulation and execution of cell death, we investigated whether there were changes in its protein expression. Our results indicate that the protein expression of Bcl-2 in the FSAP$^{-/-}$ mice is significantly reduced compared to WT mice in the occluded

hemisphere after stroke (Figure 4.19 A,C). These results confirm our *in-vitro* findings wherein exogenously added FSAP via Akt phosphorylation was able to reduce the p53 expression while increased anti-apoptotic Bcl-2 protein expression in neurons and astrocytes under ischemic conditions.

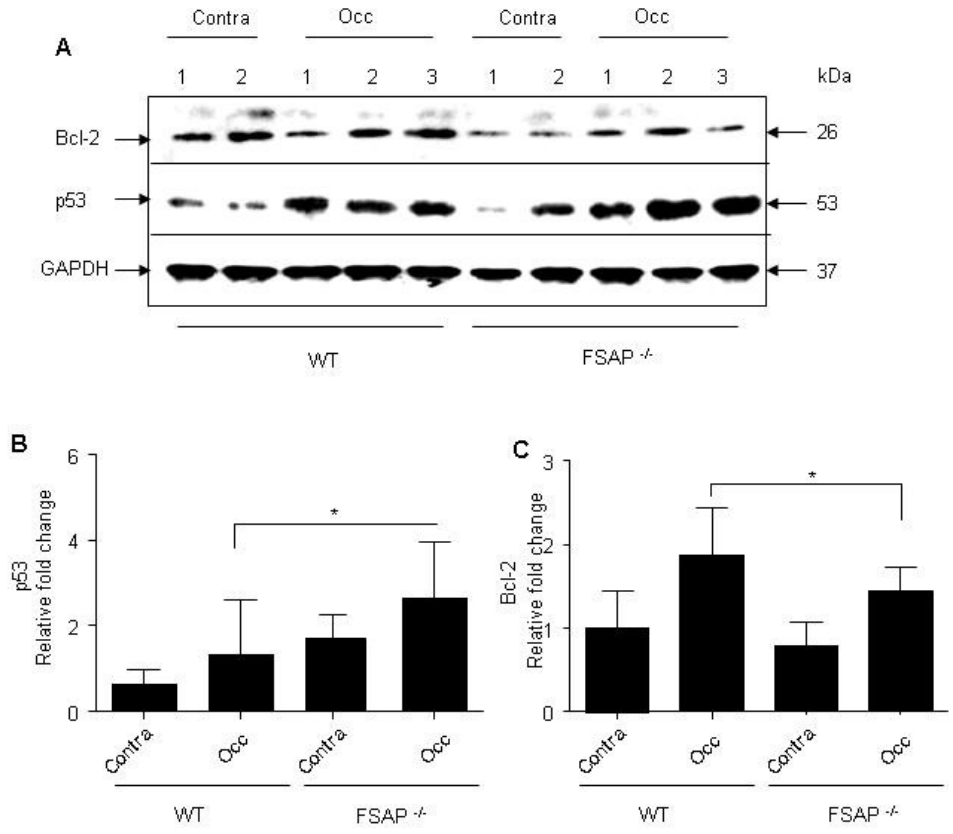

Figure 4.19: ***Western blot analysis of Bcl-2 and p53 from WT and FSAP $^{-/-}$ mice after embolic stroke.***

(A) Representative Western blot analysis for Bcl-2, p53 and GAPDH in brain extracts from WT and FSAP $^{-/-}$ mice 24 hours after stroke (B) Mean density of the band for pAkt in wild-type and FSAP$^{-/-}$ mice 24 hours after occlusion as measured by scanning densiometry. n = 6. Data represented as Mean ± SD. One-way ANOVA and post hoc Tukey's multiple comparison test. *P<0.05

5. Discussion

Ischemic stroke is one of the leading causes of mortality and economic burden across the globe (Moskowitz et al., 2010). About 85% of all strokes are ischemic and occur due to decreased or complete loss of arterial blood supply to the brain culminating in a brain infarction. Arterial occlusion is most commonly caused by a thrombus, which can either form locally at the site of occlusion and partially or completely interrupt the blood supply (thrombotic stroke), or form in another part of the circulation and then follow the blood stream until it obstructs arteries in the brain (embolic stroke). This free-roaming clot is called an embolus and often forms in the heart or on atherosclerotic plaques in large arteries, e.g. cervical arteries or aortic arch.

FSAP-MI is a significant risk predictor for the evolution and progression of carotid stenosis (Willeit et al., 2003). It was also shown that the FSAP-MI SNP is associated with an increased risk for clinical stroke and stroke related mortality (Trompet et al., 2011). They observed that Marburg I associated increase in mortality was mainly due to the increased risk of fatal stroke. The observed increase in stroke risk in Marburg I patients could be due to hyper proliferation of smooth muscle cells, since FSAP can inhibit PDGF-BB induced proliferation. FSAP through prothrombotic mechanisms, perhaps by activation of FVII (Kanse et al., 2008) and/or inhibition of TFPI (Kanse et al., 2012) could also contribute to the pathophysiology of ischemic stroke. Inflammatory responses play a critical role in the post stroke outcome. FSAP was shown to have an anti-inflammatory effect in bile duct model of liver fibrosis which is known to produce hypoxic conditions (Borkham-Kamphorst et al., 2013). This protective effect was lost in $FSAP^{-/-}$ mice which suggests a potential role for FSAP in modulating inflammation in stroke patients and the absence of which might lead to heightened post stoke inflammation worsening the outcome.

Recently, we showed that FSAP antigen and activity are elevated in patients with ischemic stroke (Hanson et al., 2012). We postulate that this might be due to the presence of cellular debris such as nucleic acids, histones and post-apoptotic cells that activate FSAP (Kanse et al., 2008). Since, 5% of Europeans are carriers of FSAP-MI there is a compelling case for further investigations into the pathophysiological role of FSAP in ischemic stroke. Hence in the present study, we investigated the role of FSAP in detail using both *in-vitro* and *in-vivo* strategies to elucidate the mechanisms and physiological role of FSAP in the context ischemic stroke.

5.1. FSAP and the blood brain barrier

In-vitro BBB models are valuable and easy to use supporting tools that can precede and complement animal and human studies. Since, the immortalized brain endothelial cell lines fail to show BBB-specific property of being able to form a tight permeability barrier under culture conditions, BBB models consisting of primary brain endothelial cells are better suitable for studying transport mechanisms across the BBB *in-vitro* (Garberg et al., 2005). Most of these well known models use primary endothelial cells from different sources, bovine, porcine, rat, and even human brain tissues. However, only a few models exist with primary endothelial cells derived from mouse brain (Deli et al., 2005). Hence, we used a model described by Coisne *et al* (Coisne et al., 2005) and further validated by Prof. Britta Engelhardt and colleagues that uses primary mouse brain microvascular endothelial cells (pMBMECs) in co culture with primary mouse astrocytes (Gorina et al., 2013). In this model, the pMBMECs form a fully differentiated endothelial monolayer with preserved characteristics of the CNS microvasculature, such as complex tight-junctions and barrier formation due to the addition of abluminal astrocytes, thereby inducing a phenotype closely mimicking to that found *in-vivo*. Recently, Steiner *et al* also demonstrated that pMBMECs were much better model to the study of T cell extravasation as compared to the immortalized bEND5 cells since they better reflect the *in-vivo* protein expression of tight junctions (Steiner et al., 2011).

Normally, the tight junctions severely restrict penetration of water-soluble compounds. However, lipid-soluble agents effectively diffuse due to the large surface area of the lipid membranes of the endothelium. The endothelium also contains transport/ carrier proteins for glucose, amino acids, purine bases, nucleosides, choline and other substances (Abbott et al., 2006). Some of these transporters are energy-dependent and act as efflux transporters. Most proteins in the plasma are unable to cross the blood brain barrier due to their size and hydrophilicity. However, concentrations of certain proteins, such as insulin, insulin-like growth factors and transferrin, vary as the plasma concentrations change, and uptake of these peptides in the brain is greater than expected based on their size and lipid solubility by a process called receptor-mediated transcytosis (Abbott et al., 2006). Polycationic proteins and lectins can cross the blood brain barrier by a nonspecific yet similar process called absorptive-mediated transcytosis (Abbott et al., 2006). Thus, transmembrane

diffusion, harnessing of transporters, adsorptive endocytosis, and extracellular pathways are some of the mechanisms by which various molecules reach the brain parenchyma.

By using a brain vascular perfusion technique, Rashid Deane and colleagues showed that ^{125}I-labeled plasma-derived mouse APC entered the brain from cerebrovascular circulation by a concentration-dependent mechanism (Deane et al., 2009). Their data suggested that APC and its variants with reduced anticoagulant activity crossed the BBB via EPCR-mediated saturable transport. In other studies, tPA was shown to cross the BBB via LRP dependent (Benchenane et al., 2005b) and independent mechanisms irrespective of its proteolytic activity (Benchenane et al., 2005a). López-Atalaya and colleagues showed that Desmoteplase, a recombinant form of the plasminogen activator DSPAα1 from *Desmodus rotundus*, crossed the intact BBB by LRP-mediated transcytosis and this mechanism remained unaltered after OGD exposure (Lopez-Atalaya et al., 2007). Thus, certain plasma proteins are able to cross the BBB through diverse mechanisms.

Since FSAP is a plasma protease circulating with concentration of 12 μg/ml (180 nM) and no detectable expression in the brain (Kanse et al., 2008), it was first essential for us to establish if FSAP could cross the blood brain barrier. To this end, we used an *in-vitro* model of the BBB comprising of pMBMECs and astrocytes. In order to validate our model, we first measured the barrier permeability to FITC-dextran. Permeability coefficient obtained from the passage of dextran is an accurate estimation of the barrier integrity and suitability. An incomplete barrier tends to have higher permeability due to the improper expression of tight-junctions or due to lack of adequate cells to form a complete barrier. The model used in this study had a permeability coefficient of 0.2×10^{-3} cm/ min which corresponded to the permeability coefficient calculated in earlier experiments (Gorina et al., 2013). We used maximum dose of 100 nM FSAP in our experiments based on the observation that, under pro-inflammatory conditions only 18-40% of FSAP was activated and subsequently formed complexes with inhibitors (Yamamichi et al., 2011). To measure if FSAP crossed the *in-vitro* BBB, we added FSAP to the luminal side and collected samples from the abluminal side of the BBB. Using a FSAP ELISA, we observed that FSAP was able to cross the *in-vitro* BBB under normal conditions. However, the exact

mechanism by which FSAP could cross the barrier was not further defined in this study.

We further investigated if FSAP played any role in the post hypoxic regulation of the BBB. The BBB has a critical role in maintaining homeostasis in the central nervous system. OGD/reoxygenation is an *in-vitro* model that has been used to mimick conditions of ischemic stroke. This model is well suited to analyze the molecular mechanisms and physiological changes that occur post ischemia. The OGD model consists of replacing the conventional culture medium by another medium without glucose and transferring the cells to a temperature controlled hypoxia chamber connected to a constant N_2 flux maintained in a humidified atmosphere with 0-2% O_2. Reperfusion is then performed which consists of replacing the OGD medium with a glucose-containing medium and then maintaining the cells in normoxic incubator to mimic the establishment of the brain blood flow and post-stroke reoxygenation. In this *in-vitro* system, low oxygen pressure, low nutrient levels (glucose), and the accumulation of cellular products that are thought to contribute to damage during ischemia occur thus effectively mimicking the clinical situation (Camos and Mallolas, 2010).

Studies have shown that hypoxia increased the permeability to FITC-labeled dextran in an *in-vitro* model of the blood–brain barrier consisting of brain microvascular endothelial cells (Li et al., 2010; Liu, J. et al., 2012). Previous investigations have documented that disorganization of tight-junction proteins are likely to occur within hours to days after ischemia, especially in models of ischemia followed by reperfusion. Zonula occludens-1 (ZO-1), occludin, claudin-5 proteins are important components of tight-junction structure and are implicated in the maintenance of integrity of tight-junctions (Jiao et al., 2011). ZO-1 links transmembrane proteins of the tight-junction to the actin cytoskeleton (Zehendner et al., 2011). Thus, changes in ZO-1 expression can accurately reflect the pathological changes of BBB, making it a valuable marker of endothelial barrier. It was shown that hypoxia disrupts the continuous pericellular distribution of the tight junction protein ZO-1 and this absence of ZO-1 is one of the mechanisms by which hyper permeability is produced (Zehendner et al., 2011).

We observed that FSAP improved cell survival of the pMBMECs and also preserved the junction expression of ZO-1. This in turn translated to improve the barrier function as measured by the decreased dextran passage. Inactivating FSAP failed to improve cell survival, ZO-1 junctional expression and BBB permeability to dextran after OGD/ reoxygenation. Surprisingly, significantly higher levels of FSAP crossed the barrier after OGD/ reoxygenation while improving the permeability.

5.2. FSAP protects against cell death and apoptosis in astrocytes

It has now become increasingly clear that the interplay between astrocytes and neurons is critical in determining the infarct volume following a stroke. Astrocytic survival post ischemia is important since they have many functions that support the viability of neurons. Also due to the difference in their cellular metabolism, neurons are more susceptible to ischemia than astrocytes. Thus, strategies targeting astrocyte survival can help salvage the ischemic tissue. Since, from our earlier results we observed that FSAP could cross the BBB, we investigated if FSAP could influence cell survival in astrocytes. For this, we used two models of cell death induction, OGD and hydrogen peroxide (H_2O_2) injury. Using mitochondrial function assays and LDH release, we observed that FSAP treatment could improve cell survival under both forms of injury. FSAP also diminished the ischemia induced caspase 3/7 activity in stressed astrocytes.

In order to further investigate the mechanisms involved in the protection, we analyzed the PI3K-Akt survival pathway. Multiple studies have shown that targeting this pathway promotes cell survival under ischemic conditions (Zhao et al., 2006; Xie et al., 2013). Akt activity is suggested to be up-regulated by phosphorylation through the activation of receptor tyrosine kinases by growth factors (Zhao et al., 2006). Although the upstream signaling components PDK-1 and integrin linked kinase enhance the activity of Akt, phosphatase and PTEN are known to decrease it. Upon activation, Akt phosphorylates an array of other molecules, including Bcl-2-associated death protein, thereby blocking mitochondrial cytochrome c release and resultant caspase activity. Generally, the level of Akt phosphorylation at site Ser^{473} has been reported to transiently increase after focal ischemia, while the levels of phosphorylation of PTEN, PDK1, forkhead transcription factor, and GSK3β decreased (Zhao et al., 2006). Gottlieb and colleagues demonstrated that depending on

the balance of signals, p53-dependent down-regulation of Akt may promote an irreversible commitment to apoptotic cell death, whereas effective recruitment of Akt by appropriate survival signals may lead to activation of Mdm2, inactivation of p53, and eventually inhibition of p53-dependent apoptosis thus promoting cell survival (Gottlieb et al., 2002). Also, Bcl-2 and its related family member Bcl-xL are among the most powerful death-suppressing proteins and inhibit both caspase-dependent and caspase-independent cell death. Akt phosphorylation is known to increase the endogenous expression of Bcl-2 proteins (Pugazhenthi et al., 2000).

Our data shows that the FSAP mediated protection after hypoxia was indeed by phosphorylating Akt leading to a protective signaling cascade in a dose dependent manner (12.5 nM – 100 nM) with 100 nM showing the maximal protective effect. We observed that FSAP blocked the p53 mediated cell death via Akt phosphorylation. p53 blockade is known to reduce BAX levels in turn promoting an increase in anti-apoptotic Bcl-2 levels. FSAP via Akt phosphorylation and p53 down-regulation was able to up regulate Bcl-2 protein levels thereby promoting cell survival post ischemia.

Having defined the pathway by which FSAP mediates its protective effects, we decided to investigate the receptor upstream of PI3K with which FSAP might interact. Since it has been previously shown that FSAP can signal via PAR-1 receptors on endothelial cells, enhanced expression of PAR-1 has been reported on astrocytes and neurons under ischemia (Rohatgi et al., 2004) , we focused on this candidate receptor. Protease-activated receptors are a subfamily of related G protein-coupled receptors that are activated by cleavage of part of their extracellular domain by coagulation proteases and play an important role in modulating cellular responses in endothelial and other cells. Thrombin (high dose)-PAR1 signaling has well established pro-inflammatory effects, including disruption of endothelial barrier function (Bae et al., 2009). However, incubation of an endothelial monolayer with APC as well as very low concentrations of thrombin potently enhanced barrier integrity through PAR1-dependent transactivation of the barrier protective sphingosine 1-phosphate (S1P) signaling pathway (Feistritzer and Riewald, 2005). It was also reported that APC-PAR1, but not thrombin-PAR1, downregulated transcript levels of several pro-apoptotic proteins including p53 and thrombospondin-1 (Resendiz et al., 2007). It was also shown that cleavage of PAR-1 by APC and

thrombin leads to the activation of phosphatidylinositol-3-kinases (PI3Ks) and downstream Akt signaling pathway (Guo et al., 2013). Thus, activating PAR-1 can lead to diverse cellular outcomes based on the stimulus.

We observed that blocking this receptor with an antagonist, SCH79797, completely removed the protective effect of FSAP. We also observed that abolishing the activity of FSAP with PPACK or Aprotinin, removed the protective effect of FSAP. FSAP also protected the astrocytes from H_2O_2 induced oxidative stress injury via the activation of PAR-1 mediated Akt phosphorylation and subsequent down-regulation of p53 and caspase 3/7 activity.

Astrocytes play a crucial role in modulating inflammation after hypoxic injury (Ceulemans et al., 2010). In earlier studies, we observed an anti-inflammatory role for FSAP in liver fibrosis. Hence, we investigated if FSAP played a role in attenuating the astrocytic inflammatory response. We observed that FSAP was able to significantly down regulate pro-inflammatory IL-6, COX-2, iNOS and TNF-α gene expression while up-regulated the expression of IL-4 and IL-10 anti-inflammatory genes indicating a shift in inflammatory phenotype in astrocytes after OGD reperfusion injury. This effect was modulated only by the active variant of FSAP indicating a secondary mechanism of protection conferred by FSAP in ischemic stroke.

5.3. FSAP prevents cell death and apoptosis in cortical neurons

Devastating loss of neurons occurs in stroke, which triggers a series of complex cascades that leads to total breakdown of cellular integrity and eventually cell death. Multiple mechanisms have been identified that contribute to the loss of neurons in the penumbra. Promoting neuronal survival post ischemia has thus become an important target for therapeutic intervention. After ischemic stroke, neurons are the most susceptible to damage in the peri-infarct region, with excitotoxicity being a key component. Normally, extracellular levels of glutamate are highly regulated by brain cells via glutamate transporters. Excess glutamate which is released from the injured cells disturbs this balance and results in hyper depolarization of neurons leading to necrosis and apoptosis (Nakka et al., 2008). Furthermore, tPA, the primary thrombolytic agent in treatment of ischemic stroke, is known to cross the blood brain

barrier and enhance this damage. It has been proposed that tPA cleaves the NR1 subunit of NMDARs potentiating NMDA-induced calcium influx and neurotoxicity or that NR2D-containing NMDARs mediate tPA-induced neuronal excitotoxicity (Parcq et al., 2012). Thus preventing this excitotoxicity is of utmost scientific significance.

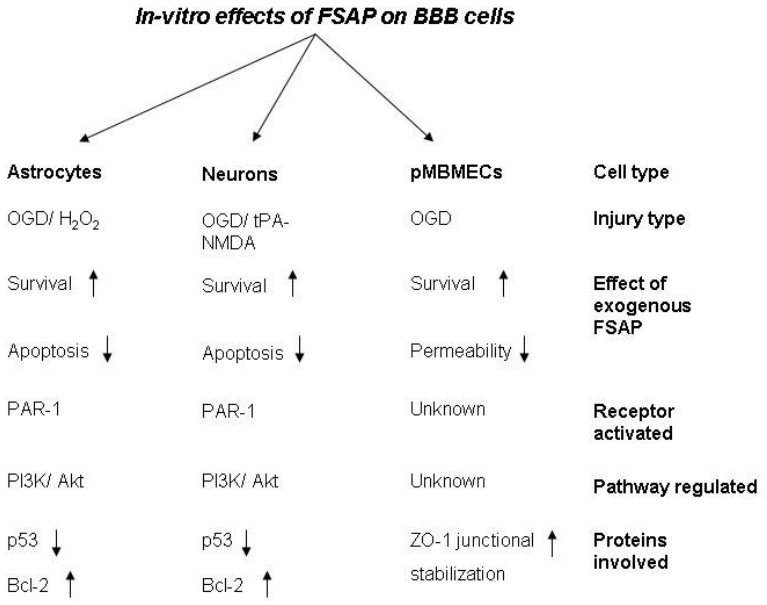

Figure 5.1. ***Effect of FSAP on astrocytes, neurons and the blood brain barrier.***
FSAP was able to influence cell death and apoptosis in astrocytes, neurons and pMBMECs exposed to conditions mimicking stroke. We observed that FSAP increased cell survival in neurons and astrocytes by regulating the PI3K-Akt pathway signaling mediated via PAR-1 receptor increasing the Bcl-2 expression and preventing p53 accumulation. In pMBMECs, we observed that FSAP reduced endothelial permeability via reducing cell death and preventing ZO-1 translocation to the nuclei thus maintaining the tight-junction structure after OGD/ reoxygenation injury.

Cell death after hypoxic injury is primarily thought to be due to the overstimulation of NMDA- receptors and hypoxia induced apoptosis (Lipton, 1999; Won et al., 2002). Neurons from mice genetically deficient in caspase 3 are relatively resistant to cell death caused by oxygen-glucose deprivation *in-vitro* and to mild brain ischemia after middle cerebral artery occlusion (Le et al., 2002). Various studies have reported that p53 is an important upstream initiator of excitotoxic NMDA-induced neuronal death and that it can increase Bax/Bcl-2 pro-apoptotic ratio through transcriptional Bax up-regulation and/or Bax oligomerization thus increasing cell

death (Liu et al., 2004; Guo et al., 2011). Depending on the stimulus intensity and neuronal cell type, some death pathways usually dominate over the others. Thus, after having seen the protective effect of FSAP on primary astrocytes and the blood brain barrier, we investigated if FSAP conferred the protection to primary cortical neurons under conditions mimicking ischemic stroke.

In the current study, we used two models of neuronal damage, tPA/NMDA excitotoxicity or OGD/ reoxygenation. Consistent with the earlier reports, we observed that overstimulation of NMDA receptor with tPA/NMDA as well as OGD/reoxygenation increased caspase 3/7 mediated cell death (Plesnila et al., 2001; Le et al., 2002; Zhong et al., 2010) . FSAP was able to reverse this caspase activation thereby promoting neuronal survival. Our data indicates that FSAP was able to improve mitochondrial function in neurons. Proteolytic activity of FSAP was required for this neuroprotective effect. As in astrocytes, FSAP was able to phosphorylate and sustain the Akt survival pathway in neurons. We observed that FSAP treatment reversed the accumulation of p53 in neurons post injury, presumably by regulating MDM2 and also restored the Bcl-2 protein levels. This effect was mediated via PAR-1 receptor and similar to the previous observations in astrocytes and APC. Thus in this thesis, we present a neuroprotective signaling pathway involving PAR-1-Akt-p53-Bcl-2 which FSAP can regulate in neurons under hypoxic injury. However, whether FSAP can act directly on NMDARs to attenuate the neurotoxic signaling during a tPA/NMDA-mediated insult should be addressed by the future studies.

5.4. FSAP $^{-/-}$ mice have worsened outcome after embolic stroke

Even though *in-vitro* models of ischemia/ reperfusion injury mimick the clinical situation, their role is limited to characterization of the pathways involved in the progression of injury or providing targets for neuroprotective agents since they are isolated systems devoid of any plasma mediators of injury. Rodent stroke models hence are the experimental standards for the *in-vivo* determination of the mechanisms of cell death and neural repair, and for the initial testing of neuroprotective compounds. Models of cerebral ischemia can be categorized into focal and global ischemia models. Focal ischemia is characterized by a reduction of cerebral blood flow in a distinct region of the brain, whereas in global ischemia the reduction of

blood flow affects the entire brain or forebrain (Carmichael, 2005; Durukan and Tatlisumak, 2007). In focal cerebral ischemia, either an artery or vein is occluded mechanically or by cerebral thromboembolism. Stroke caused by an acute cerebral vessel occlusion can be reproduced by different techniques, namely by mechanical occlusion of either the proximal middle cerebral artery (pMCAo) (large vessel occlusion) or distal MCA (dMCAo) (small vessel occlusion), or by thrombotic occlusion either *via* injection of blood clots or thrombin into the MCA (Durukan and Tatlisumak, 2007; Orset et al., 2007).

Since majority of the ischemic strokes are of embolic origin, we used a model of *in-situ* thromboembolic stroke developed by Dr. Cyrille Orset and colleagues (Orset et al., 2007). In this model, embolism was induced by the local injection of murine purified thrombin into the middle cerebral artery that results in reproducible ischemic brain damage. MRI provides a non-invasive method to estimate the infarct volumes which help minimize the use of animals. T2 weighted images obtained from the MRI display the infarcted area as a hyper intense region. To account for differences in total brain volumes, we analyzed the infarcted area as percentage of the contralateral hemisphere. We observed that $FSAP^{-/-}$ mice had larger infarctions compared to WT mice 24 hours post injury. Larger infarct volumes have been associated with worsened neurological deficits in mice. The increased infarct volume that we observed in the $FSAP^{-/-}$ mice significantly correlated with worsened neurological deficit. Even though all our mice survived the 24 hours end point, these results correlated with the clinical findings of FSAP-MI and increased risk of stroke.

Since, higher infarct volumes have been associated with secondary edema formation, we then evaluated if $FSAP^{-/-}$ mice showed the presence of edema. Edema formation occurs post ischemic stroke which further accelerates the pathological outcome. This occurs due to the influx of neutrophils and leukocytes during reperfusion which enhances the MMP-9 expression in the brain leading to increased vascular permeability (Ludewig et al., 2013). After thromboembolic stroke, $FSAP^{-/-}$ mice exhibited a tendency towards edema formation as measured by the contralateral vs ispilateral ratio which indicated the increased space occupying effect due to higher water accumulation.

Then we investigated if the increased infarct volumes in FSAP$^{-/-}$ mice were associated with deficient reperfusion in the cerebral vasculature, since FSAP has a potential role in coagulation and hemostasis via modulating TFPI. In our model of thromboembolic stroke, it has been reported that the endogenous fibrinolytic pathway is activated within 1 h after the onset of stroke and the clot resolution is completed within 24 hours. Laser speckle flowmetry (LSF) is useful to noninvasively assess two-dimensional cerebral blood flow (CBF) with high temporal and spatial resolution (Strong et al., 2006). We compared the difference in the flow between the two hemispheres and observed that 24 hours post ischemic event, there was no difference in the relative cerebral reperfusion in WT and FSAP$^{-/-}$ mice.

MR angiography using a time-of-flight technique can be used to visualize the incomplete resolution of blood flow after MCA occlusion. The arterial vascular supply of the mouse brain can also be clearly analyzed by using 3D MR angiography and thus define the cerebral anatomy (Langhauser et al., 2012). Using a predefined protocol, we analyzed the WT and FSAP$^{-/-}$ mice post stroke to visualize the deficits in the cerebral vasculature and observed no significant difference in occluded blood vessels. Magnetic resonance angiograms also revealed no difference in the cerebral vasculature of the FSAP$^{-/-}$ mice.

In stroke, it has been reported that the circulating levels of nucleosomes is elevated (Geiger et al., 2006; Geiger et al., 2007). Similarly, it was shown that plasma DNA concentrations correlated with stroke severity (Rainer et al., 2003). Since FSAP is activated by these factors; we analyzed the mouse plasma from WT and FSAP$^{-/-}$ mice in this study. We observed significantly elevated levels of FSAP antigen and activity in the WT mice 24 hours after embolic stroke. These results provide further support to the idea that endogenous active FSAP plays a critical role in the pathophysiology of stroke and correlated with the clinical observations wherein FSAP antigen and activity levels were elevated after ischemic stroke.

Thromboembolic Stroke model

WT mice	FSAP $^{-/-}$ mice	
+++	++++	Infarct Volume
+++	++++	Neuroscore
++	++	Reperfusion
++	++	Edema
++	++	Inflammatory genes
+++	n.d.	FSAP Activity
++	+	pAkt levels
++	+++	p53 levels
++	+	Bcl-2 levels

Figure 5.2. ***Effects of endogenous FSAP on stroke outcome*****.**
Absence of endogenous FSAP resulted in increased infarct volumes and neural deficits in FSAP$^{-/-}$ mice. No apparent differences were observed in cerebral vasculature and reperfusion post thromboembolic stroke in WT and FSAP$^{-/-}$ mice. However, Akt phosphorylation and subsequent Bcl-2 expression was significantly reduced in FSAP$^{-/-}$ mice. Also, p53 accumulation was significantly higher in FSAP$^{-/-}$ mice indicating a failure in protection and higher cell death after thromboembolic stroke.

Next we investigated if FSAP influenced the transcription of inflammatory genes in the brain after ischemic insult since FSAP was shown recently to have an anti-inflammatory role in liver fibrosis. In inflammation after cerebral ischemia, pro-inflammatory cytokines, IL-6, TNF-α and reactive oxygen species are released by necrotic and injured tissue. Consequently, astrocytes, microglia and endothelial cells (EC) are activated which initiates the post-ischemic inflammatory response. In FSAP$^{-/-}$ mice, we observed that the IL-6 mRNA expression was pronouncedly up-regulated. Even though, FSAP deficiency did not significantly alter the expression of TNF-α, IL-10, IL-4, COX-2 and iNOS, there was a tendency towards pro-inflammatory phenotype in FSAP$^{-/-}$ mice after stroke, thus providing a parallel cascade for limiting neuronal damage.

Having described the mechanisms for FSAP mediated neuroprotection in both neurons and astrocytes; we investigated if endogenous FSAP provided neuroprotection by regulating phosphorylation of Akt *in-vivo*. We observed that in FSAP$^{-/-}$ mice, phosphorylated Akt protein levels were significantly reduced as compared to WT mice 24 hours after embolic stroke. We also observed higher levels

of p53 protein accumulation and reduced levels of anti-apoptotic Bcl-2 in the infarcted hemisphere in $FSAP^{-/-}$ mice in comparison with WT infarcted hemispheres further providing evidence to the observation that $FSAP^{-/-}$ mice have increased infarct volumes. Thus from the data presented in this thesis, we show that endogenous FSAP plays an important role in the pathophysiology of ischemic stroke and has been summarized in Figure 5.2.

5.5 Conclusions

As the population ages, the number of ischemic stroke events are expected to rise and increase the socio-economic burden. In previous studies, FSAP-MI variant, 5% of Caucasian population, was found to be a significant risk predictor for carotid stenosis, ischemic stroke and cardiovascular disease. We had also observed elevated plasma levels of FSAP antigen and activity in human stroke patients. Thus, elucidating the role of FSAP in stroke is of importance. In the present study, we described a mechanism by which FSAP might influence stroke outcome and have been summarized in Figure 5.3.

With the herein presented data new findings that shed light on the complex mechanism by which active FSAP modulates ischemic stroke are provided. We have shown that FSAP protected the blood brain barrier (BBB) exposed to conditions modeling ischemic stroke *in-vitro*. We propose that FSAP can preserve barrier integrity after ischemia and concomitantly it can cross the endothelial BBB and activate the canonical pro-survival Akt pathway in astrocytes and neurons. In response to OGD/reoxygenation or oxidative stress or excitotoxicity, only the enzymatically active FSAP protected neurons and astrocytes, while enzymatically inactivated FSAP was ineffective. Active FSAP also modulates post stroke inflammatory responses.

In the final part of this study, we have shown the endogenous FSAP is essential in determining the stroke outcome. $FSAP^{-/-}$ mice showed more pronounced infarct volumes and neurological deficits, which could not be attributed to defective perfusion. Hence, we investigated at molecular level the role of endogenous FSAP in brain infarct evolution. Endogenous FSAP was essential for the activation of Akt survival pathway which leads to the subsequent observations in p53 and Bcl-2 levels.

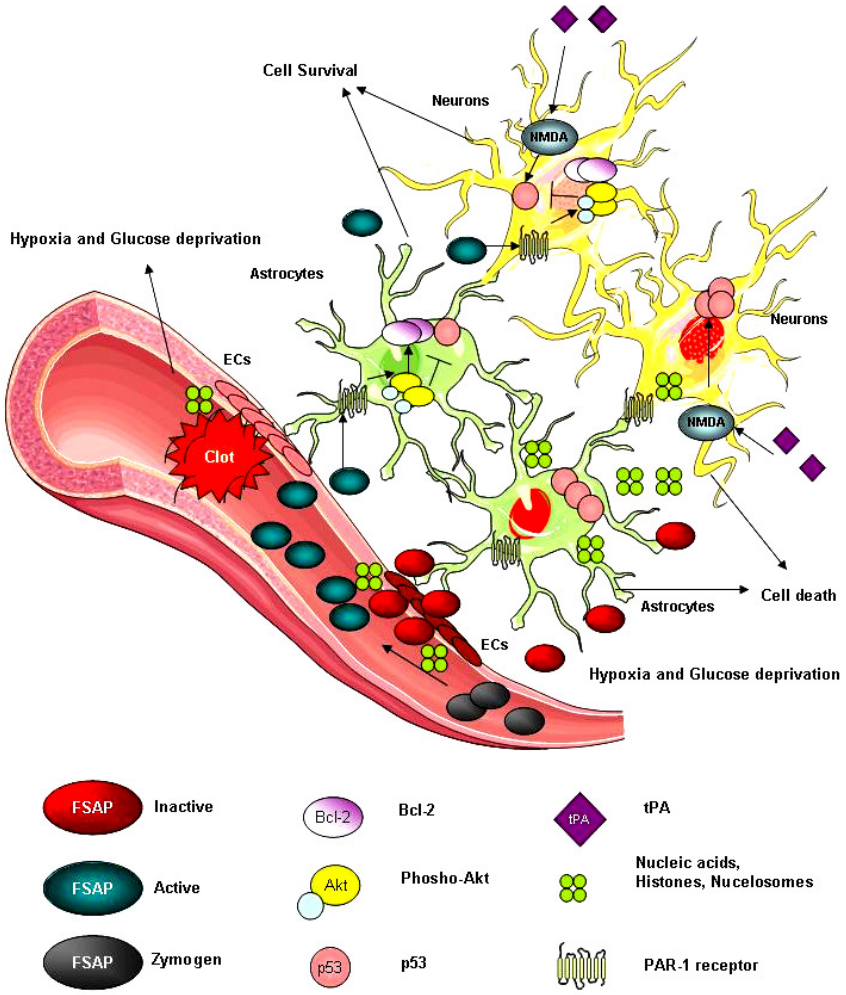

Figure 5.3: ***Active FSAP protects the cells from Ischemia and limits infarct volume.*** After embolic stroke, the BBB permeability increases which leads to the efflux of dead cells and factors released by them into circulation. FSAP which circulates as an inactive zymogen is then activated and more FSAP crosses the BBB. During this process, FSAP stabilizes the BBB and reduces the permeability. Once in the brain parenchyma, FSAP activates the PAR-1 receptor and induces phosphorylation of Akt which further leads to increased Bcl-2 and decreased p53 levels. This pathway prevents cell death and apoptosis. However, inactive FSAP as in the case of FSAP-MI patients, crosses the BBB but fails to reduce permeability. In the brain parenchyma, it fails to activate the PAR-1 receptor mediated Akt phosphorylation. Subsequently, there is accumulation of p53 which results in increased cell death.

FSAP-MI SNP is associated with low proteolytic activity and has been associated with increased risk of ischemic stroke. We observed that only active FSAP could induce Akt phosphorylation in neurons, astrocytes and mouse brain; and leading to a subsequent protective effect (Figure 5.3). Failure of the FSAP pathway exacerbates the damaging consequences of ischemic stroke and perhaps is the reason

why MI-carriers, with low FSAP enzymatic activity are associated with an increased risk of clinical stroke and mortality.

Although we were able to shed more light on the *in-vitro* and *in-vivo* effects of FSAP in the ischemic brain, this work was just the beginning of more complex and refined methodical studies in the future. Future studies should confirm these findings in additional models of stroke, including permanent ischemic and hemorrhagic models of stroke, and in female and at risk populations, in order to expand the potential role of FSAP in general stroke pathophysiology. Further experiments with NMDA injection model in $FSAP^{-/-}$ mice would also help dissect the *in-vivo* protective of FSAP against excitotoxic injury. Also, since FSAP is known to modulate neutrophils infiltration, it would be necessary to analyze their role in the observed effects. Furthermore, experiments with the proposed humanized FSAP-MI mice in our lab would much more closely resemble the clinical situation and give a better understanding role of FSAP in ischemic brain.

Developing agents, which mimick the neuroprotective effect of FSAP or enhance the circulating FSAP activity could help minimize the ischemic stroke severity in human carriers of Marburg I SNP. Additionally, due to the ability of FSAP to modulate post stroke inflammation and tPA/NMDA excitotoxicity, FSAP mimicking drugs could improve the therapeutic window for tPA administration thereby benefiting all stroke patients.

Factor Seven Activating Protease (FSAP) is a circulating protease with a role in coagulation, fibrinolysis and inflammation. The FSAP-Marburg I polymorphism, with low proteolytic activity, is associated with an increased risk of stroke and late complications of carotid stenosis in humans. We recently showed that FSAP antigen and activity levels are elevated in patients with Ischemic Stroke. In order to find a mechanistic explanation for this we have investigated the effect of FSAP on primary mouse brain microvascular endothelial cells, astrocytes and neurons. We demonstrate that FSAP can regulate endothelial permeability in an *in-vitro* model of the blood brain barrier (BBB) by stabilizing junctional localization of ZO-1 and by preventing the opening of the endothelial tight junctions after oxygen glucose deprivation (OGD)/reoxygenation. Furthermore, FSAP can cross the BBB and exert a protective effect on cortical astrocytes and neurons exposed to conditions mimicking stroke by activating the PI3K-Akt pathway. This protective effect was mediated by PAR-1 dependent activation of Akt pathway and dependent on its proteolytic activity. In a mouse *in-situ* thromboembolic stroke model, we observed that infarction volumes at 24 hours were significantly larger in $FSAP^{-/-}$ mice and neurological score worse. However, no difference was observed in the either cerebral reperfusion or cerebral vasculature. Increased FSAP antigen and activity levels were detected in WT mice after stroke in accordance with the clinical findings. In the absence of endogenous FSAP, there was a tendency towards a pro-inflammatory phenotype post stroke. Also, the lack of FSAP after stroke resulted in decreased Akt phosphorylation and Bcl-2 levels while increased levels of p53 were observed. Thus, from the data presented in this thesis, we propose that FSAP is a novel neuroprotective agent of the neurovascular unit and loss of FSAP activity could suggest the possible mechanism which leads to less protection in Marburg I polymorphism patients.

Die Faktor VII-aktivierende Protease (FSAP) ist eine zirkulierende Protease mit einer Rolle in der Koagulation, der Fibrinolyse und in Entzündungsprozessen. Der FSAP-Marburg-I-Polymorphismus, ohne proteolytisch Aktivität ist mit einem erhöhten Risiko für Hirn-Infarkte und späteren Komplikationen wie Karotisstenosen assoziiert. Wir zeigen, dass FSAP-Antigen und -Aktivität in Patienten mit ischämischem Schlaganfall erhöht sind. Um eine mechanistische Erklärung dafür zu finden, haben wir die Wirkung von FSAP auf primäre mikrovaskuläre Hirn-Endothelzellen, Astrozyten und Neuronen untersucht. In dieser Studie zeigen wir, dass FSAP die endotheliale Permeabilität in einem *in-vitro*-Modell der Blut-Hirn-Schranke (BBB) durch Stabilisierung der junktionalen Lokalisierung von ZO- 1 und durch die Öffnung der endothelialen tight-junctions nach Sauerstoff-Glucose-Deprivation (OGD)/ Reoxygenierung verhindern regulieren bzw kann. Darüber hinaus kann FSAP die BBB überqueren und somit eine schützende Wirkung auf kortikale Astrozyten und Neuronen ausüben, die einem Schlaganfall nach Aktivierung des PI3K-Akt-Signalweges ausgesetzt sind. Dieser schützende Effekt wird durch PAR-1-abhängige Aktivierung des Akt-Signalweges vermittelt. In einem in-situ thromboembolischen Schlaganfall-Modell der Maus beobachteten wir, dass das Infarktvolumen nach 24 Stunden deutlich größer und das neurologische Ergebnis in $FSAP^{-/-}$ Mäusen deutlich schlechter war. Es wurde kein Unterschied in der zerebralen Reperfusion oder in zerebralen Gefäßen beobachtet. In WT-Mäusen wurde mehr FSAP-Antigen und eine erhöhte FSAP-Aktivität festgestellt. In Abwesenheit von endogenem FSAP gab es eine Tendenz hin zu einem pro-inflammatorischen Phänotyp nach einem Schlaganfall . Auch das Fehlen von FSAP nach einem Schlaganfall führte zu einer verringerten Akt- Phosphorylierung und veringerten Bcl-2-Werten während erhöhte p53-Werte beobachtet wurden. So gibes eine neue Rolle für FSAP als neuroprotektives Agens in der neurovaskulären Einheit und der Verlust der FSAP-Aktivität könnte eine mögliche Ursache des geringeren Schutzes in Marburg-I-Polymorphismus Patienten sein.

References

Abbott, N. J., Ronnback, L. and Hansson, E. (2006). Astrocyte-endothelial interactions at the blood-brain barrier. *Nature reviews. Neuroscience* **7**, 41-53.

Almeida, A., Delgado-Esteban, M., Bolanos, J. P. and Medina, J. M. (2002). Oxygen and glucose deprivation induces mitochondrial dysfunction and oxidative stress in neurones but not in astrocytes in primary culture. *Journal of neurochemistry* **81**, 207-217.

Amantea, D., Nappi, G., Bernardi, G., Bagetta, G. and Corasaniti, M. T. (2009). Post-ischemic brain damage: pathophysiology and role of inflammatory mediators. *The FEBS journal* **276**, 13-26.

Arai, K. and Lo, E. H. (2010). Astrocytes protect oligodendrocyte precursor cells via MEK/ERK and PI3K/Akt signaling. *Journal of neuroscience research* **88**, 758-763.

Aronowski, J., Strong, R. and Grotta, J. C. (1997). Reperfusion injury: demonstration of brain damage produced by reperfusion after transient focal ischemia in rats. *Journal of cerebral blood flow and metabolism : official journal of the International Society of Cerebral Blood Flow and Metabolism* **17**, 1048-1056.

Arumugam, T. V., Woodruff, T. M., Lathia, J. D., Selvaraj, P. K., Mattson, M. P. and Taylor, S. M. (2009). Neuroprotection in stroke by complement inhibition and immunoglobulin therapy. *Neuroscience* **158**, 1074-1089.

Asahi, K., Mizutani, H., Tanaka, M., Miura, M., Yamanaka, K., Matsushima, K., Nakashima, K. and Shimizu, M. (1999). Intradermal transfer of caspase-1 (CASP1) DNA into mouse dissects: role of CASP1 in interleukin-1beta associated skin inflammation and apoptotic cell death. *Journal of dermatological science* **21**, 49-58.

Bae, J. S., Kim, Y. U., Park, M. K. and Rezaie, A. R. (2009). Concentration dependent dual effect of thrombin in endothelial cells via Par-1 and Pi3 Kinase. *Journal of cellular physiology* **219**, 744-751.

Bauer, A. T., Burgers, H. F., Rabie, T. and Marti, H. H. (2010). Matrix metalloproteinase-9 mediates hypoxia-induced vascular leakage in the brain via tight junction rearrangement. *Journal of cerebral blood flow and metabolism : official journal of the International Society of Cerebral Blood Flow and Metabolism* **30**, 837-848.

Benchenane, K., Berezowski, V., Fernandez-Monreal, M., Brillault, J., Valable, S., Dehouck, M. P., Cecchelli, R., Vivien, D., Touzani, O. and Ali, C. (2005a). Oxygen glucose deprivation switches the transport of tPA across the blood-brain barrier from an LRP-dependent to an increased LRP-independent process. *Stroke; a journal of cerebral circulation* **36**, 1065-1070.

Benchenane, K., Berezowski, V., Ali, C., Fernandez-Monreal, M., Lopez-Atalaya, J. P., Brillault, J., Chuquet, J., Nouvelot, A., MacKenzie, E. T., Bu, G. et al. (2005b). Tissue-type plasminogen activator crosses the intact blood-brain barrier by low-density lipoprotein receptor-related protein-mediated transcytosis. *Circulation* **111**, 2241-2249.

Bezzi, P., Gundersen, V., Galbete, J. L., Seifert, G., Steinhauser, C., Pilati, E. and Volterra, A. (2004). Astrocytes contain a vesicular compartment that is competent for regulated exocytosis of glutamate. *Nature neuroscience* **7**, 613-620.

Bondarenko, A. and Chesler, M. (2001). Rapid astrocyte death induced by transient hypoxia, acidosis, and extracellular ion shifts. *Glia* **34**, 134-142.

Borkham-Kamphorst, E., Zimmermann, H. W., Gassler, N., Bissels, U., Bosio, A., Tacke, F., Weiskirchen, R. and Kanse, S. M. (2013). Factor VII activating

protease (FSAP) exerts anti-inflammatory and anti-fibrotic effects in liver fibrosis in mice and men. *Journal of hepatology* **58**, 104-111.

Bratton, M. R., Duong, B. N., Elliott, S., Weldon, C. B., Beckman, B. S., McLachlan, J. A. and Burow, M. E. (2010). Regulation of ERalpha-mediated transcription of Bcl-2 by PI3K-AKT crosstalk: implications for breast cancer cell survival. *International journal of oncology* **37**, 541-550.

Camos, S. and Mallolas, J. (2010). Experimental models for assaying microvascular endothelial cell pathophysiology in stroke. *Molecules* **15**, 9104-9134.

Carmichael, S. T. (2005). Rodent models of focal stroke: size, mechanism, and purpose. *NeuroRx : the journal of the American Society for Experimental NeuroTherapeutics* **2**, 396-409.

Ceulemans, A. G., Zgavc, T., Kooijman, R., Hachimi-Idrissi, S., Sarre, S. and Michotte, Y. (2010). The dual role of the neuroinflammatory response after ischemic stroke: modulatory effects of hypothermia. *Journal of neuroinflammation* **7**, 74.

Choi-Miura, N. H., Tobe, T., Sumiya, J., Nakano, Y., Sano, Y., Mazda, T. and Tomita, M. (1996). Purification and characterization of a novel hyaluronan-binding protein (PHBP) from human plasma: it has three EGF, a kringle and a serine protease domain, similar to hepatocyte growth factor activator. *Journal of biochemistry* **119**, 1157-1165.

Christov, A., Ottman, J. T. and Grammas, P. (2004). Vascular inflammatory, oxidative and protease-based processes: implications for neuronal cell death in Alzheimer's disease. *Neurological research* **26**, 540-546.

Clausen, B. H., Lambertsen, K. L., Babcock, A. A., Holm, T. H., Dagnaes-Hansen, F. and Finsen, B. (2008). Interleukin-1beta and tumor necrosis factor-alpha are expressed by different subsets of microglia and macrophages after ischemic stroke in mice. *Journal of neuroinflammation* **5**, 46.

Coisne, C., Dehouck, L., Faveeuw, C., Delplace, Y., Miller, F., Landry, C., Morissette, C., Fenart, L., Cecchelli, R., Tremblay, P. et al. (2005). Mouse syngenic in vitro blood-brain barrier model: a new tool to examine inflammatory events in cerebral endothelium. *Laboratory investigation; a journal of technical methods and pathology* **85**, 734-746.

Cojocaru, I. M., Cojocaru, M., Tanasescu, R., Iliescu, I., Dumitrescu, L. and Silosi, I. (2009). Expression of IL-6 activity in patients with acute ischemic stroke. *Romanian journal of internal medicine = Revue roumaine de medecine interne* **47**, 393-396.

Crumrine, R. C., Thomas, A. L. and Morgan, P. F. (1994). Attenuation of p53 expression protects against focal ischemic damage in transgenic mice. *Journal of cerebral blood flow and metabolism : official journal of the International Society of Cerebral Blood Flow and Metabolism* **14**, 887-891.

Culmsee, C. and Mattson, M. P. (2005). p53 in neuronal apoptosis. *Biochemical and biophysical research communications* **331**, 761-777.

Deane, R., LaRue, B., Sagare, A. P., Castellino, F. J., Zhong, Z. and Zlokovic, B. V. (2009). Endothelial protein C receptor-assisted transport of activated protein C across the mouse blood-brain barrier. *Journal of cerebral blood flow and metabolism : official journal of the International Society of Cerebral Blood Flow and Metabolism* **29**, 25-33.

del Zoppo, G. J. (1998). The role of platelets in ischemic stroke. *Neurology* **51**, S9-14.

del Zoppo, G. J. (2009). Inflammation and the neurovascular unit in the setting of focal cerebral ischemia. *Neuroscience* **158**, 972-982.

Deli, M. A., Abraham, C. S., Kataoka, Y. and Niwa, M. (2005). Permeability studies on in vitro blood-brain barrier models: physiology, pathology, and pharmacology. *Cellular and molecular neurobiology* **25**, 59-127.

Dirnagl, U., Iadecola, C. and Moskowitz, M. A. (1999). Pathobiology of ischaemic stroke: an integrated view. *Trends in neurosciences* **22**, 391-397.

Durukan, A. and Tatlisumak, T. (2007). Acute ischemic stroke: overview of major experimental rodent models, pathophysiology, and therapy of focal cerebral ischemia. *Pharmacology, biochemistry, and behavior* **87**, 179-197.

Eddleston, M. and Mucke, L. (1993). Molecular profile of reactive astrocytes--implications for their role in neurologic disease. *Neuroscience* **54**, 15-36.

Endo, H., Nito, C., Kamada, H., Nishi, T. and Chan, P. H. (2006). Activation of the Akt/GSK3beta signaling pathway mediates survival of vulnerable hippocampal neurons after transient global cerebral ischemia in rats. *Journal of cerebral blood flow and metabolism : official journal of the International Society of Cerebral Blood Flow and Metabolism* **26**, 1479-1489.

Enzmann, G., Mysiorek, C., Gorina, R., Cheng, Y. J., Ghavampour, S., Hannocks, M. J., Prinz, V., Dirnagl, U., Endres, M., Prinz, M. et al. (2013). The neurovascular unit as a selective barrier to polymorphonuclear granulocyte (PMN) infiltration into the brain after ischemic injury. *Acta neuropathologica* **125**, 395-412.

Feistritzer, C. and Riewald, M. (2005). Endothelial barrier protection by activated protein C through PAR1-dependent sphingosine 1-phosphate receptor-1 crossactivation. *Blood* **105**, 3178-3184.

Fink, K. B., Andrews, L. J., Butler, W. E., Ona, V. O., Li, M., Bogdanov, M., Endres, M., Khan, S. Q., Namura, S., Stieg, P. E. et al. (1999). Reduction of post-traumatic brain injury and free radical production by inhibition of the caspase-1 cascade. *Neuroscience* **94**, 1213-1218.

Fischer, S., Wobben, M., Marti, H. H., Renz, D. and Schaper, W. (2002). Hypoxia-induced hyperpermeability in brain microvessel endothelial cells involves VEGF-mediated changes in the expression of zonula occludens-1. *Microvascular research* **63**, 70-80.

Frijns, C. J. and Kappelle, L. J. (2002). Inflammatory cell adhesion molecules in ischemic cerebrovascular disease. *Stroke; a journal of cerebral circulation* **33**, 2115-2122.

Garberg, P., Ball, M., Borg, N., Cecchelli, R., Fenart, L., Hurst, R. D., Lindmark, T., Mabondzo, A., Nilsson, J. E., Raub, T. J. et al. (2005). In vitro models for the blood-brain barrier. *Toxicology in vitro : an international journal published in association with BIBRA* **19**, 299-334.

Geiger, S., Holdenrieder, S., Stieber, P., Hamann, G. F., Bruening, R., Ma, J., Nagel, D. and Seidel, D. (2006). Nucleosomes in serum of patients with early cerebral stroke. *Cerebrovascular diseases* **21**, 32-37.

Geiger, S., Holdenrieder, S., Stieber, P., Hamann, G. F., Bruening, R., Ma, J., Nagel, D. and Seidel, D. (2007). Nucleosomes as a new prognostic marker in early cerebral stroke. *Journal of neurology* **254**, 617-623.

Gertz, K., Kronenberg, G., Kalin, R. E., Baldinger, T., Werner, C., Balkaya, M., Eom, G. D., Hellmann-Regen, J., Krober, J., Miller, K. R. et al. (2012). Essential role of interleukin-6 in post-stroke angiogenesis. *Brain : a journal of neurology* **135**, 1964-1980.

Giffard, R. G., Monyer, H., Christine, C. W. and Choi, D. W. (1990). Acidosis reduces NMDA receptor activation, glutamate neurotoxicity, and oxygen-glucose deprivation neuronal injury in cortical cultures. *Brain research* **506**, 339-342.

Goeckeler, Z. M. and Wysolmerski, R. B. (1995). Myosin light chain kinase-regulated endothelial cell contraction: the relationship between isometric tension, actin polymerization, and myosin phosphorylation. *The Journal of cell biology* **130**, 613-627.

Gorina, R., Lyck, R., Vestweber, D. and Engelhardt, B. (2013). beta2 Integrin-Mediated Crawling on Endothelial ICAM-1 and ICAM-2 Is a Prerequisite for Transcellular Neutrophil Diapedesis across the Inflamed Blood-Brain Barrier. *Journal of immunology*.

Gorina, R., Santalucia, T., Petegnief, V., Ejarque-Ortiz, A., Saura, J. and Planas, A. M. (2009). Astrocytes are very sensitive to develop innate immune responses to lipid-carried short interfering RNA. *Glia* **57**, 93-107.

Gottlieb, T. M., Leal, J. F., Seger, R., Taya, Y. and Oren, M. (2002). Cross-talk between Akt, p53 and Mdm2: possible implications for the regulation of apoptosis. *Oncogene* **21**, 1299-1303.

Griffin, J. H., Zlokovic, B. V. and Mosnier, L. O. (2012). Protein C anticoagulant and cytoprotective pathways. *International journal of hematology* **95**, 333-345.

Guo, H., Barrett, T. M., Zhong, Z., Fernandez, J. A., Griffin, J. H., Freeman, R. S. and Zlokovic, B. V. (2011). Protein S blocks the extrinsic apoptotic cascade in tissue plasminogen activator/N-methyl D-aspartate-treated neurons via Tyro3-Akt-FKHRL1 signaling pathway. *Molecular neurodegeneration* **6**, 13.

Guo, H., Liu, D., Gelbard, H., Cheng, T., Insalaco, R., Fernandez, J. A., Griffin, J. H. and Zlokovic, B. V. (2004). Activated protein C prevents neuronal apoptosis via protease activated receptors 1 and 3. *Neuron* **41**, 563-572.

Guo, H., Zhao, Z., Yang, Q., Wang, M., Bell, R. D., Wang, S., Chow, N., Davis, T. P., Griffin, J. H., Goldman, S. A. et al. (2013). An activated protein C analog stimulates neuronal production by human neural progenitor cells via a PAR1-PAR3-S1PR1-Akt pathway. *The Journal of neuroscience : the official journal of the Society for Neuroscience* **33**, 6181-6190.

Hacke, W., Kaste, M., Bluhmki, E., Brozman, M., Davalos, A., Guidetti, D., Larrue, V., Lees, K. R., Medeghri, Z., Machnig, T. et al. (2008). Thrombolysis with alteplase 3 to 4.5 hours after acute ischemic stroke. *The New England journal of medicine* **359**, 1317-1329.

Hanson, E., Kanse, S. M., Joshi, A., Jood, K., Nilsson, S., Blomstrand, C. and Jern, C. (2012). Plasma factor VII-activating protease antigen levels and activity are increased in ischemic stroke. *Journal of thrombosis and haemostasis : JTH* **10**, 848-856.

Harukuni, I. and Bhardwaj, A. (2006). Mechanisms of brain injury after global cerebral ischemia. *Neurologic clinics* **24**, 1-21.

Hosomi, N., Ban, C. R., Naya, T., Takahashi, T., Guo, P., Song, X. Y. and Kohno, M. (2005). Tumor necrosis factor-alpha neutralization reduced cerebral edema through inhibition of matrix metalloproteinase production after transient focal cerebral ischemia. *Journal of cerebral blood flow and metabolism : official journal of the International Society of Cerebral Blood Flow and Metabolism* **25**, 959-967.

Hu, X., Pandolfi, P. P., Li, Y., Koutcher, J. A., Rosenblum, M. and Holland, E. C. (2005). mTOR promotes survival and astrocytic characteristics induced by Pten/AKT signaling in glioblastoma. *Neoplasia* **7**, 356-368.

Huang, J., Upadhyay, U. M. and Tamargo, R. J. (2006). Inflammation in stroke and focal cerebral ischemia. *Surgical neurology* **66**, 232-245.

Iredale, J. P. (2007). Models of liver fibrosis: exploring the dynamic nature of inflammation and repair in a solid organ. *The Journal of clinical investigation* **117**, 539-548.

Ishida, Y., Nagai, A., Kobayashi, S. and Kim, S. U. (2006). Upregulation of protease-activated receptor-1 in astrocytes in Parkinson disease: astrocyte-mediated neuroprotection through increased levels of glutathione peroxidase. *Journal of neuropathology and experimental neurology* **65**, 66-77.

Jiao, H., Wang, Z., Liu, Y., Wang, P. and Xue, Y. (2011). Specific role of tight junction proteins claudin-5, occludin, and ZO-1 of the blood-brain barrier in a focal cerebral ischemic insult. *Journal of molecular neuroscience : MN* **44**, 130-139.

Kannemeier, C., Feussner, A., Stohr, H. A., Weisse, J., Preissner, K. T. and Romisch, J. (2001). Factor VII and single-chain plasminogen activator-activating protease: activation and autoactivation of the proenzyme. *European journal of biochemistry / FEBS* **268**, 3789-3796.

Kanse, S. M., Declerck, P. J., Ruf, W., Broze, G. and Etscheid, M. (2012). Factor VII-activating protease promotes the proteolysis and inhibition of tissue factor pathway inhibitor. *Arteriosclerosis, thrombosis, and vascular biology* **32**, 427-433.

Kanse, S. M., Parahuleva, M., Muhl, L., Kemkes-Matthes, B., Sedding, D. and Preissner, K. T. (2008). Factor VII-activating protease (FSAP): vascular functions and role in atherosclerosis. *Thrombosis and haemostasis* **99**, 286-289.

Koto, T., Takubo, K., Ishida, S., Shinoda, H., Inoue, M., Tsubota, K., Okada, Y. and Ikeda, E. (2007). Hypoxia disrupts the barrier function of neural blood vessels through changes in the expression of claudin-5 in endothelial cells. *The American journal of pathology* **170**, 1389-1397.

Koubi, D., Jiang, H., Zhang, L., Tang, W., Kuo, J., Rodriguez, A. I., Hunter, T. J., Seidman, M. D., Corcoran, G. B. and Levine, R. A. (2005). Role of Bcl-2 family of proteins in mediating apoptotic death of PC12 cells exposed to oxygen and glucose deprivation. *Neurochemistry international* **46**, 73-81.

Lan, R., Xiang, J., Zhang, Y., Wang, G. H., Bao, J., Li, W. W., Zhang, W., Xu, L. L. and Cai, D. F. (2013). PI3K/Akt Pathway Contributes to Neurovascular Unit Protection of Xiao-Xu-Ming Decoction against Focal Cerebral Ischemia and Reperfusion Injury in Rats. *Evidence-based complementary and alternative medicine : eCAM* **2013**, 459467.

Langhauser, F. L., Heiler, P. M., Grudzenski, S., Lemke, A., Alonso, A., Schad, L. R., Hennerici, M. G., Meairs, S. and Fatar, M. (2012). Thromboembolic stroke in C57BL/6 mice monitored by 9.4 T MRI using a 1H cryo probe. *Experimental & translational stroke medicine* **4**, 18.

Le, D. A., Wu, Y., Huang, Z., Matsushita, K., Plesnila, N., Augustinack, J. C., Hyman, B. T., Yuan, J., Kuida, K., Flavell, R. A. et al. (2002). Caspase activation and neuroprotection in caspase-3- deficient mice after in vivo cerebral ischemia and in vitro oxygen glucose deprivation. *Proceedings of the National Academy of Sciences of the United States of America* **99**, 15188-15193.

Li, G., Simon, M. J., Cancel, L. M., Shi, Z. D., Ji, X., Tarbell, J. M., Morrison, B., 3rd and Fu, B. M. (2010). Permeability of endothelial and astrocyte cocultures: in vitro blood-brain barrier models for drug delivery studies. *Annals of biomedical engineering* **38**, 2499-2511.

Li, J., Lang, J., Zeng, Z. and McCullough, L. D. (2008). Akt1 gene deletion and stroke. *Journal of the neurological sciences* **269**, 105-112.

Li, Y., Xu, N., Cai, L., Gao, Z., Shen, L., Zhang, Q., Hou, W., Zhong, H., Wang, Q. and Xiong, L. (2013). NDRG2 is a novel p53-associated regulator of apoptosis in C6-originated astrocytes exposed to oxygen-glucose deprivation. *PloS one* **8**, e57130.

Lin, B., Ginsberg, M. D. and Busto, R. (1998). Hyperglycemic exacerbation of neuronal damage following forebrain ischemia: microglial, astrocytic and endothelial alterations. *Acta neuropathologica* **96**, 610-620.

Lin, C. H., Cheng, F. C., Lu, Y. Z., Chu, L. F., Wang, C. H. and Hsueh, C. M. (2006). Protection of ischemic brain cells is dependent on astrocyte-derived growth factors and their receptors. *Experimental neurology* **201**, 225-233.

Lipton, P. (1999). Ischemic cell death in brain neurons. *Physiological reviews* **79**, 1431-1568.

Liu, B. and Neufeld, A. H. (2004). Activation of epidermal growth factor receptor causes astrocytes to form cribriform structures. *Glia* **46**, 153-168.

Liu, D., Cheng, T., Guo, H., Fernandez, J. A., Griffin, J. H., Song, X. and Zlokovic, B. V. (2004). Tissue plasminogen activator neurovascular toxicity is controlled by activated protein C. *Nature medicine* **10**, 1379-1383.

Liu, G. P., Wei, W., Zhou, X., Zhang, Y., Shi, H. H., Yin, J., Yao, X. Q., Peng, C. X., Hu, J., Wang, Q. et al. (2012). I(2)(PP2A) regulates p53 and Akt correlatively and leads the neurons to abort apoptosis. *Neurobiology of aging* **33**, 254-264.

Liu, J., Jin, X., Liu, K. J. and Liu, W. (2012). Matrix metalloproteinase-2-mediated occludin degradation and caveolin-1-mediated claudin-5 redistribution contribute to blood-brain barrier damage in early ischemic stroke stage. *The Journal of neuroscience : the official journal of the Society for Neuroscience* **32**, 3044-3057.

Lo, E. H., Dalkara, T. and Moskowitz, M. A. (2003). Mechanisms, challenges and opportunities in stroke. *Nature reviews. Neuroscience* **4**, 399-415.

Lopez-Atalaya, J. P., Roussel, B. D., Ali, C., Maubert, E., Petersen, K. U., Berezowski, V., Cecchelli, R., Orset, C. and Vivien, D. (2007). Recombinant Desmodus rotundus salivary plasminogen activator crosses the blood-brain barrier through a low-density lipoprotein receptor-related protein-dependent mechanism without exerting neurotoxic effects. *Stroke; a journal of cerebral circulation* **38**, 1036-1043.

Ludewig, P., Sedlacik, J., Gelderblom, M., Bernreuther, C., Korkusuz, Y., Wagener, C., Gerloff, C., Fiehler, J., Magnus, T. and Horst, A. K. (2013). Carcinoembryonic antigen-related cell adhesion molecule 1 inhibits MMP-9-mediated blood-brain-barrier breakdown in a mouse model for ischemic stroke. *Circulation research* **113**, 1013-1022.

Mambetsariev, N., Mirzapoiazova, T., Mambetsariev, B., Sammani, S., Lennon, F. E., Garcia, J. G. and Singleton, P. A. (2010). Hyaluronic Acid binding protein 2 is a novel regulator of vascular integrity. *Arteriosclerosis, thrombosis, and vascular biology* **30**, 483-490.

Manwani, B., Friedler, B., Verma, R., Venna, V. R., McCullough, L. D. and Liu, F. (2013). Perfusion of Ischemic Brain in Young and Aged Animals: A Laser Speckle Flowmetry Study. *Stroke; a journal of cerebral circulation*.

Mark, K. S. and Davis, T. P. (2002). Cerebral microvascular changes in permeability and tight junctions induced by hypoxia-reoxygenation. *American journal of physiology. Heart and circulatory physiology* **282**, H1485-1494.

Martin-Schild, S. (2012). tPA for stroke--are we ready to remove the barriers? *European journal of neurology : the official journal of the European Federation of Neurological Societies* **19**, 359.

Martinez-Hernandez, A., Bell, K. P. and Norenberg, M. D. (1977). Glutamine synthetase: glial localization in brain. *Science* **195**, 1356-1358.
Martinez, A. D. and Saez, J. C. (2000). Regulation of astrocyte gap junctions by hypoxia-reoxygenation. *Brain research. Brain research reviews* **32**, 250-258.
Mehta, S. L., Manhas, N. and Raghubir, R. (2007). Molecular targets in cerebral ischemia for developing novel therapeutics. *Brain research reviews* **54**, 34-66.
Moskowitz, M. A., Lo, E. H. and Iadecola, C. (2010). The science of stroke: mechanisms in search of treatments. *Neuron* **67**, 181-198.
Mosnier, L. O., Zlokovic, B. V. and Griffin, J. H. (2007). The cytoprotective protein C pathway. *Blood* **109**, 3161-3172.
Mosnier, L. O., Sinha, R. K., Burnier, L., Bouwens, E. A. and Griffin, J. H. (2012). Biased agonism of protease-activated receptor 1 by activated protein C caused by noncanonical cleavage at Arg46. *Blood* **120**, 5237-5246.
Muhl, L., Hersemeyer, K., Preissner, K. T., Weimer, T. and Kanse, S. M. (2009). Structure-function analysis of factor VII activating protease (FSAP): sequence determinants for heparin binding and cellular functions. *FEBS letters* **583**, 1994-1998.
Muhl, L., Nykjaer, A., Wygrecka, M., Monard, D., Preissner, K. T. and Kanse, S. M. (2007). Inhibition of PDGF-BB by Factor VII-activating protease (FSAP) is neutralized by protease nexin-1, and the FSAP-inhibitor complexes are internalized via LRP. *The Biochemical journal* **404**, 191-196.
Nakka, V. P., Gusain, A., Mehta, S. L. and Raghubir, R. (2008). Molecular mechanisms of apoptosis in cerebral ischemia: multiple neuroprotective opportunities. *Molecular neurobiology* **37**, 7-38.
Namura, S., Zhu, J., Fink, K., Endres, M., Srinivasan, A., Tomaselli, K. J., Yuan, J. and Moskowitz, M. A. (1998). Activation and cleavage of caspase-3 in apoptosis induced by experimental cerebral ischemia. *The Journal of neuroscience : the official journal of the Society for Neuroscience* **18**, 3659-3668.
Neary, J. T., Kang, Y., Tran, M. and Feld, J. (2005). Traumatic injury activates protein kinase B/Akt in cultured astrocytes: role of extracellular ATP and P2 purinergic receptors. *Journal of neurotrauma* **22**, 491-500.
Nilupul Perera, M., Ma, H. K., Arakawa, S., Howells, D. W., Markus, R., Rowe, C. C. and Donnan, G. A. (2006). Inflammation following stroke. *Journal of clinical neuroscience : official journal of the Neurosurgical Society of Australasia* **13**, 1-8.
Ogawara, Y., Kishishita, S., Obata, T., Isazawa, Y., Suzuki, T., Tanaka, K., Masuyama, N. and Gotoh, Y. (2002). Akt enhances Mdm2-mediated ubiquitination and degradation of p53. *The Journal of biological chemistry* **277**, 21843-21850.
Orset, C., Macrez, R., Young, A. R., Panthou, D., Angles-Cano, E., Maubert, E., Agin, V. and Vivien, D. (2007). Mouse model of in situ thromboembolic stroke and reperfusion. *Stroke; a journal of cerebral circulation* **38**, 2771-2778.
Pan, J., Konstas, A. A., Bateman, B., Ortolano, G. A. and Pile-Spellman, J. (2007). Reperfusion injury following cerebral ischemia: pathophysiology, MR imaging, and potential therapies. *Neuroradiology* **49**, 93-102.
Pan, W. and Kastin, A. J. (2007). Tumor necrosis factor and stroke: role of the blood-brain barrier. *Progress in neurobiology* **83**, 363-374.
Parcq, J., Bertrand, T., Montagne, A., Baron, A. F., Macrez, R., Billard, J. M., Briens, A., Hommet, Y., Wu, J., Yepes, M. et al. (2012). Unveiling an exceptional zymogen: the single-chain form of tPA is a selective activator of NMDA receptor-dependent signaling and neurotoxicity. *Cell death and differentiation* **19**, 1983-1991.

Planas, A. M., Gorina, R. and Chamorro, A. (2006). Signalling pathways mediating inflammatory responses in brain ischaemia. *Biochemical Society transactions* **34**, 1267-1270.

Plesnila, N., Zinkel, S., Le, D. A., Amin-Hanjani, S., Wu, Y., Qiu, J., Chiarugi, A., Thomas, S. S., Kohane, D. S., Korsmeyer, S. J. et al. (2001). BID mediates neuronal cell death after oxygen/ glucose deprivation and focal cerebral ischemia. *Proceedings of the National Academy of Sciences of the United States of America* **98**, 15318-15323.

Pugazhenthi, S., Nesterova, A., Sable, C., Heidenreich, K. A., Boxer, L. M., Heasley, L. E. and Reusch, J. E. (2000). Akt/protein kinase B up-regulates Bcl-2 expression through cAMP-response element-binding protein. *The Journal of biological chemistry* **275**, 10761-10766.

Rainer, T. H., Wong, L. K., Lam, W., Yuen, E., Lam, N. Y., Metreweli, C. and Lo, Y. M. (2003). Prognostic use of circulating plasma nucleic acid concentrations in patients with acute stroke. *Clinical chemistry* **49**, 562-569.

Ransom, B. R. and Ransom, C. B. (2012). Astrocytes: multitalented stars of the central nervous system. *Methods in molecular biology* **814**, 3-7.

Reddrop, C., Moldrich, R. X., Beart, P. M., Farso, M., Liberatore, G. T., Howells, D. W., Petersen, K. U., Schleuning, W. D. and Medcalf, R. L. (2005). Vampire bat salivary plasminogen activator (desmoteplase) inhibits tissue-type plasminogen activator-induced potentiation of excitotoxic injury. *Stroke; a journal of cerebral circulation* **36**, 1241-1246.

Resendiz, J. C., Kroll, M. H. and Lassila, R. (2007). Protease-activated receptor-induced Akt activation--regulation and possible function. *Journal of thrombosis and haemostasis : JTH* **5**, 2484-2493.

Roedel, E. K., Schwarz, E. and Kanse, S. M. (2013). The factor VII-activating protease (FSAP) enhances the activity of bone morphogenetic protein-2 (BMP-2). *The Journal of biological chemistry* **288**, 7193-7203.

Rohatgi, T., Sedehizade, F., Reymann, K. G. and Reiser, G. (2004). Protease-activated receptors in neuronal development, neurodegeneration, and neuroprotection: thrombin as signaling molecule in the brain. *The Neuroscientist : a review journal bringing neurobiology, neurology and psychiatry* **10**, 501-512.

Romera, C., Hurtado, O., Botella, S. H., Lizasoain, I., Cardenas, A., Fernandez-Tome, P., Leza, J. C., Lorenzo, P. and Moro, M. A. (2004). In vitro ischemic tolerance involves upregulation of glutamate transport partly mediated by the TACE/ADAM17-tumor necrosis factor-alpha pathway. *The Journal of neuroscience : the official journal of the Society for Neuroscience* **24**, 1350-1357.

Romisch, J., Feussner, A. and Stohr, H. A. (2001). Quantitation of the factor VII- and single-chain plasminogen activator-activating protease in plasmas of healthy subjects. *Blood coagulation & fibrinolysis : an international journal in haemostasis and thrombosis* **12**, 375-383.

Rosmorduc, O., Wendum, D., Corpechot, C., Galy, B., Sebbagh, N., Raleigh, J., Housset, C. and Poupon, R. (1999). Hepatocellular hypoxia-induced vascular endothelial growth factor expression and angiogenesis in experimental biliary cirrhosis. *The American journal of pathology* **155**, 1065-1073.

Rothwell, N. (2003). Interleukin-1 and neuronal injury: mechanisms, modification, and therapeutic potential. *Brain, behavior, and immunity* **17**, 152-157.

Rothwell, N. J. and Luheshi, G. N. (2000). Interleukin 1 in the brain: biology, pathology and therapeutic target. *Trends in neurosciences* **23**, 618-625.

Roussel, B. D., Mysiorek, C., Rouhiainen, A., Jullienne, A., Parcq, J., Hommet, Y., Culot, M., Berezowski, V., Cecchelli, R., Rauvala, H. et al. (2011). HMGB-1 promotes fibrinolysis and reduces neurotoxicity mediated by tissue plasminogen activator. *Journal of cell science* **124**, 2070-2076.

Sari, S., Hashemi, M., Mahdian, R., Parivar, K. and Rezayat, M. (2013). The Effect of Pentoxifylline on bcl-2 Gene Expression Changes in Hippocampus after Ischemia-Reperfusion in Wistar Rats by a Quatitative RT-PCR Method. *Iranian journal of pharmaceutical research : IJPR* **12**, 495-501.

Sharma, S., Yang, B., Xi, X., Grotta, J. C., Aronowski, J. and Savitz, S. I. (2011). IL-10 directly protects cortical neurons by activating PI-3 kinase and STAT-3 pathways. *Brain research* **1373**, 189-194.

Shichita, T., Ago, T., Kamouchi, M., Kitazono, T., Yoshimura, A. and Ooboshi, H. (2012). Novel therapeutic strategies targeting innate immune responses and early inflammation after stroke. *Journal of neurochemistry* **123 Suppl 2**, 29-38.

Silver, J. and Miller, J. H. (2004). Regeneration beyond the glial scar. *Nature reviews. Neuroscience* **5**, 146-156.

Soane, L. and Fiskum, G. (2005). Inhibition of mitochondrial neural cell death pathways by protein transduction of Bcl-2 family proteins. *Journal of bioenergetics and biomembranes* **37**, 179-190.

Sochocka, E., Juurlink, B. H., Code, W. E., Hertz, V., Peng, L. and Hertz, L. (1994). Cell death in primary cultures of mouse neurons and astrocytes during exposure to and 'recovery' from hypoxia, substrate deprivation and simulated ischemia. *Brain research* **638**, 21-28.

Steiner, O., Coisne, C., Engelhardt, B. and Lyck, R. (2011). Comparison of immortalized bEnd5 and primary mouse brain microvascular endothelial cells as in vitro blood-brain barrier models for the study of T cell extravasation. *Journal of cerebral blood flow and metabolism : official journal of the International Society of Cerebral Blood Flow and Metabolism* **31**, 315-327.

Stephan, F., Hazelzet, J. A., Bulder, I., Boermeester, M. A., van Till, J. O., van der Poll, T., Wuillemin, W. A., Aarden, L. A. and Zeerleder, S. (2011). Activation of factor VII-activating protease in human inflammation: a sensor for cell death. *Critical care* **15**, R110.

Strong, A. J., Bezzina, E. L., Anderson, P. J., Boutelle, M. G., Hopwood, S. E. and Dunn, A. K. (2006). Evaluation of laser speckle flowmetry for imaging cortical perfusion in experimental stroke studies: quantitation of perfusion and detection of peri-infarct depolarisations. *Journal of cerebral blood flow and metabolism : official journal of the International Society of Cerebral Blood Flow and Metabolism* **26**, 645-653.

Supanc, V., Biloglav, Z., Kes, V. B. and Demarin, V. (2011). Role of cell adhesion molecules in acute ischemic stroke. *Annals of Saudi medicine* **31**, 365-370.

Swanson, R. A., Farrell, K. and Stein, B. A. (1997). Astrocyte energetics, function, and death under conditions of incomplete ischemia: a mechanism of glial death in the penumbra. *Glia* **21**, 142-153.

Trompet, S., Pons, D., Kanse, S. M., de Craen, A. J., Ikram, M. A., Verschuren, J. J., Zwinderman, A. H., Doevendans, P. A., Tio, R. A., de Winter, R. J. et al. (2011). Factor VII Activating Protease Polymorphism (G534E) Is Associated with Increased Risk for Stroke and Mortality. *Stroke research and treatment* **2011**, 424759.

Unal-Cevik, I., Kilinc, M., Can, A., Gursoy-Ozdemir, Y. and Dalkara, T. (2004). Apoptotic and necrotic death mechanisms are concomitantly activated in the same cell after cerebral ischemia. *Stroke; a journal of cerebral circulation* **35**, 2189-2194.

Vaseva, A. V., Marchenko, N. D., Ji, K., Tsirka, S. E., Holzmann, S. and Moll, U. M. (2012). p53 opens the mitochondrial permeability transition pore to trigger necrosis. *Cell* **149**, 1536-1548.

Wang, Q., Tang, X. N. and Yenari, M. A. (2007). The inflammatory response in stroke. *Journal of neuroimmunology* **184**, 53-68.

Wang, Y., Yang, J., Zheng, H., Tomasek, G. J., Zhang, P., McKeever, P. E., Lee, E. Y. and Zhu, Y. (2009). Expression of mutant p53 proteins implicates a lineage relationship between neural stem cells and malignant astrocytic glioma in a murine model. *Cancer cell* **15**, 514-526.

White, B. C., Sullivan, J. M., DeGracia, D. J., O'Neil, B. J., Neumar, R. W., Grossman, L. I., Rafols, J. A. and Krause, G. S. (2000). Brain ischemia and reperfusion: molecular mechanisms of neuronal injury. *Journal of the neurological sciences* **179**, 1-33.

Willeit, J., Kiechl, S., Weimer, T., Mair, A., Santer, P., Wiedermann, C. J. and Roemisch, J. (2003). Marburg I polymorphism of factor VII--activating protease: a prominent risk predictor of carotid stenosis. *Circulation* **107**, 667-670.

Won, S. J., Kim, D. Y. and Gwag, B. J. (2002). Cellular and molecular pathways of ischemic neuronal death. *Journal of biochemistry and molecular biology* **35**, 67-86.

Xie, R., Cheng, M., Li, M., Xiong, X., Daadi, M., Sapolsky, R. M. and Zhao, H. (2013). Akt isoforms differentially protect against stroke-induced neuronal injury by regulating mTOR activities. *Journal of cerebral blood flow and metabolism : official journal of the International Society of Cerebral Blood Flow and Metabolism* **33**, 1875-1885.

Yamamichi, S., Fujiwara, Y., Kikuchi, T., Nishitani, M., Matsushita, Y. and Hasumi, K. (2011). Extracellular histone induces plasma hyaluronan-binding protein (factor VII activating protease) activation in vivo. *Biochemical and biophysical research communications* **409**, 483-488.

Yang, G. Y., Gong, C., Qin, Z., Ye, W., Mao, Y. and Bertz, A. L. (1998). Inhibition of TNFalpha attenuates infarct volume and ICAM-1 expression in ischemic mouse brain. *Neuroreport* **9**, 2131-2134.

Yang, Y., Estrada, E. Y., Thompson, J. F., Liu, W. and Rosenberg, G. A. (2007). Matrix metalloproteinase-mediated disruption of tight junction proteins in cerebral vessels is reversed by synthetic matrix metalloproteinase inhibitor in focal ischemia in rat. *Journal of cerebral blood flow and metabolism : official journal of the International Society of Cerebral Blood Flow and Metabolism* **27**, 697-709.

Zehendner, C. M., Librizzi, L., de Curtis, M., Kuhlmann, C. R. and Luhmann, H. J. (2011). Caspase-3 contributes to ZO-1 and Cl-5 tight-junction disruption in rapid anoxic neurovascular unit damage. *PloS one* **6**, e16760.

Zhao, H., Sapolsky, R. M. and Steinberg, G. K. (2006). Phosphoinositide-3-kinase/akt survival signal pathways are implicated in neuronal survival after stroke. *Molecular neurobiology* **34**, 249-270.

Zhao, H., Yenari, M. A., Cheng, D., Sapolsky, R. M. and Steinberg, G. K. (2003). Bcl-2 overexpression protects against neuron loss within the ischemic margin following experimental stroke and inhibits cytochrome c translocation and caspase-3 activity. *Journal of neurochemistry* **85**, 1026-1036.

Zhao, H., Shimohata, T., Wang, J. Q., Sun, G., Schaal, D. W., Sapolsky, R. M. and Steinberg, G. K. (2005). Akt contributes to neuroprotection by hypothermia against cerebral ischemia in rats. *The Journal of neuroscience : the official journal of the Society for Neuroscience* **25**, 9794-9806.

Zhong, Z., Wang, Y., Guo, H., Sagare, A., Fernandez, J. A., Bell, R. D., Barrett, T. M., Griffin, J. H., Freeman, R. S. and Zlokovic, B. V. (2010). Protein S protects neurons from excitotoxic injury by activating the TAM receptor Tyro3-phosphatidylinositol 3-kinase-Akt pathway through its sex hormone-binding globulin-like region. *The Journal of neuroscience : the official journal of the Society for Neuroscience* **30**, 15521-15534.

Declaration

I declare that I have completed this dissertation single-handedly without the unauthorized help of a second party and only with the assistance acknowledged therein. I have appropriately acknowledged and referenced all text passages that are derived literally from or are based on the content of published or unpublished work of others, and all information that relates to verbal communications. I have abided by the principles of good scientific conduct laid down in the charter of the Justus Liebig University of Giessen in carrying out the investigations described in the dissertation

Date:_____ AMIT UMESH JOSHI

10. Publications

10.1. Articles

1. **Deficiency of FSAP exacerbates stroke outcome after thromboembolic stroke in mice.**
   A.U. Joshi, C. Orset, D. Vivien, S.M. Kanse.
   In preparation

2. **Factor Seven Activating Protease (FSAP) regulates blood brain barrier permeability and astrocyte survival after ischemic and oxidative injury *in vitro*.**
   A.U. Joshi, R. Gorina, B. Engelhardt, S.M. Kanse.
   Submitted

3. **Factor Seven Activating Protease (FSAP) imparts neuroprotection *in-vitro* to primary cortical neurons against excitotoxic and hypoxic injury.**
   A.U. Joshi, S.M. Kanse.
   Submitted.

4. **Plasma FVII-Activating Protease (FSAP) Antigen and Activity Levels are increased in Ischemic Stroke.**
   E. Hanson, S. M. Kanse, A. Joshi, K. Jood, S. Nilsson, C. Blomstrand, and C. Jern.
   J Thromb Haemost. 2012 May; 10(5):848-56.

10.2. Abstracts

1. **Novel role for Factor VII activating protease (FSAP) in Ischemic Stroke**
   A.U. Joshi, R. Gorina, C. Orset, B. Engelhardt, D. Vivien, S. M. Kanse.
   Submitted to 8th International Symposium Neuroprotection & Neurorepair, 9th April – 12th September 2014, Magdeburg, Germany

2. **FVII-activating protease (FSAP) protects astrocytes and neurons via activation of anti-apoptotic pathways of survival in hypoxic injury models**
   A.U. Joshi, R. Gorina, N. Schleicher, T. Gerriets, B. Engelhardt, S. M. Kanse.
   Accepted as a poster presentation at the 6th GGL Annual Conference, 11th – 12th September 2013, Giessen, Germany

3. **FVII-activating protease (FSAP) confers protection to Primary Astrocytes and Neurons exposed to Oxygen-Glucose deprived conditions**
   A.U. Joshi, N. Schleicher, K. Mayer, T. Gerriets, S. M. Kanse
   Accepted as a poster presentation in Group A at XXIV Congress of the International Society on Thrombosis and Haemostasis, 29th June – 4th July 2013, Amsterdam, Netherlands.

4. **The effect of Factor VII Activating Protease (FSAP) on neurons and astrocytes**
   A.U. Joshi, S.M. Kanse
   Accepted as a poster presentation at the 5th GGL Annual Conference, 18th – 19th September 2012, Giessen, Germany

5. **Role of Factor VII activating protease (FSAP) in the pathogenesis of stroke**
   A.U. Joshi, E. Hanson, N. Schleicher, K. Mayer, T. Gerriets, K. Jood, C. Blomstrand, C. Jern and S.M. Kanse
   Accepted as a poster presentation at the ECCPS Symposium, 16th – 18th June 2011, Bad Nauheim, Germany

AKT	Protein Kinase B	**ELISA**	Enzyme-linked immunosorbent assay
AMPA	α-amino-3-hydroxy-5-methyl-4-isoxazolepropionic acid	**FBS**	Fetal Bovin Serum
APC	Activated Protein C	**FKHR**	forkhead transcription factor Foxo1
APO	Aprotinin	**FSAP**	Factor VII activating protease
ARA-C	cytosine arabinoside	**FV**	Factor V
BBB	Blood Brain Barrier	**FVIII**	Factor VIII
BDNF	Brain-derived neurotrophic factor	**GAPDH**	Glyceraldehyde 3-phosphate dehydrogenase
bFGF	basic Fibroblast growth factor	**GFAP**	Glial fibrillary acidic protein
BSA	Bovine Serum Albumin	**GPCRs**	G protein-coupled receptors
CNS	Central Nervous System	**GS**	Glutamine synthetase
ct	Threshold cycles	**GSK3β**	Glycogen synthase kinase 3 beta
DIV	Days *in-vitro*	**H_2O_2**	Hyrogen Peroxide
DMEM	Dulbecco's modified Eagle's medium	**HBSS**	Hank's Balanced Salt Solution
DMSO	Dimethyl sulfoxide	**HMWK**	High-molecular-weight kininogen
DWI	Diffusion-weighted imaging	**HT**	Hyper tension
ECs	Endothelial Cells	**ICAM**	Intercellular Adhesion Molecule
EDTA	Ethylenediaminetetraacetic acid	**IL**	Interlukin
EGF	Epidermal growth factor	**LDH**	Lactate dehydrogenase
LSF	Laser Speckle Flowmetry	**NO**	Nitric Oxide
MCA	Middle Cerebral Artery	**OGD**	Oxygen Glucose Deprivation
MCAO	Middle Cerebral Artery Occlusion	**PAR**	Protease activated receptor
MDM2	Mouse double minute 2 homolog	**PBS**	Phosphate buffered saline
MLCK	Myosin light-chain kinase	**PCR**	polymerase chain reaction
MMP	Matrix metalloproteinases	**PDGF BB**	platelet-derived growth factor
MRA	Magnetic resonance angiography	**PDK-1**	Pyruvate dehydrogenase lipoamide kinase isozyme 1

MRI	Magnetic resonance imaging	**PECAM**	Platelet endothelial cell adhesion molecule
MTT	3-(4,5-dimethylthiazol-2-yl)-2,5-diphenyltetrazolium bromide	**PI3K**	Phosphoinositide 3-kinase
Na_3VO_4	Sodium orthovanadate	**pMBMECs**	primary mouse brain microvascular endothelial cells
NaCl	Sodium Choride	**PPACK**	D-Phenylalanyl-L-prolyl-L-arginine chloromethyl ketone
NaF	Sodium Floride	**PTEN**	Phosphatase and tensin homolog
NaN_3	Sodium Azide	**PVDF**	Polyvinylidene difluoride
NaPyr	Sodium Pyruvate	**ROS**	Reactive oxygen species
NEAA	Non-Essential Amino Acid	**SNP**	Single Nucleotide - polymorphism
NeuN	Neuronal Nuclei	**STAT**	Signal Transducer and Activator of Transcription
NGF	Nerve growth factor	**TBS**	Tris buffered saline
NMDA	N-Methyl-D-aspartate	**TdT**	terminal deoxynucleotidyl transferase
LSF	Laser Speckle Flowmetry	**NO**	Nitric Oxide
TEER	Trans-Endothelial Electrical Resistance	**uPA**	Urokinase
TFPI	Tissue factor pathway inhibitor	**VCAM**	Vascular cell adhesion protein
TGFβ-1	Transforming growth factor beta 1	**VEGF**	Vascular endothelial growth factor
TIA	transient ischemic attack	**ZO-1**	Zona Occludens -1
TMB	3,3',5,5'-Tetramethylbenzidine		
TNFα	Tumor necrosis factor alpha		
TOF	Time of Flight		
tPA	Tissue plasminogen activator		
TUNEL	Terminal deoxynucleotidyl transferase dUTP nick end labeling		

1. List of devices used

Product	*Company*
BD GasPak ™ EZ Container Systems	BD Biosciences, CA, USA
Bruker PharmaScan 7.0 T, 16 cm	Bruker Corportation, Germany
Dissecting microscope: Leica S4E	Leica Microsystems, Wetzlar, Germany
Fluorescence microscope: Leica DMRB	Leica Microsystems, Wetzlar, Germany
GraphPad Prism 6	GraphPad Software, Inc., La Jolla, CA, USA
Innova CO_2 incubator CO-48	New Brunswick Scientific, NJ, USA
Metamorph Imaging software 7.0	Molecular Devices, Downingtown, PA, USA
Microplate reader EL808	Biotek Instruments, Winooski, OR, USA

2. Reagents

Product	*Company*
2-Mercaptoethanol	Carl Roth, Karlsruhe, Germany
2-Propanol	Carl Roth, Karlsruhe, Germany
3,3,5,5-tetramethylbenzidine (TMB)	EUROPA (Cambridge, UK)
Acetic acid	Carl Roth, Karlsruhe, Germany
Acetone 99,8%	Merck, Darmstadt, Germany
Agarose	Molecular Probes, Leiden, The Netherlands
Arginine	Sigma-Aldrich Chemie, Munich, Germany
Bovine serum albumin (BSA)	Sigma-Aldrich Chemie, Munich, Germany
Calcium chloride	Carl Roth, Karlsruhe, Germany
DAPI	Linaris, Wertheim, Germany
Dry milk, fat-free	Sigma-Aldrich Chemie, Munich, Germany
Dulbecco's modified eagle medium (D-MEM)	Invitrogen, Karsruhe, Germany

Dulbecco's modified eagle medium (D-MEM) F12	Invitrogen, Karsruhe, Germany
Dulbecco's modified eagle medium (D-MEM) without Glucose	Invitrogen, Karsruhe, Germany
Dulbecco‟s phosphate buffered saline (PBS)	PAA Laboratories, Pasching, Austria
Ethanol	Riedel-de Haën Sigma-Aldrich, Seelsze, Germany
Fetal calf serum (FCS)	Invitrogen, Karsruhe, Germany
FITC dextran 30 kDA	Invitrogen (Karlsruhe, Germany)
Formalin solution (PFA)	Carl Roth, Karlsruhe, Germany
Gelatin 2% solution	Invitrogen (Karlsruhe, Germany)
Glucose	Carl Roth, Karlsruhe, Germany
Glycerol	Sigma-Aldrich Chemie, Munich, Germany
Glycine	Sigma-Aldrich Chemie, Munich, Germany
Hank's Balanced Salt Solution	Invitrogen (Karlsruhe, Germany)
Horse Serum	Invitrogen (Karlsruhe, Germany)
Hydrogen Peroxide 30% (H_2O_2)	Merck, Darmstadt, Germany
Isopropanol	Carl Roth, Karlsruhe, Germany
Laminin	Invitrogen (Karlsruhe, Germany)
Lysine	Sigma-Aldrich Chemie, Munich, Germany
Methanol	Carl Roth, Karlsruhe, Germany
MTT	Sigma-Aldrich Chemie, Munich, Germany
NMDA	Sigma-Aldrich Chemie, Munich, Germany
PageRuler Prestained Protein Ladder	Fermentas (St. Leon-Rot, Germany)
Penicillin / Streptomycin	Invitrogen, Karsruhe, Germany
Plasminogen	From blood of healthy volunteers

Poly-D-Lysine	Sigma-Aldrich Chemie, Munich, Germany
Poly-L-Lysine	Sigma-Aldrich Chemie, Munich, Germany
RNeasy Mini Kit	Sigma-Aldrich Chemie, Munich, Germany
Sodium acetate	Carl Roth, Karlsruhe, Germany
Sodium chloride 0,9% (NaCl)	Carl Roth, Karlsruhe, Germany
Sodium chloride solution	Carl Roth, Karlsruhe, Germany
Sodium citrate	Carl Roth, Karlsruhe, Germany
Sodium dodecyl sulfate (SDS)	Carl Roth, Karlsruhe, Germany
TEMED	Carl Roth, Karlsruhe, Germany
Tissue plasminogen activator (Activase® (Alteplase))	Genentech, Inc., CA., USA
Triton X-100	Carl Roth, Karlsruhe, Germany
Tween 20	Sigma-Aldrich Chemie, Munich, Germany
Tween 80	Sigma-Aldrich Chemie, Munich, Germany
Vectashield mounting medium H 1000 for Fluorescence	Vector Laboratories, Burlington, CA, USA

All other chemicals were obtained from Sigma (Munich, Germany) or Roth (Karlsruhe, Germany).

3. Primer sequence of oligonucleotides used for quantitative realtime PCR

Gene Primer	**Sequence**
COX-2 Forward	ATGGTAGAAGTTGGAGCACCA
COX-2 Reverse	GGAGCGGGAAGAACTTGCA
GADPH Reverse	CGGCCAAATCCGTTCACACCGA
GAPDH Forward	CGCCACCAGTTCGCCATGGA
IL-10 Forward	GCTCTTACTGACTGGCATGAG
IL-10 Reverse	CGCAGCTCTAGGAGCATGTG

IL-4 Forward	ACAGGAGAAGGGACGCCAT
IL-4 Reverse	GAAGCCCTACAGACGAGCTCA
IL-6 Forward	ACAACGATGATGCACTTGCAGA
IL-6 Reverse	TCCAGGTAGCTATGGTACTCCA
iNOS - Forward	CAGGCCAATGGCCGTGA
iNOS - Reverse	TAGTTCAGCATCTCCTGGTGA
TNF alpha Forward	CCCTCACACTCAGATCATCTTCT
TNF alpha Reverse	GCTACGACGTGGGCTACAG

4. Primary and secondary antibodies for Western blotting

Antibody	**Species**	**Isotype**	**Source**	**Dilution**
Anti- pAKT	Rabbit	Polyclonal	Cell Signaling Technology Inc., USA	1:1000
Anti- Total Akt	Rabbit	Polyclonal	Cell Signaling Technology Inc., USA	1:1000
Anti- β-Actin	Rabbit	Polyclonal	Cell Signaling Technology Inc., USA	1:1000
Anti- p53	Rabbit	Polyclonal	Cell Signaling Technology Inc., USA	1:1000
Anti- Bcl-2	Rabbit	Polyclonal	Cell Signaling Technology Inc., USA	1:1000
Anti- GAPDH	Rabbit	Polyclonal	Cell Signaling Technology Inc., USA	1:1000
Anti- FSAP (MENEW)	Rabbit	Polyclonal	A gift from Dr. Michael Etscheid (Langen)	1:1000
Anti- Rabbit POD	Swine	Polyclonal	DAKO, Hamburg, Germany	1:2000

5. Antibodies used for staining

Antibody	Species	Isotype	Source	Dilution
Anti- GFAP	Mouse	Monoclonal	Millipore, Billerica, MA, USA	1:400
Anti- NeuN	Mouse	Monoclonal	Millipore, Billerica, MA, USA	1:400
Anti- ZO-1	Rabbit	Polyclonal	Invitrogen (Switzerland)	1:100
Alexa Fluor 488-Anti Rabbit	Goat	Polyclonal	Molecular Probes, Eugene, OR, USA	1:1000
Alexa Furo 488 – Anti mouse	Goat	Polyclonal	Molecular Probes, Eugene, OR, USA	1:1000

Dedication

This work is dedicated to

My father, Dr. Umesh K. Joshi
You inspired me to be everything that I am today and hope to be tomorrow.

&

My mother, Mrs. Janaki U. Joshi
You have always been there with me as a friend, loving mother and a true supporter.

This thesis would not have been completed without all the support and encouragement that I have received from my surroundings during these exciting years. I would like to express my gratitude to the wonderful people who in one or another way contributed to the completion of this thesis. I particular would like to thank:

My Supervisor, Prof. Sandip Kanse, for making my dream of pursuing a PhD a reality. Thank you for your incredible support, patience and help in teaching me the ways of scientific research, for always being helpful and available when needed. Your enormous enthusiasm for research and your ability to find ways out of impossible situations are simply amazing. I learned how to work independently and be flexible in research.

Prof. Britta Engelhardt and Dr. Roser Gorina, A special thanks for hosting me in Bern. It was a memorable month filled with ideas and discussions which I will always remember.

Prof. Denis Vivien and Dr. Cyrille Orset, Thank you for hosting me at your lab in Caen and teaching me new techniques related to stroke studies.

Prof. Klaus Preissner, for being supportive and great discussions during all these years. You have always had valuable inputs on my work, which has led me to really think things through.

Prof. Lienhard Schmitz, for the guidance with hypoxia chamber experiments,

Thomas Schmidt-Wöll, Susanne Tannert-Otto, Karin Hersemeyer and Baerbel Fuehler for excellent technical assistance and for being there whenever I needed,

Elfie, Silke, Mareike, Saravanan and Paul for creating a great environment in and outside the lab,

All the members of AG Preissner who provide a friendly atmosphere in the lab, their friendship and their assistance,

I would also like to thank the GGL International for providing me with the funding to perform collaborative research,

Parth, my brother, for being such an amazing brother and always supporting me in my endeavors,

Mom & Dad, for standing by me through my ups and downs for all these years,

My grandparents, for all the love and caring,

I am also very grateful for the continuous support and the love of my entire family, friends and well wishers.

Finally, and most importantly, I would like to thank my wife, Ketkee. Your support, encouragement, quiet patience and unwavering love have been the reasons why I have been able to complete this thesis. I owe you everything.

Der Lebenslauf wurde aus der elektronischen Version der Arbeit entfernt.

The curriculum vitae was removed from the electronic version of the paper.

Publications:

- **A.U. Joshi,** C. Orset, D. Vivien, S.M. Kanse., *"Deficiency of FSAP exacerbates stroke outcome after thromboembolic stroke in mice". In preparation*
- **A.U. Joshi,** R. Gorina, B. Engelhardt, S.M. Kanse. *"Factor Seven Activating Protease (FSAP) regulates blood brain barrier permeability and astrocyte survival after ischemic and oxidative injury in-vitro." Submitted.*
- **A.U. Joshi,** S.M. Kanse. *"Factor Seven Activating Protease (FSAP) Imparts Neuroprotection In-Vitro to primary cortical neurons against excitotoxic and hypoxic injury". Submitted*
- E. Hanson, S. M. Kanse, **A. Joshi**, K. Jood, S. Nilsson, C. Blomstrand, and C. Jern. "*Plasma FVII-Activating Protease (FSAP) Antigen and Activity Levels are increased in Ischemic Stroke*". **J Thromb Haemost. 2012 May; 10(5):848-56.**
- **A. Joshi,** S. Rajput, C. Wang, J. Ma, D. Cao. *"Murine Aldo-Keto Reductases: Identification of AKR1B8 as an ortholog of human AKR1B10".* **Biol Chem. 2010 Dec; 391(12):1371-8.**
- **A. Joshi,** D. Cao. *"TGF-β signaling, tumor microenvironment and tumor progression: The butterfly effect".* **Front Biosci. 2010 Jan 1; 15:180-94**.

Abstracts:

- International Giessen Graduate Centre for the Life Sciences (GGL) annual conference, Giessen, Germany 2013
- XXIV Congress of the International Society on Thrombosis and Hemostasis, Amsterdam, Netherlands 2013
- International Giessen Graduate Centre for the Life Sciences (GGL) annual conference, Giessen, Germany 2012
- 2nd International Symposium of the Excellence Cluster Cardio Pulmonary System (ECCPS), Max Plank institute for Heart and Lung, Bad Nauheim, Germany 2011
- International Giessen Graduate Centre for the Life Sciences (GGL) annual conference, Giessen, Germany 2011
- Southern Illinois University, MMICB conference, Springfield, IL, USA 2009
- International PRRSV symposium, Chicago, Illinois, USA 2006
- Roslin Institute Annual Conference, Edinburgh, UK 2006

Academic Honors:

- **DAAD Travel fellowship 2013** – Cyceron, University of Caen, Caen, France
- **DAAD STIBET** teaching assistantship 2013 - Courses in Bioinformatics
- **DAAD Travel fellowship 2013** – Theodor Kocher Institute, Bern, Switzerland
- **DAAD STIBET** teaching assistantship 2012 - Courses in Bioinformatics
- **DAAD STIBET** teaching assistantship 2011 - Courses in Bioinformatics

Technical and analytical skills:

- Cell culture –
    - Cell lines (HEK293, COS-7, RAW 267.1, U937, bEND3, bEND5),
    - Primary culture - cortical neurons, astrocytes, brain microvascular endothelial cells (pBMEMCs), *in-vitro* blood brain barrier (pBMEMCs + Glia).
- Biochemistry techniques – SDS – PAGE, Western Blot, ELISA, Activity assays, Enzyme kinetic assays, Permeability assay, Gelatin/Casein Zymography, Trans-well Migration assay, Wound Assay, Cell death/ cell survival assays.
- Molecular Biology techniques – cDNA synthesis, Cloning, Site mutagenesis, Plasmid extraction and purification, RNA extraction and purification, DNA extraction and purification, Real time PCR, Transfection, Transformation and Microbiological techniques.
- Microscopy – Immocytochemistry, Immunohistochemistry, Confocal Microscopy.
- Bioinformatics – BLAST, pFAM, Swiss-Prot, Deep View, Rasmol, Prosite, nnPredict, ClustalW, PDBsum, SOPMA, CINEMA.
- Mouse Thromboembolic Stroke model.
- Imaging & Statistical softwares – moorFLPI-2, MRI, LabImage 1D, Image J, Photoshop, GIMP, Graphpad Prism.